TETRA TECH

December 13, 2012

Mary Wohleb
King County WTD
201 S Jackson Street, Suite 500
Seattle, WA 98104-3855

Subject: North Beach Force Main Evaluation

Dear Mary:

Please find attached Norton Corrosion Limited's final report relating to the August coupon testing of the North Beach Force Main.

Field testing of the North Beach force main was conducted in August, 2012 after considerable planning and permitting by County staff. Tetra Tech arranged for survey support by True North Land Surveying and for field/laboratory services by Norton Corrosion Limited (NCL).

NCL staff members were present during the coupon sampling. NCL conducted field testing of soil and water conditions and conducted evaluation of corrosion products on the pipe exterior. They performed a general inspection of the exposed portions of the pipe prior to the attachment of the tapping tee. They collected soil and water samples as well as the pipe coupons for additional study in the lab. NCL's report describes all of their work and their results and conclusions.

Locations of samples are shown in the attached figure. Samples were collected at Locations 1, 2, and 3. No excavation was conducted at Location 4 due to tidal conditions, thus no pipe sample was collected. No analytical work was conducted at this location.

NCL's conclusions include a discussion of potential corrosion rates that is based on pitting depths. Their report states that if pitting continues at the average rate calculated, the pipe wall at similar pits on the pipeline may be breached in 30-40 years. The report notes that this is based on the limited samples they collected. Obviously, there could be deeper pits elsewhere and pitting rates are not likely to be consistent over time. With a pressurized pipe, some minimum wall thickness is required, depending on operating pressures, to prevent failure at a pit.

Pitting is one measure of loss of structural integrity of the pipe. NCL's analyses also documents graphitization, or loss of iron from the iron/graphite cast iron pipe material, leaving only the more brittle graphite. This process occurs across the surface of the pipe, but would vary as environmental conditions change along the length of the pipe. The loss of iron from the pipe wall decreases the strength of the pipe and increases the risk of failure over time. NCL noted a significant penetration of graphitization corrosion and estimated complete graphitization, based on the limited sampling, in a 30-40 year range. As with pitting, some amount of sound pipe material is required to maintain the pipe's structural integrity. The required remaining thickness depends on operating pressures and external loading conditions.

This assessment of the force main did not reveal conditions indicating an imminent risk of failure of the pipeline. The analyses confirmed that the pipe is located in an environment that contributes to an increased rate of corrosion relative to dryer, upland locations. As such, the County should continue to monitor the condition of the pipe over time and should expect to find that it requires rehabilitation or replacement some time prior to the life span indicated by the pitting rate calculation, but not in the immediate future.

Please call me directly with any questions. I can be reached at 206-883-9348.

Sincerely,
Tetra Tech, Inc.

R. Goss

Kevin R. Goss, P.E.
Project Manager, Engineering & Consulting Services

KRG:kg

Attachments (2)
c: Central Files

135-12539-11001-12

NOTES:

1. SAMPLE LOCATIONS PER KING COUNTY BASED ON AIR POCKET LOCATIONS.
    a. STATION 03+56. SAMPLE COLLECTED ON 8-14-2012
    b. STATION 11+39. SAMPLE COLLECTED ON 8-15-2012
    c. STATION 13+67. SAMPLE COLLECTED ON 8-16-2012
    d. STATION 31+02. NO SAMPLING CONDUCTED
2. FORCEMAIN ALIGNMENT PER TRUE NORTH LAND SURVEYING TOPOGRAPHIC SURVEY OF PIPE LOCATIONS MARKED BY KING COUNTY.

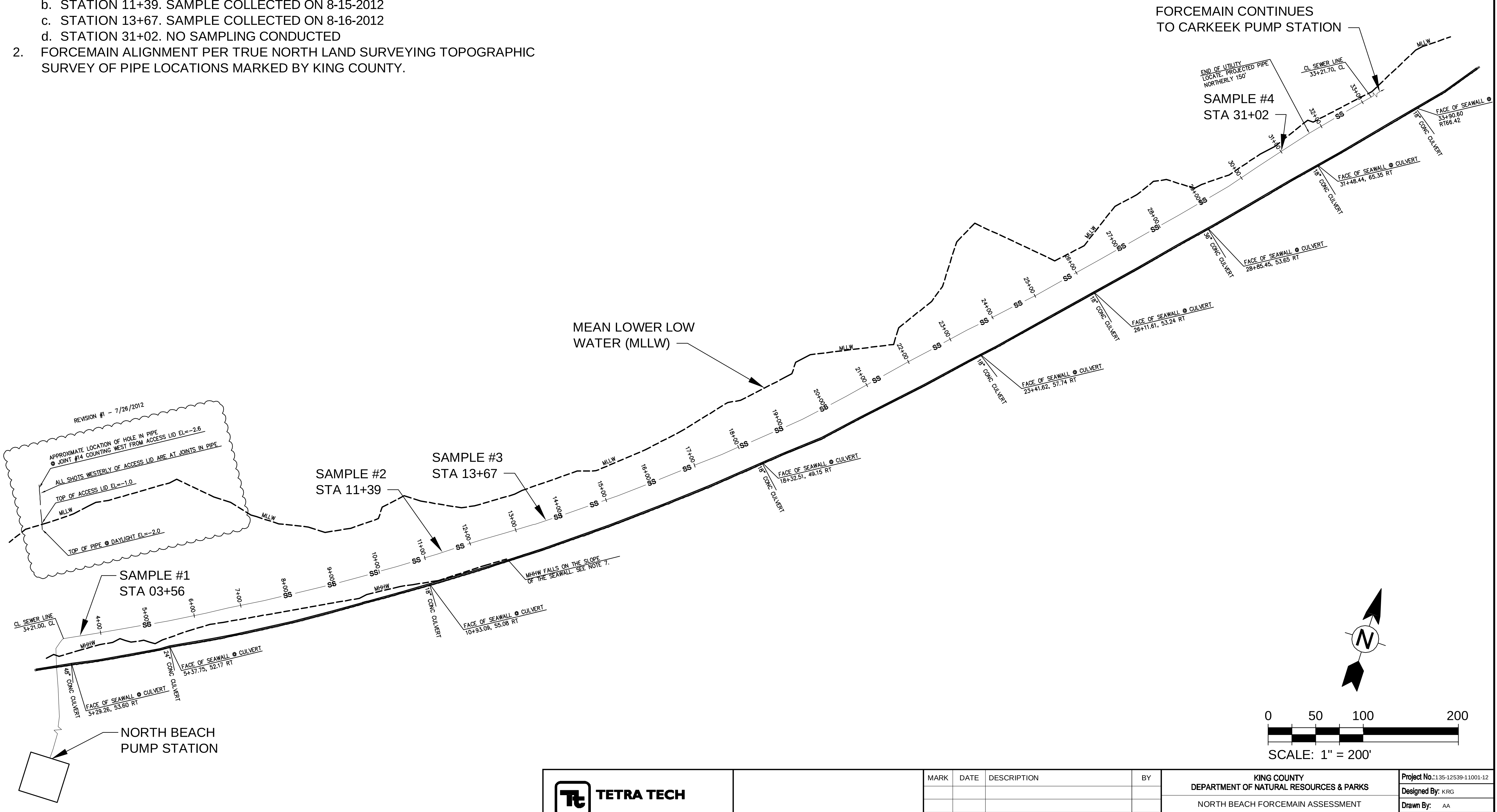

TETRA TECH

www.tetratech.com
1420 5th Ave, Ste 600
Seattle, WA 98101

MARK	DATE	DESCRIPTION	BY

KING COUNTY
DEPARTMENT OF NATURAL RESOURCES & PARKS

NORTH BEACH FORCEMAIN ASSESSMENT

SAMPLE LOCATIONS

Project No.: 135-12539-11001-12
Designed By: KRG
Drawn By: AA
Checked By: KRG

FIGURE 1

Bar Measures 1 inch

12/12/2012 1:41:53 PM - P:\12539\135-12539-11001-12\CAD\SHEETFILES\NORTH BEACH - FIGURE 1.DWG - ARIFIN, ANDERSON

NORTON CORROSION LIMITED

TETRA TECH, INC.
KING COUNTY WTD
NORTH BEACH FORCE MAIN
CONDITION ASSESSMENT PROJECT
FINAL REPORT

Prepared for: Tetra Tech, Inc.
1420 Fifth Ave Ste. 600
Seattle, WA 98101

December 2012
NCL File No. E-20806

CORROSION CONTROL SPECIALISTS SINCE 1959

8820 222nd Street SE
Woodinville, WA 98077
1-800-426-3111
Phone: 425-483-1616
Fax: 425-485-1754

TETRA TECH, INC.
KING COUNTY WTD
NORTH BEACH FORCE MAIN
CONDITION ASSESSMENT PROJECT

TABLE OF CONTENTS

TETRA TECH, INC.
KING COUNTY WTD
NORTH BEACH FORCE MAIN
CONDITION ASSESSMENT PROJECT

INTRODUCTION

Norton Corrosion Limited (NCL) was retained by Tetra Tech, Inc. to assist with a condition assessment of King County WTD North Beach Force Main located in Seattle, Washington. NCL developed an inspection/sampling program to be conducted at select excavation sites with field activities to collect necessary data and laboratory analysis to support formation of a professional opinion on present conditions. Authorization was by Consulting Services Agreement dated September 5, 2012. The field portion of the inspection/sampling occurred during the week of August 17, 2012.

GENERAL INFORMATION

North Beach Force Main transfers wastewater through Puget Sound tide flats from North Beach Pump Station to Carkeek Pump Station. The Force Main consists of 14-inch cast iron pipe with un-bonded bell and spigot joints. The pipe is internally lined with concrete for internal corrosion control and is externally uncoated except for the standard thin bitumastic paint provided for temporary corrosion control prior to installation. The Force Main was installed more than 50 years ago and was inspected under a similar analysis conducted in 1989. That work was conducted by Specialty Consultants Group and reported through Brown and Caldwell Consulting Engineers on May 31, 1989.

INVESTIGATION DETAILS

During August 14-16, 2012, NCL participated in coupon sampling of North Beach Force Main at three inspection locations selected by King County. At each location, the pipe was exposed and two soil samples were collected at pipe depth along with a water sample at the same elevation. Pipe-to-soil potentials were recorded, and a sample of the graphitization layer was also collected at Excavation No. 2 for analysis in the laboratory. A visual corrosion survey was conducted at each location to provide an approximation of the pipe condition.

A pipe tap was then attached to the pipe by others and a small coupon section of pipe was removed. That three-inch diameter coupon was preserved for metallurgical analysis. The force main was then re-sealed by installing a band with a valve bolted to the top of the band. A blind flange was then installed over the top of the valve assembly sealing the entire system, and the excavation was closed.

CAST IRON DETERIORATION

Cast iron and ductile iron pipe (DIP) both consist of an iron matrix surrounded by graphite particles. The distinction is simply the shape of the graphite particles. The iron portion is naturally susceptible to a corrosive environment exposure while the graphite is relatively immune from attack. The typical corrosion scenario consists of degradation of the outer iron surface exposed to the elements while the graphite remains unaffected. This process can continue until a condition known as graphitization results, meaning a large portion of the iron is corroded and only the more brittle graphite constituent remains, or local pitting can extend through the wall until failure may occur, depending upon local environmental conditions.

Cast iron normally enjoys a longer service life than carbon steel piping due to substantial wall section and less active materials when installed in most environments. The centrifugal casting process and subsequent annealing during production provides a corrosion resistant protective iron oxide layer. The Ductile Iron Pipe Research Association (DIPRA) currently utilizes a design decision model based upon likelihood and consequence factors to determine optimum corrosion control measures necessary for realizing service life demands. Likelihood factors are developed by DIPRA utilizing a 10-point soil evaluation guide as a basis with other factors considered to determine if specific soils are expected to be aggressive. Those results are combined with consequence factors toward DIP failure to justify corrosion mitigation measures.

The following tests are often considered in evaluating soil corrosivity: resistivity, pH, redox potential, sulfides, sulfates, and moisture characteristics. For each of these tests, results are categorized according to their contribution to corrosivity. Point values are assigned based upon the index as indicated below. When the total point value meets or exceeds 10 points, the soil is considered corrosive toward cast iron or DIP, and supplemental protection against external corrosion is recommended. Protection options usually include high-build coating, polyethylene encasement, bonded joints and/or cathodic protection.

DIPRA CORROSION INDEX

		Points
Resistivity (ohm-cm)	Less than 1,500	10
	1,500 – 1,800	8
	1,800 - 2,100	5
	2,100 - 2,500	2
	2,500 - 3,000	1
	More than 3,000	0
pH	0.0 - 2.0	5
	2.0 - 4.0	3
	4.0 - 6.5	0
	6.5 - 7.5	0*
	7.5 - 8.5	0
	More than 8.5	3
Redox (millivolts)	More than 100	0
	50 - 100	3.5
	0 - 50	4
	Negative	5
Sulfides	Positive	3.5
	Trace	2
	Negative	0
Moisture	Continuously wet	2
	Generally moist	1
	Generally dry	0

*Three (3) points when sulfides are present and redox potential is low or negative.

The use of this index is discussed in detail in Appendix A of ANSI/AWWA Standard C-105 entitled "American National Standard for Polyethylene Encasement for Ductile-Iron Pipe Systems".

FIELD INVESTIGATION

Field investigation included collection of samples, pipe-to-soil potential monitoring, and visual pothole inspections. Pothole inspections included photography and recording data revealed from each site relative to local conditions, including water level, soil type, pipe condition; construction details (select bedding, joint bonding, coating, polyethylene encasement and CP). Additional testing was conducted to identify extent of graphitization and pit depths. Pit depth was determined by removal of most corrosion products and measured by use of a standard hand-held pit gauge.

Since corrosion is an electrochemical process, the level of corrosion activity is often determined by the pipe-to-soil potential monitored in reference to a standard electrode contacting the soil. That monitoring was conducted as established by NACE International (National Association of Corrosion Engineers) Standard Test Method TM0497-2002-01 entitled "Measurement Techniques Related to Criteria for Cathodic Protection on Underground or Submerged Metallic Piping Systems”. When there is no CP operating on the force main, the pipe-to-soil potentials recorded in reference to the saturated silver-silver chloride (AgAgCl [sat.]) cell typically mean potentials more negative than -500 mV are generally considered representative of actively corroding cast iron when monitored in proximity to the reference cell location.

Excavation No. 1

The first excavation of the force main occurred on August 14, 2012. The location was at approximately Station 3+45’ near the secondary overflow pipe from the North Beach Pump Station.

The force main had roughly 5’ of cover at this location. There were significant volumes of fresh water that saturated the soil because of the proximity to the overflow pipe; therefore, the soils around the excavation were very moist and acted as flowing sand. The soils consisted of a grey sand, containing small rocks (<1” diameter). This soil extended from the surface to the pipe invert.

Two soil samples and a water sample were collected from the pipe depth. A second water sample was also collected at the discharge point for the dewatering system. This was done to get an accurate representation of the mixing between the fresh water and salt water. The pipe-to-soil potential was recorded as -532 mV (AgAgCl sat).

The coupon removal process began at 9:55 AM and was completed at 10:35 AM. At that time NCL took possession of the coupon and photographed the external surfaces of the pipe.

Excavation No. 2

The excavation was completed on August 15, 2012 and was located at Station 11+39'. This location was within 100' of a fresh water outfall. This outfall had saturated the area with fresh water since the tide was receding.

There were several pits evident with the deepest field measured at 100 mils. These pits were covered by the graphitization layer and were revealed by scraping a blade across the pipe surface removing corrosion product. In the locations where bright white metal was not evident, further investigation was conducted. It was in those locations, where the layer of graphite was removed that pits were revealed. Photographs of several such pits are shown in the appendices.

Coupon No. 2 does not contain the largest pits from that excavation. At the time of removal, the tapping crew was unable to collect the portion with the deepest pit because of the proximity of the graphitization layer and soil spilling into the work space.

The metal that was under the outer graphite layer was quite soft and was easily removed indicating further corrosion to an unknown depth. Because the pipe was not cleanly blasted and access to the bottom of the pipe was limited at best, the exposed pits may have not been the most severe. A limited time frame was allowed for the visual corrosion survey in Excavation No. 2 because of the incoming tide.

The surface soil conditions at Excavation No. 2 were similar to Excavation No. 1. The surface soil (<2’ in depth) were a grey sand that contained small rocks (<1” dia.). On occasion the excavation did find large rocks (1.5’ dia.). One of these rocks was directly on top of the pipe. There was no apparent damage from the large rock. At a depth greater than 2’, the soils changed to sandy, grey clay. This clay was saturated with water from both Puget Sound and the fresh water outfall. The pipe-to-soil potential was recorded as -572 mV (AgAgCl sat).

While a similar buildup of corrosion product was found on the pipe in Excavation No. 2, there were significantly fewer rocks imbedded into it. This may be because the clays prevented the migration of rocks through the soils.

Excavation No. 3

The excavation was completed on August 16, 2012, located at station 13+67’. This location did not have above ground features that would influence the local environment in the pipe area.

As with the previous two locations, Excavation No. 3 has a top soil layer composed of sand and small rock. This granular layer extended to roughly 2 feet in depth. The soils then changed to gray sandy clay. They clay did have some smaller (<2” dia.) stones imbedded in it. The grey, sandy clay layer was approximately 2 feet in depth as well. The soils around pipe depth were another type of clay. This clay was again grey in color and did contain some sands but was very dry. As this soil was excavated, it would break off in small sheets.

As the pipe was exposed, there was a layer of graphitization that generally surrounded the pipe. Similar to Excavation No. 2, there were not many rocks embedded in the layer when compared with Excavation No. 1. The pipe-to-soil potential was recorded as -559 mV (AgAgCl sat).

When the graphitization layer was removed and bare pipe exposed, several pits were revealed. In the time that was given to investigate the pipe surface, 11 separate pits were found and measured. The depths of these pits are included in the following table.

EXCAVATION NO. 3

CORROSION PIT DEPTHS

Pit Number	Depth (mils)
1	120
2	210
3	215
4	135
5	90
6	215

Pit Number	Depth (mils)
7	215
8	300
9	250
10	325
11	300

Pit locations 10 and 11 appeared to be associated with some prior damage to the pipe. The damage may have occurred at the time of installation. When the corrosion cell was initiated in these locations, the damage allowed the pitting to become more significant.

The coupon that was removed from Excavation No. 3 contained one of the major pits but not the deepest. The pit contained in the coupon was pit number 3 in the above chart.

LABORATORY INVESTIGATION

Soil and water samples were collected from the potholes from different depths. Laboratory testing of soil and water are performed under specified conditions which supply characteristics known to affect corrosion. Laboratory testing is often done where field test locations lack adequate exposed space for standard field testing and when other specific characteristics are desired.

The following is a summary of laboratory analysis conducted on the collected samples to measure characteristics known to affect pipe corrosion.

Resistivity	Low resistivity supports corrosion currents
pH	Low pH means higher corrosion rate & damage to concrete
Sulfides	Elevated sulfides damage exposed steel
Sulfates	Elevated sulfates physically damage concrete
Chlorides	Cause concrete coated steel to actively corrode
Redox	Low to negative Redox means poorly aerated soil
Class	Granular is less corrosive

Resistivity is an inverse function of electric current flow as produced by corrosion and is tested per ASTM G-187 Standard Test Method for Measurement of Soil Resistivity Using the Two Electrode Soil Box Method . Table 1 is useful in predicting the corrosivity of a soil with respect to resistivity alone.

Table 1: Anticipated Corrosivity

Classification	Electrolyte Resistivity (ohm-cm)	Anticipated Corrosivity
Low Resistance	0 - 2,000	Severe
Medium	2,000 - 10,000	Moderate
High	10,000 - 30,000	Mild
Very High	Greater than 30,000	Increasingly Less

pH is a measurement of hydrogen ion concentration describing environmental acidity and tested per ASTM D4972 Standard Test Method for pH of Soils. A pH value between 6.5 and 7.5 is generally considered to be neutral. A lower pH (acidic) indicates an excess number of hydrogen ions are available to readily support a corrosion cell. Higher pH represents an alkaline condition which suppresses corrosion activity to exposed carbon steel, CI or DI pipe. Table 2 illustrates how pH considered alone can be interpreted as an indicator of potential corrosion toward exposed piping.

Table 2: pH

pH	Corrosivity	Acid/Alkaline
< 5.5	Severe	Acidic
5.5 – 6.5	Moderate	Slightly Acidic
6.5 – 7.5	Neutral (low)	Neutral
> 7.5	None (low)	Alkaline

The presence of sulfides indicates the soil or water may contain and support Sulfate Reducing Bacteria (SRB), a species known to cause corrosion. EPA 9030B Acid Soluble and Acid Insoluble Sulfides by distillation is the test method used to detect sulfide level.

Under certain circumstances such as anaerobic conditions (low or negative Redox Potential) and neutral pH, SRB are able to proliferate. SRB reduce (consume) naturally occurring sulfates and hydrogen in the soil producing unstable and damaging sulfides.

The presence of sulfates in soil or water can significantly increase the corrosion rate of metallic pipe at concentrations greater than 1,500 parts per million (ppm). EPA 300.0 Determination of Inorganic Anions by Ion Chromatography is the test method used to determine sulfate concentration. Table 3 shows the acceptable range of sulfates.

Table 3: Acceptable Sulfate Limits

Classification	Sulfates (PPM)	Anticipated Corrosivity
High	>10,000	Severe
Medium	1,500 - 10,000	Considerable
Low	150 - 1,500	Detectable
Very Low	0 – 150	Negligible

Chlorides damage concrete coated cast iron that is normally passivated by the elevated pH of the concrete. Chlorides migrate through the concrete by diffusion and activate the metal when concentration exceeds 300 ppm by weight of concrete. Chloride concentration is tested by EPA 300.0 Determination of Inorganic Anions by Ion Chromatography. Table 4 shows the acceptable range of chlorides.

Table 4. Chemistry – Chlorides

Classification	Chlorides (PPM)	Corrosivity
Very High	>5,000	Severe
High	1,500 – 5,000	Considerable
Medium	500 – 1,500	Corrosive
Low	100 - 500	Threshold

Oxidation-Reduction potential, commonly referred to as Redox Potential, is a measurement of soil aeration or oxygen availability. ASTM D1498 Standard Test Method for Oxidation-Reduction Potential of Water is the method used to determine Redox.

That is important because SRB is known to be responsible for establishing local chemical conditions resulting in high corrosion rates, proliferate in oxygen free environments. Redox potential greater than +100 mV indicates the soil to be sufficiently aerated so SRB are not readily supported. Potentials of 0 to +100 mV may or may not indicate anaerobic conditions, while a negative Redox potential indicates anaerobic conditions under which SRB are readily supported. Heavy clays, mucks and organic soils are often anaerobic. Table 5 shows the acceptable range of Redox Potential in soil.

Table 5. Soil Chemistry – Redox Potential

Redox Potential (standard H Scale)	Aeration	Soil Corrosivity
Negative	Not aerated	Extremely severe
0 to 100 mV	None to weak	Severe
100 to 200 mV	Weakly aerated	Moderate
200 to 400 mV	Aerated	Slight
> 400 mV	Strongly aerated	Noncorrosive

Soil classification by grain size and type is also relative. Finer soils tend to have more surface area exposed, allowing minerals and salts to dissolve more easily than larger grains. At the same time, finer soils have a lower percolation rate, so the dissolved ions are not as easily flushed out of the soil. Fine-grain soils; such as, clay tend to be far more corrosive than course-grain soils such as sand and gravel. They also tend to hold moisture longer.

Variations in soil composition typically result in more corrosive soil conditions, both on a micro and macro scale. Long structures such as pipelines usually contact various soil types. Corrosion is accelerated by differences in the metal (such as hot/cold, welds, stress at bends, and bimetallic couples) and variations in the environment (such as above or below the ground water table, temperature and oxygen content). A site with significant variations in soil composition can be more corrosive than a homogeneous site of more corrosive soil.

Microbiologically Influenced Corrosion (MIC) can be a multi-faceted biological process from naturally occurring microorganisms that often exacerbates corrosion through several different methods. Some types of bacteria colonize in a voluminous biomass covering a portion of a structure or create a protective covering of corrosion product as tuberculation; thereby, limiting free oxygen availability to an otherwise oxygen rich environment. That environmental difference spanned by a single continuous structure creates an oxygen concentration cell where corrosion is accelerated under the deposit. Others cause compromise to metal through the direct result of natural biologic activity.

Bacteria known to cause corrosion exist in both aerobic and anaerobic conditions and often co-exist in a symbiotic relationship with other species. SRB for instance, is a well-known corrosion-causing organism on cast iron but it requires an anaerobic environment and essential nutrients not found naturally occurring to flourish; therefore, it is often found existing with other species. Other species are known to colonize under positive conditions and their natural biologic activities produce acidic waste products that then directly attack metal. These types of bacteria are often grouped as Acid Producing Bacteria (APB) and it is not uncommon to find depressed pH as low as 1 or 2 in contact with the underlying metal.

MIC activity was monitored by creating slurry from a swab collected from the exterior coupon surfaces. That was used to inoculate various growth media known to support specific bacteria that influence corrosion. A sterile syringe was utilized to transfer 1 cubic centimeter (cc) of slurry to a string of growth media by serial decimal dilutions. Specific media were used to monitor the presence of APB, SRB, Anaerobic Bacteria (ANA), Low Nutrient Bacteria (LNB) and Iron Related Bacteria (IRB) all of which are known to affect corrosion in natural waters and are species easily incubated. Some other corrosion related bacterial species including Sulfur Oxidizing Bacteria (SOB) are so difficult to incubate and isolate, that detecting SRB species alone allows one to assume the presence of the former. These species of bacteria are all naturally occurring and not harmful to the public but can be responsible for serious corrosion damage.

The inoculated MIC samples were set aside and allowed to incubate for over 30 days at room temperature after which microbial activity was determined by noting which media indicated positive reactions and the range of viable bacteria per milliliter (ml) was then estimated by noting which minimum dilution sample of each series indicated a positive reaction.

The pipe coupons and corrosion product were closely examined by low power microscope to detect significant details of the corrosion damage. The samples were further analyzed using Scanning Electron Microscope (SEM) and Energy Dispersive Spectroscopy (EDS) techniques to detect greater detail with spectrographic analysis used to determine specific make-up. The stereomicroscopy SEM/EDS analysis allow one to microscopically view and photograph the samples at great magnification and to then select specific microscopic portions of the samples for further chemical analysis. That specific portion of the sample is bombarded by x-rays, which excite electrons and produce a unique spectrum, which can then be used to identify the material composition.

TEST RESULTS

Soil Analysis

Two soil samples were collected from each excavation and preserved for analysis. The samples were removed from the spring line level of the pipe to most accurately represent the conditions immediately around the pipe. Each soil sample was tested in accordance with the DIPRA scale with the following results:

Excavation 1:

Soil Sample 1 -1

Resistivity	170,000 Ω-cm
PH	8.1
Redox	-143.7 mV
Sulfides	<1 ppm
Sulfates	32 ppm
Moisture	11.07%
DIPRA Index	7

Soil Sample 1-2

Resistivity	6,700 Ω-cm
PH	6.9
Redox	-125.8 mV
Sulfides	<1 ppm
Sulfates	32 ppm
Moisture	13.15%
DIPRA Index	7

Excavation 2:

Soil Sample 2-1

Resistivity	370 Ω-cm
PH	7.6
Redox	-158.5 mV
Sulfides	<1 ppm
Sulfates	67 ppm
Moisture	17.29%
DIPRA Index	17

Soil Sample 2-2

Resistivity	230 Ω-cm
PH	8.1
Redox	-180.7 mV
Sulfides	<1 ppm
Sulfates	50 ppm
Moisture	21.80%
DIPRA Index	17

Excavation 3:

Soil Sample 3-1

Resistivity	170 Ω-cm
PH	8.0
Redox	-266.9 mV
Sulfides	<1 ppm
Sulfates	280 ppm
Moisture	23.45%
DIPRA Index	17

Soil Sample 3-2

Resistivity	170 Ω-cm
PH	7.6
Redox	-370.8 mV
Sulfides	<1 ppm
Sulfates	130 ppm
Moisture	31.15%
DIPRA Index	17

Water Analysis

A water sample was collected from each excavation and preserved for analysis. Each sample was taken from the bottom of the excavation to better get a representation of the water normally contacting the pipe. In Excavations No. 1 and 2, there was a significant flow of fresh water into the local soils due to the proximity of two freshwater overflows. The fresh water could be flushing out the salt water that may have been present otherwise.

Each water sample was tested for pH, sulfate, sulfide, chlorides and resistivity. The results are tabulated in the below tables.

Excavation 1:

Water Sample 1-1

Resistivity	2,350 Ω-cm
PH	7.6
Sulfides	<1 ppm
Sulfates	27 ppm
Chlorides	37 ppm

Excavation 2:

Water Sample 2-1

Resistivity	46 Ω-cm
PH	7.5
Sulfides	<1 ppm
Sulfates	1,700 ppm
Chlorides	11,000 ppm

Excavation 3:

Water Sample 3-1

Resistivity	390 Ω-cm
PH	7.1
Sulfides	<1 ppm
Sulfates	1,900 ppm
Chlorides	11,000 ppm

All soil samples collected had negative Redox potentials indicating anaerobic conditions where damaging SRB could proliferate. The results of the soil analysis considering only the DIPRA Index indicate Excavation No. 1 is compatible toward cast iron with no additional corrosion mitigation, while Excavations No. 2 and 3 both exceed the 10 point total identified as soil that should include extra corrosion protection for cast iron. No extra exterior corrosion protection had been provided for this pipe. The water analysis found normal salt water conditions with some fresh water intrusion.

MIC Results

The MIC testing detected limited populations of APB in all three excavations and ANA was detected in Excavation No. 1 only where soils were much more granular than found at the other two excavations. SRB, IRB and LNB were not detected in any of the three excavations, though local conditions were optimal for colonization. These results do not suggest that species known for support of corrosion were not present, rather were not colonized in sufficient numbers to be detected, thus are not likely contributing to corrosion.

SEM/EDS Results

The visual examination revealed areas of piping suffering significant external loss of section primarily through pitting. There was no visual internal degradation evident. The coupon collected from Excavation No. 2 included a fractured cement mortar lining that was damaged during removal. The other two coupons collected from Excavation No. 1 and Excavation No. 2 had no lining recovered with coupon removal.

Excavation No.1 (Coupon 1) had residue of a mortar lining remaining and minor exterior surface corrosion with no pitting evident.

Excavation No 2 (Coupon 2) had loose pieces of the mortar lining (approximately ¼ inch thick) with a minor internal seal coat tar lining and minor exterior surface corrosion with no pitting evident.

Excavation No. 3 (Coupon 3) had residue of a mortar lining remaining and one deep exterior pit and other minor exterior surface corrosion.

The corrosion product sample collected from Excavation No. 2 contained pebbles and clay. The corrosion product revealed a black layer when sectioned that rapidly turned dark brown after drying with air exposure.

Pipe Wall

Pipe wall section was measured from coupons using a standard micrometer at locations free of detectable pitting with the following results in mils:

Reading	Coupon 1	Coupon 2	Coupon 3
1	662	665	687
2	667	660	687
3	665	672	691
Average	665	666	688

Chemical Analysis

Pipe chemical analysis was determined by Inductively Coupled Plasma Atomic Emission Spectroscopy (ICP-AES) and combustion analysis as follows with results in % and remainder as iron:

Element	Coupon 1	Coupon 2	Coupon 3
Carbon C	3.44	3.37	3.44
Manganese Mn	0.35	0.34	0.36
Sulfur S	0.060	0.067	0.073
Silicon Si	1.15	1.11	1.16
Nickel Ni	0.05	0.05	0.06
Chromium Cr	0.07	0.07	0.08
Phosphorus P	0.39	0.36	0.35
Copper C	0.07	0.17	0.15

Metallurgical

The coupons were then sectioned and mounted to better examine the extent and depth of corrosion (Figures 17 to 26).

Coupon 1 had corroded to a depth of approximately 2mm (80 mils) from the exterior leaving graphite matrix (figures 24, 27, 28 and 33-35).

Coupon 2 had limited exterior corrosion to a depth of less than 1mm (40 mils) leaving graphite matrix and minor interior corrosion pitting of approximately 1mm (40 mils) (Figures 25, 29-30 and 36-39).

Coupon 3 had corroded with a pit to a depth of approximately 6mm (240 mils) from the exterior leaving graphite matrix (Figures 26, 31, 32, 40-44).

SEMS-EDS

The mounted cross sections and samples of corrosion scale were then submitted to SEM-EDS for chemical fingerprinting and detailed pit depth measurement.

Coupon 1 had deepest areas of graphitization approximately 2mm from OD with generalized areas of about 1mm (Figures 45-47).

> Chemical fingerprinting revealed elevated levels of phosphorous, sulfur and chlorides with corrosion byproducts (Figures 48-53).

Coupon 2 had deepest areas of graphitization approximately 0.3mm from OD with 1.1mm pitting from ID (Figures 54-57 and 60).

> Chemical fingerprinting of the scale revealed elevated levels of phosphorous, sulfur and chlorides (Figures 58-65).

Coupon 3 had deepest pit extending about 6.43mm from OD (figures 66-67) with areas of graphitization approximately 4.7mm from OD (Figures 66-70).

> Chemical fingerprinting revealed elevated levels of phosphorous, sulfur and chlorides with corrosion byproducts (Figures 71-73).

The corrosion product collected from Excavation No.2 contained no sound metal and the corrosion scale had elevated levels of phosphorous, sulfur and chlorides (Figures 74-81).

CONCLUSIONS

Coupon 1 had corrosion penetration approximately 2.0 mm of the 16.9 mm wall section from the OD.

Coupon 2 had corrosion penetration approximately 0.3 mm from OD and 1.1 mm from ID of the 16.9 mm wall section.

Coupon 3 had corrosion pit extending approximately 6.43 mm from OD of the 16.9 mm wall section.

Sample 4 had no sound metal and was composed of soil stones and corrosion product.

New or original cast iron pipe wall depends upon pipe class used. The original class is not known but was assumed to be Class 27 in earlier Brown and Caldwell report, and no evidence was found to refute that. Class 27 pipe has wall section range of 670 to 830 mils.

Assuming this was Class 27 cast iron pipe with maximum wall of 830 mils, average corrosion rates over past 51 years are: Coupon 1, 3.23 mpy, Coupon 2, 3.21 mpy & Coupon 3 2.78 mpy; therefore, the maximum general corrosion loss over that period was 165 mils at Coupon 1 collected from Excavation No. 1.

The maximum pit found was on Coupon 3 from Excavation No. 3 which was 325 mils deep. Average remaining wall section of that coupon was measured at 688 mils so remaining section below the pit was 363 mils. The maximum pitting rate has then been: 830 mils -363 mils = 467 mils over 51 years or 9.16 mpy and if that is worst case, the first penetration should be expected during year 90 which is 39 years in the future.

The most serious compromise was found at Excavation No. 3 and yet the remaining wall section there was 363 mils. In this location, graphitization corrosion has penetrated 56.2% of the pipe wall, reducing the original structural properties of the pipe. If that is the worst case for the entire force main and the corrosion process has been and will remain linear, the first corrosion penetration is not expected until approximately 30 to 40 years in the future. These conclusions must be recognized as being based upon very limited examination of the entire force main and they are based entirely on only that evidence revealed.

APPENDIX A

FIELD NOTES

Site 1 (Sta: 3+56)

Site selection because of air pockets in the force main that were found in “Smart Ball Technology” conducted at a previous date. This was a rough estimate of air pocket locations. Also “Smart Ball” found no leaks during its survey.

6:00 AM Arrived on site, excavation had begun and was roughly 3 feet deep. Pipe had not been exposed or found.

Site Conditions

Top 3 feet soil conditions: Sandy with small to moderate sized aggregate. As excavations continue the soil conditions remain similar in materials but become more hard-packed.

On arrival the tide was receding at a relatively fast pace. The tide line was roughly 60’ below the excavation. At this location there was a fresh water outfall on the beach side of the tracks. This was a fast flowing stream that had significant relevance to the area because fresh water was continually flushing into the excavation. Therefore it is highly likely that the water samples collected at the pipe depth were not true representations of the typical water around the pipe.

6:20 AM top of pipe is found but not exposed. Fresh water is still pouring into the excavation. Soil conditions have changed slightly with larger aggregate in the sand.

8:00 AM top of pipe exposed. Exterior appears to have large concentrations of corrosion product around the pipe. The corrosion product also has a significant amount of aggregate that is imbedded in the corrosion product.

9:00 AM pipe exterior was cleaned by tapping company and samples were taken from the Puget Sound side of the pipe. Also collected were two soil samples one from the Puget sound side of the pipe (Sample 1) and one from the land side of the pipe (Sample 2). Also a water sample was taken from the pipe area. This area had significant fresh water flow due to the outfall proximity.

As corrosion product was removed the pipe surface was inspected for any major pitting and or the presence of graphitization. There were many small pits of less than 100 mils and the pipe surface appeared to be hard and not much graphitization.

It is possible that the pipe had been coated. In the 1989 report it was noted that there was no coating, but this could a location that had coating installed for some reason. This location is very near the 90 degree bend that comes from the pump station and turns down the beach. There are as built plans that are available through Mary Beth Gilbrough. (marybeth.gilbrough@kingcounty.com)

10:00 AM the bottom of the pipe was exposed and cleaned by tapping company. John Keppler did the inspection at this point because of limited room and time constraints. A thorough invert inspection was not completed because of time constraints so there are no photos of the bottom of the pipe.

10:30 AM Coupon has been removed and the chain of custody was transferred to Norton Corrosion Limited. The sample was wrapped in a clean cloth and placed in a zip lock bag after several rounds of pictures were taken. The sample was then double bagged and NCL left the site shortly thereafter.

The metal sample was then taken to the lab and a MIC Kit was inoculated by Isaac Reinholdt. Soil samples were also started and will be completed by Randy Hunt and Isaac Reinhold in following days. The samples were transported to the lab in a cooler with ice packs and then were placed in a refrigerator.

Site specifics:

There are two sewer overflow outfalls in close proximity to Site 1. The first was discussed at length at the fresh water outfall this is supposed to be a secondary overflow but in past years has become the primary. The other overflow is a pipe leading out into the water this pipe has become clogged with sand but does continue to spill some overflow.

Site 2 (Sta. 11+39)

Site was selected in the same fashion as location 1 the “Smart Ball Technology” found air pockets in this area and had a higher likelihood of internal corrosion due to the sulfur presence.

Site conditions:

There is a smaller fresh water outfall that is within 100’ of the excavation. This does have some influence on the excavation area but has been removed by a pump on the uphill side of the excavation. This area is much more susceptible to the influence of sea water for the duration of the excavation and survey.

Soil:

The surface soils are sand with some small (<1”) stones within it. Sporadically there are large (1.5’ dia) stones in the soils up to 3-3.5’ in depth

At 3-3.5’ the soils change dramatically. The soil becomes a sandy clay. The clay has a grey brown color and has little odor. This clay also has large rocks sporadically imbedded in it. There is also a layer of round rocks separating the sand from the clay. This layer is very minimal at 3-4.” The rocks were small in diameter.

Soil and water samples were taken at pipe depth at 9:35 am. A sample of the discharge water was also taken to give a more accurate evaluation of the mixed types of water that the pipe area may be exposed to.

6:00 AM Arrived on site to find excavations just beginning. Water levels are within 50’ of excavation at time of arrival but are receding at a rapid pace.

9:30 AM Pipe was exposed. A buildup of a corrosion product was present as with location 1. This was not as thick as it was with excavation 1 and had a more grey color to the exterior of the corrosion product. A sample was collected to determine the thickness and makeup of the material. The water levels of the Puget Sound were +100’ from the excavation site.

10:00 AM not many pictures were taken on the pipe surface other than the pit locations as there was additional pressure to have the tapping crew in immediately.

There were three pits found on the top surface of the pipe. The deepest was 0.140” deep and roughly ½“ long. The material that was below this pit was soft possibly from micro corrosion cells. The total depth of these cells was not determined due to time constraints.

All pits were scraped using a pocket knife to look for white metal (when the blade runs over the surface). Where white metal was not found, further investigation was done to determine the depth of the pit. There are no guarantees that the pits that were found were the deepest on that section (2 LF of pipe). The bottom of the pipe was never available for inspection.

11:15 AM the coupon was removed and an internal concrete lining was found. This lining also had a black film that was built up on the surface (sewage side) of the C.C. It is possible that location 1 had a lining as well but was lost in the tapping efforts. No pits were removed with the coupon. A very small pit was evident but has not been explored for depth. After NCL took possession of the coupon, pictures were taken. NCL then wrapped the sample in a clean cloth and placed it in two zip lock bags. The coupon and soil samples were then transported back to NCL's office in a cooler with ice packs.

The metal coupon was taken to the lab and a MIC Kit was inoculated by Isaac Reinholdt. The soil samples were also started to be completed by Randy Hunt and Isaac Reinholdt in the following days.

Site 3 (Sta. 13+67)

Site was selected in the same fashion as locations 1 and 2. This was because of the “Smart Ball Technology” findings. This location was expected to have an air pocket on the inside of the pipe.

Site conditions:

Site had no fresh water outfall nearby. The surface soil was typical beach sand and small cobble (<1”) as noted been at the sites 1 and 2. This condition persisted up to 2’ in depth.

At depths greater than 2’, the soils around the pipe were dry grey clay that came off in sheets. The samples that were taken do not evidence this as they were taken from the excavation site and had water running over them and were saturated. The soil samples were taken one from the beach side of the pipe and one from the sound side.

9:00 AM Arrived on site. Excavation activities were well underway upon arrival. Weather conditions were warming and sunny.

9:30 AM At first exposure, the pipe was 50’ from the sound water line. There was a minimal inflow of seawater into the excavation because of the clay layer and the water level.

10:00 AM The pipe was exposed and cleaned by the tapping crew and NCL. The first inspection was of the carbonaceous deposit that was upward of 4” thick. Once the deposits were removed, a thorough inspection of the pipe surface was completed. This inspection was much more thorough than at the previous sites because the excavation activities progressed at a more rapid pace. There were several pits found in this location. The depths are detailed below.

Pit Locations:

Pits were located on the top of the pipe and on the sides. The deepest pits were located roughly 30-38” from first exposure from the pump station side. Pits 10 and 11 appeared to be initiated from installation damage and progressed from there. Pits were up to an inch wide and half an inch in length.

Pit depths

Description	Depth (inch)
1	0.12
2	0.210
3	0.215
4	0.135
5	0.090
6	0.215
7	0.215
8	0.300
9	0.250
10	0.325
11	0.300

Locations of pits on the small section are shown in a drawing that is included in the packet of daily information. Sites 8-11 are not on this list.

Because of the number of pits found on this section, NCL was not allowed time to investigate for additional pitting.. It is possible that there were more pits elsewhere in this section.

12:20 PM The coupon was removed by the tapping crew and NCL took possession of the coupon for further evaluation. This coupon had a significant pit included in it. This pit was number three on the above chart. This coupon did show small signs that a concrete lining may have originally existed, but it is impossible to give a definitive answer because no large chunks of the lining came out with the sample.

After NCL took possession of the coupon, pictures were taken. NCL then wrapped the sample in a clean cloth and placed it in two zip lock bags. The coupon and soil samples were then transported back to NCL's office in a cooler with ice packs.

The metal coupon was taken to the lab and a MIC Kit was inoculated by Isaac Reinholdt. The soil samples were started to be completed by Randy Hunt and Isaac Reinholdt in the following days.

APPENDIX B

FIELD PICTURES

Pictures of Excavation No. 1

Picture 1-1: General Overview of Excavation

Picture 1-2: Excavation at Beginning Stages Depicting Water Level

Picture 1-3: Pipe with Carbonation Layer Intact

Picture 1-4: Carbonation Layer Removed to Bare Pipe Surface

Picture 1-5: Thickness of the Carbonation/Corrosion Product Layer of 1”

Picture 1-6: Profile Cleaned Cast Iron

Picture 1-7: Clamp and Tapping Machine

Pictures of Excavation No. 2

Picture 2-1: General Overview of Excavation

Picture 2-2: General Soil Conditions Surrounding Pipe

Picture 2-3: Carbonation/Corrosion Layer Being Removed by Tapping Crew

Picture 2-4: General Profile of Pipe with Carbonation Layer Removed

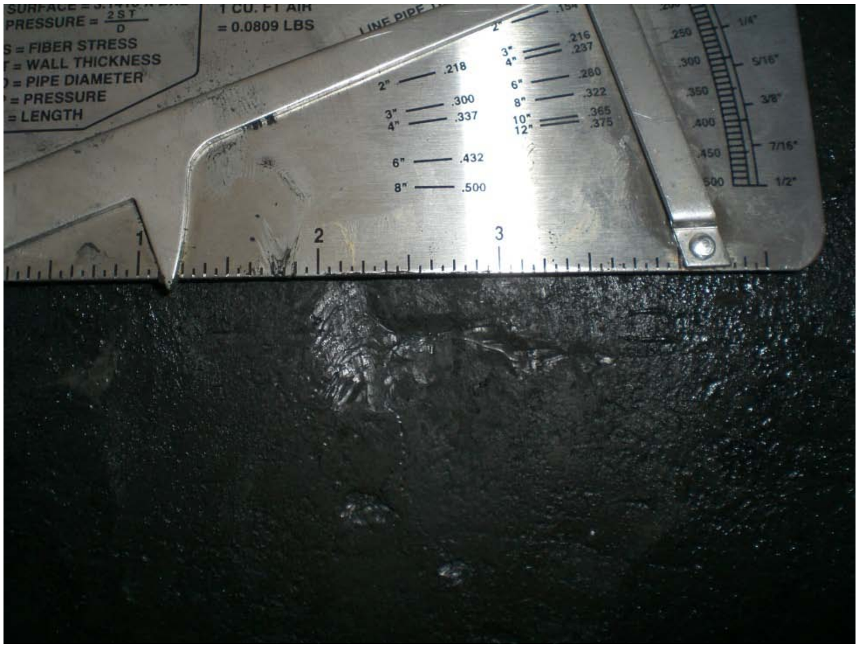

Picture 2-5: Depicts Length of Largest Pit in this Section of Exposed Pipe

Picture 2-6: Tapping Machine with Coupon Inside
& Concrete Lining
(This is the only sample that retained the concrete lining.)

Pictures of Excavation No. 3


Picture 3-1: General Overview of Excavation


Picture 3-2: Pipe Surface Visible while Tapping Crew Removes Carbonation Layer

Picture 3-3: Carbonization/Corrosion Layer Shown
of Approximately 4” Thickness

Picture 3-4: General Profile of Cleaned Pipe

Picture 3-5: Depth of Pit 3

Picture 3-6: Depths of Pits 10 and 11
These pits appeared to be initiated by slight damage most likely from installation.

Picture 3-7: Profile of Pit 6
The scrape marks through the pit are from the knife used to dig out the soft graphite layer that filled the pit.

APPENDIX C

METALURGICAL

FIGURES – E86580

Fig. 1: Overall view of the four (4) submitted coupons.

Fig. 2: Overall view of the ID of sample #1. Note, the white material is residue from the concrete liner.

Fig. 3: Overall view of the OD of sample #1.

Fig. 4: Overall view of the ID of sample #2. Note, the tar (asphalt) coated concrete was retained with this sample.

Fig. 5: Same as Fig. 4 with the concrete liner removed.

Fig. 6: Same as Fig. 5 except the OD of the pipe is viewed.

Fig. 7: Overall view of the ID of sample #3.

Fig. 8: Overall view of the OD of sample #3.

Fig. 9: Close-up of the deep pit on the OD of sample #3.

Fig. 10: Overall view of sample #4.

Fig. 11: Same as Fig. 10 except the opposite side is viewed.

Fig. 12: Same as Fig. 10 after breaking the sample in half.

Fig. 13: Close-up of one half of sample #4. Note, the rocks in the corrosion scale.

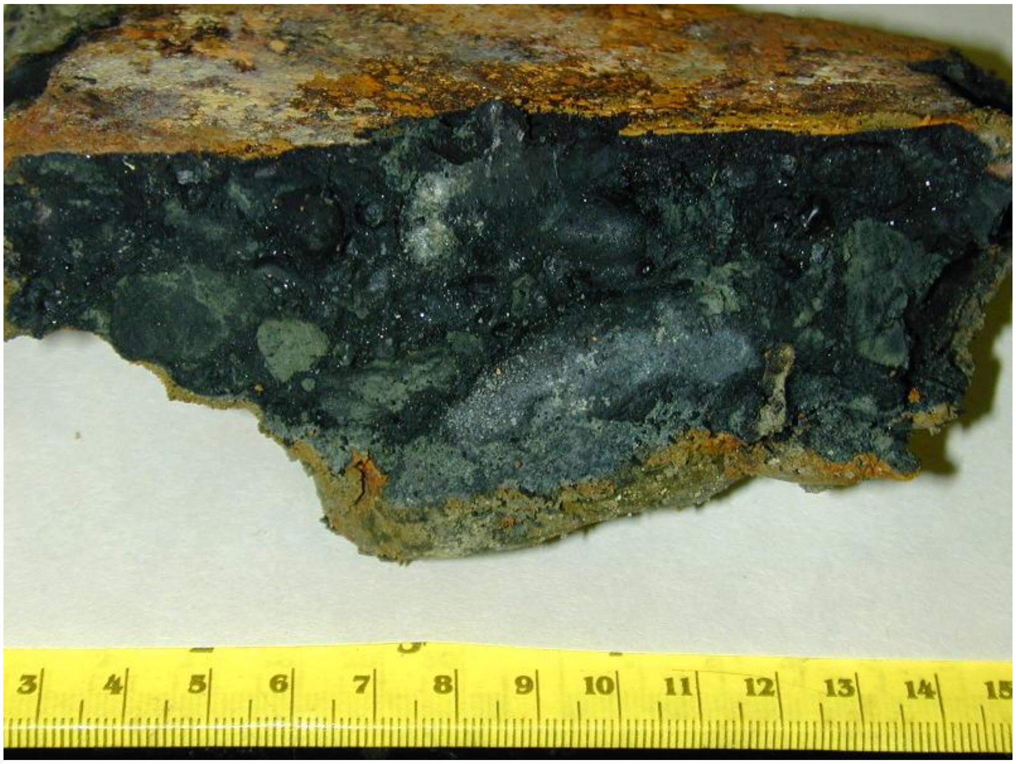

Fig. 14: Same as Fig. 13 except the opposite half is viewed.

Fig. 15: Same as Fig. 12 after allowing to air dry.

Fig. 16: Same as Fig. 13 after drying.

Fig. 17: Overall view of sample #1 after sectioning for metallurgical examination.

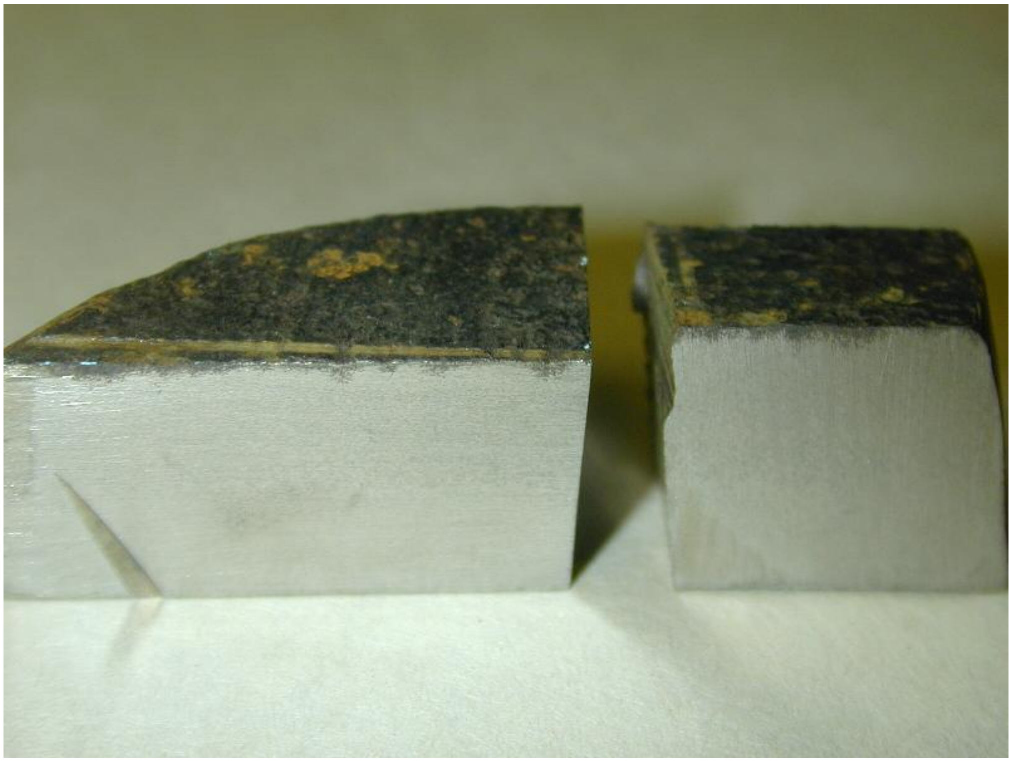

Fig. 18: Close-up of the corrosion on sample 1 from the OD.

Fig. 19: Overall view of sample # after sectioning.

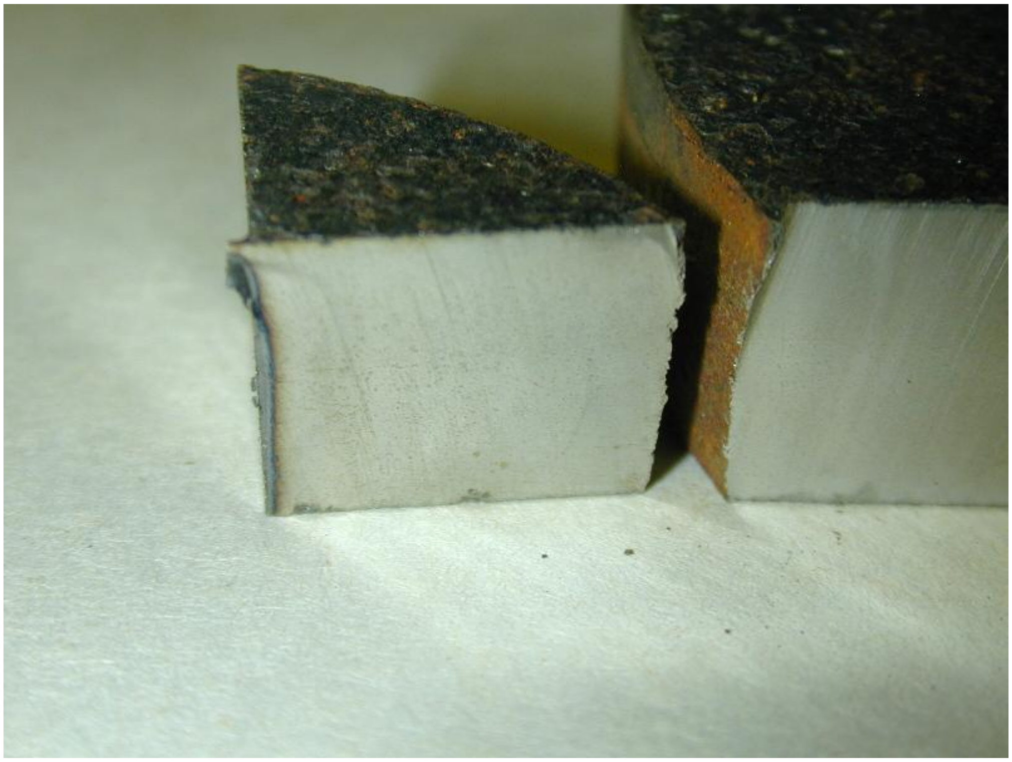

Fig. 20: Close-up of the cross-sectioned piece. Note, the pitting at the ID.

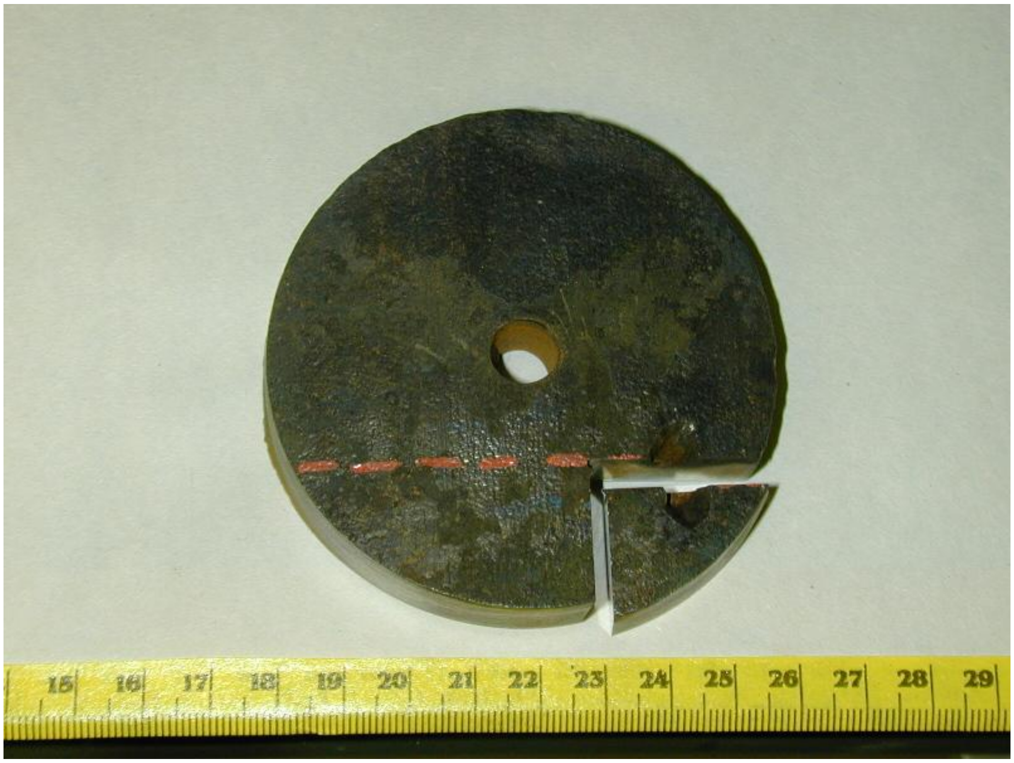

Fig. 21: Overall view of sample #3 sectioned through the pit.

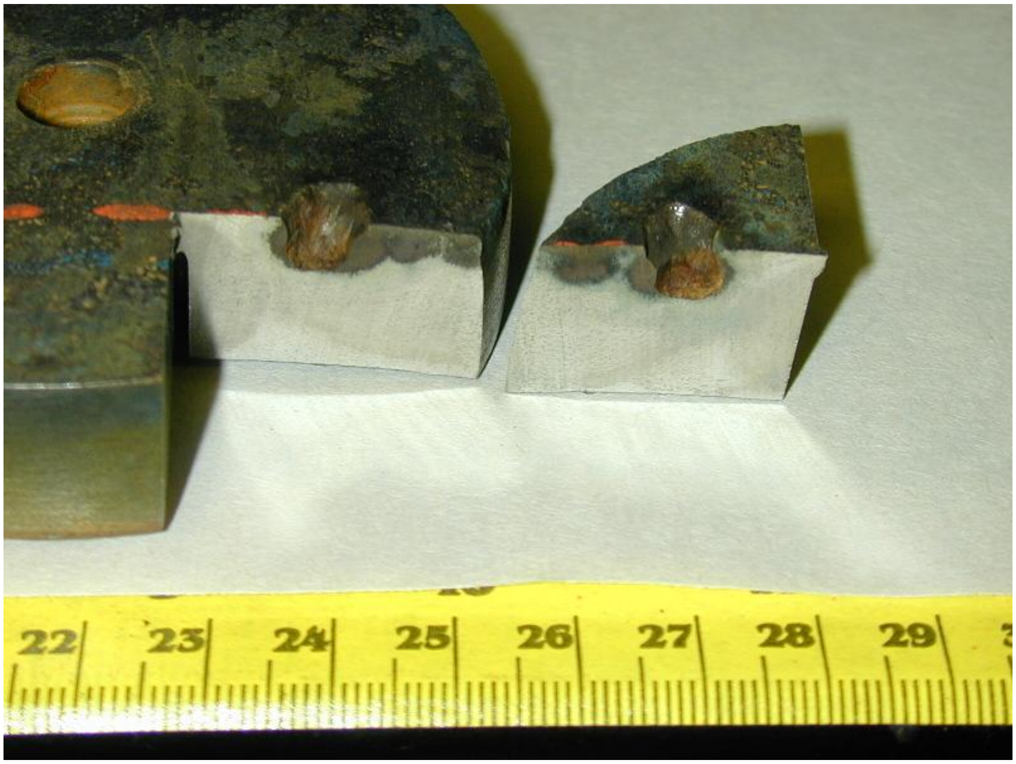

Fig. 22: Cross-sectional view of the pitting and graphitic corrosion.

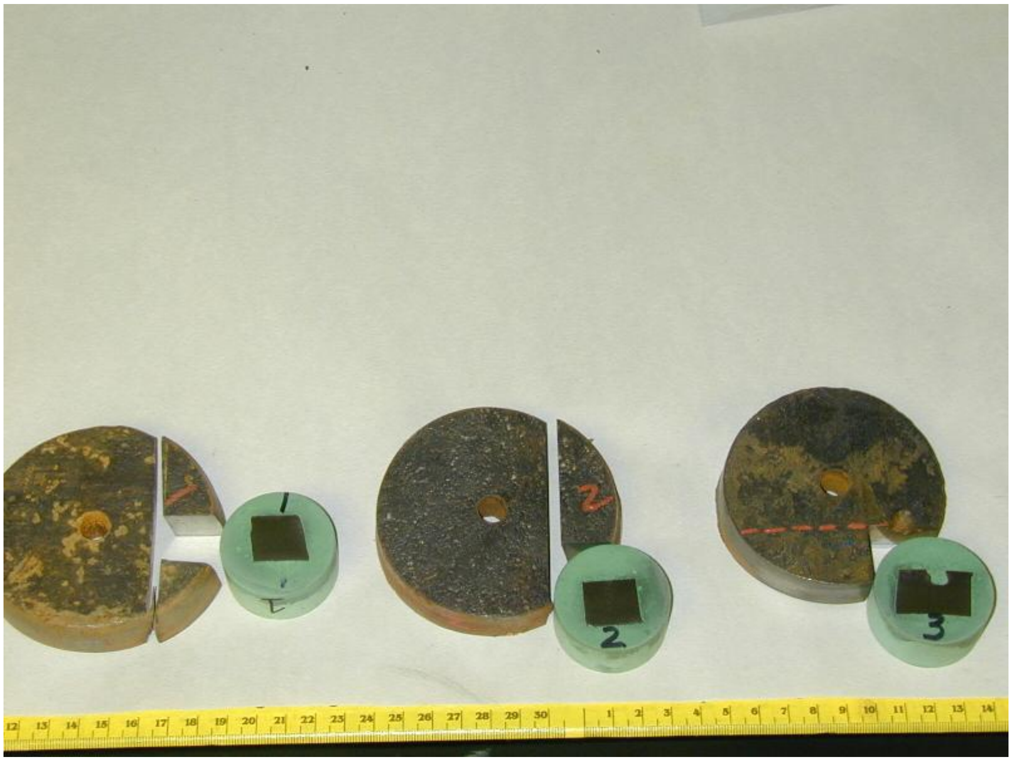

Fig. 23: Overall view of samples #1 – 3 after metallurgically mounting and polishing the cross-sections.

Fig. 24: Overall view of sample #1.

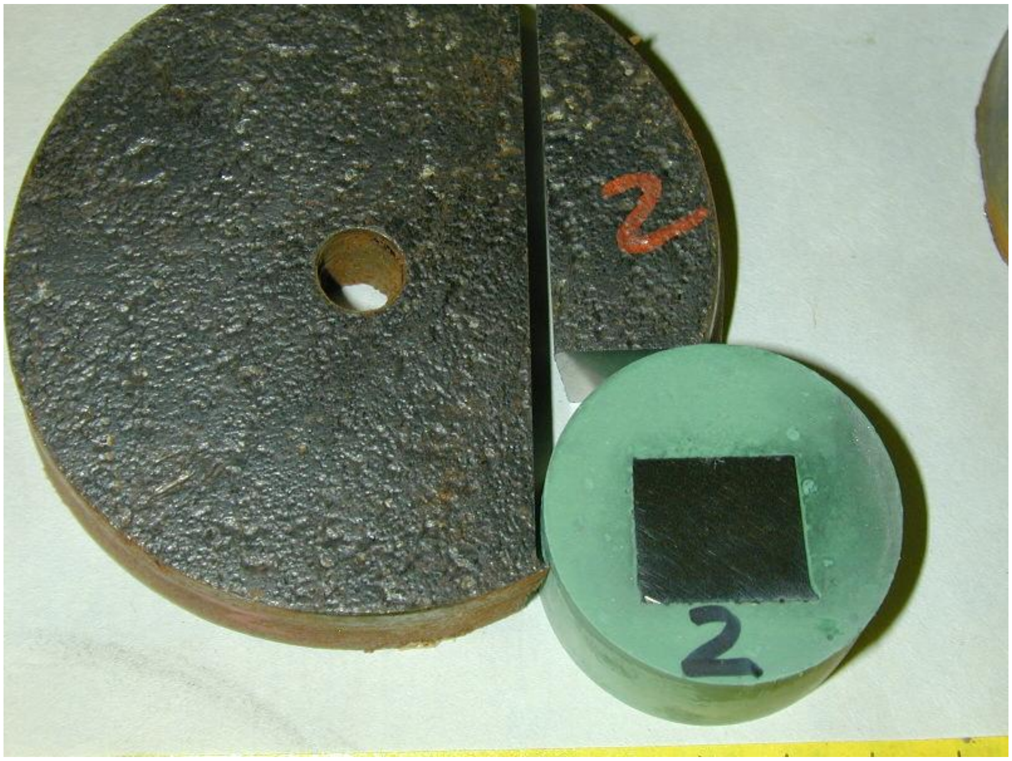

Fig. 25: Overall view of sample #2.

Fig. 26: Overall view of sample #3.

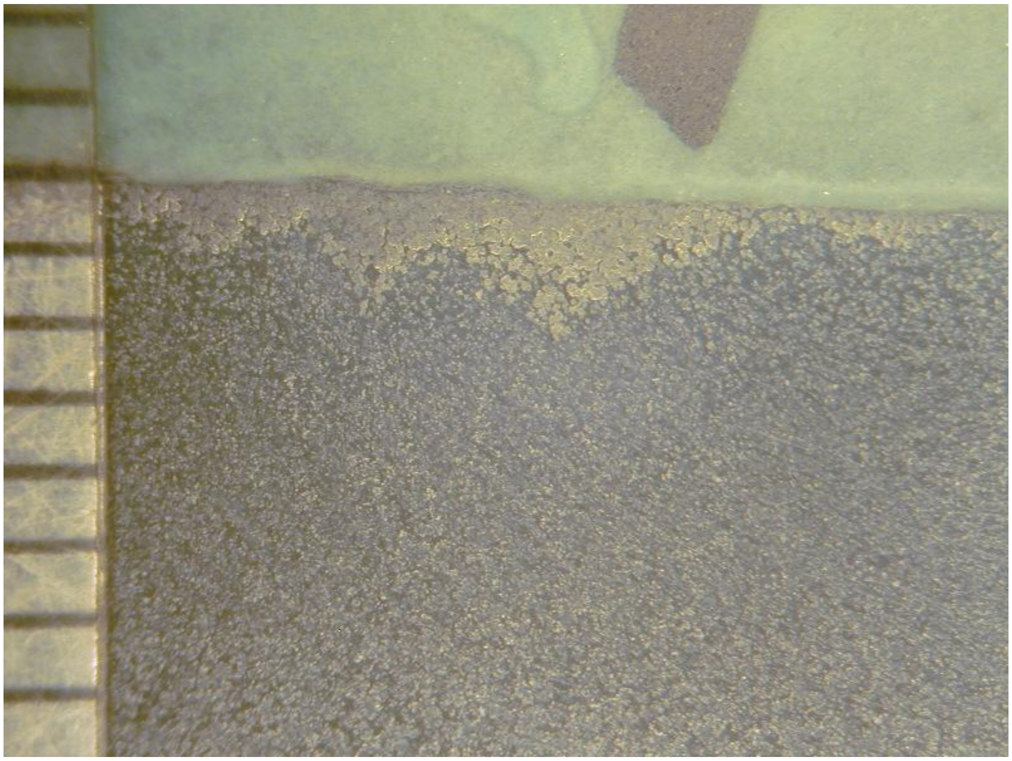

Fig. 27: 7x cross-sectional view of the depth of graphitic corrosion from the OD. Note, the demarcations on the scale are 1mm.

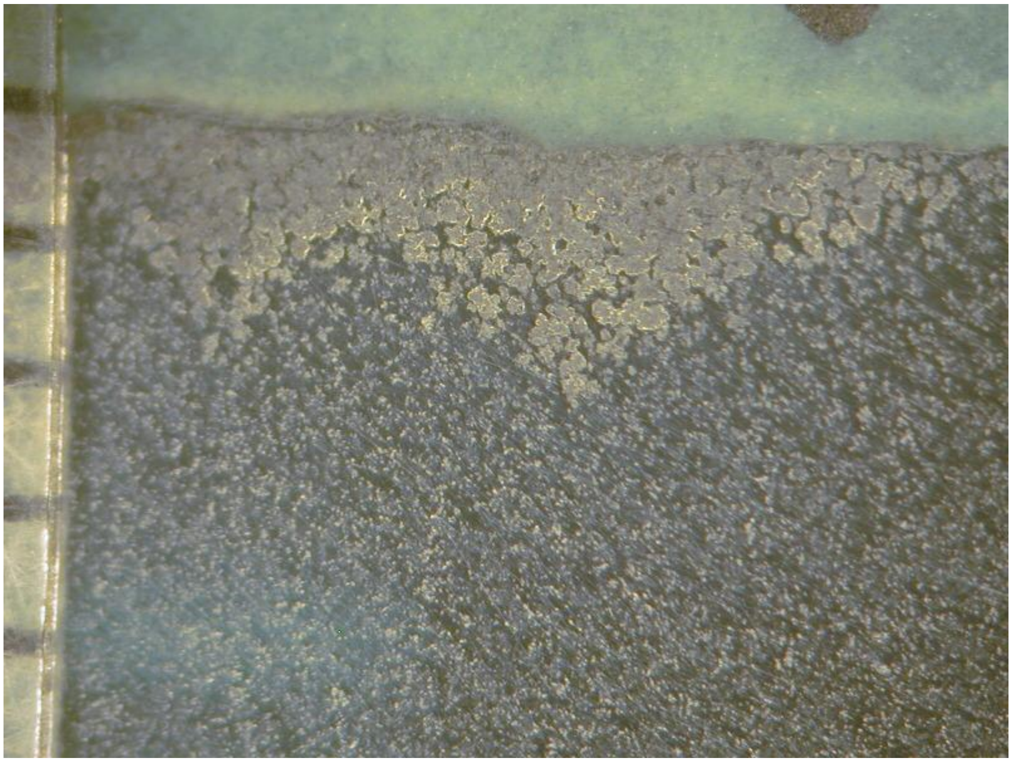

Fig. 28: 15x view of Fig. 27.

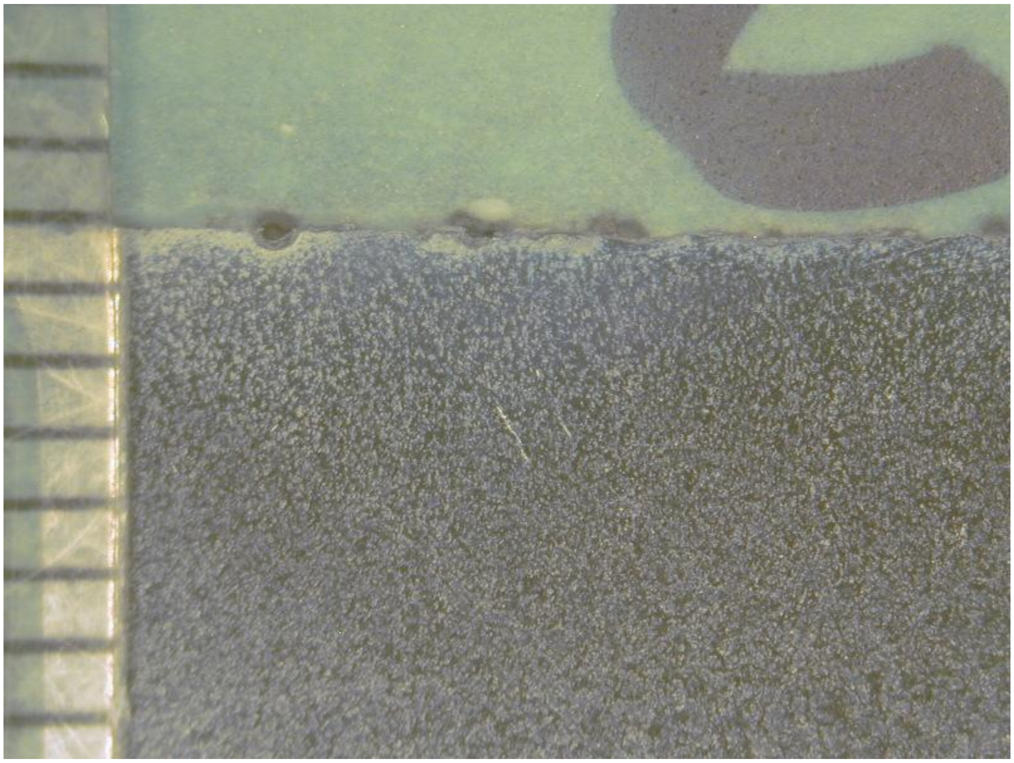

Fig. 29: 7x cross-sectional view of the corrosion at the OD of sample #2.

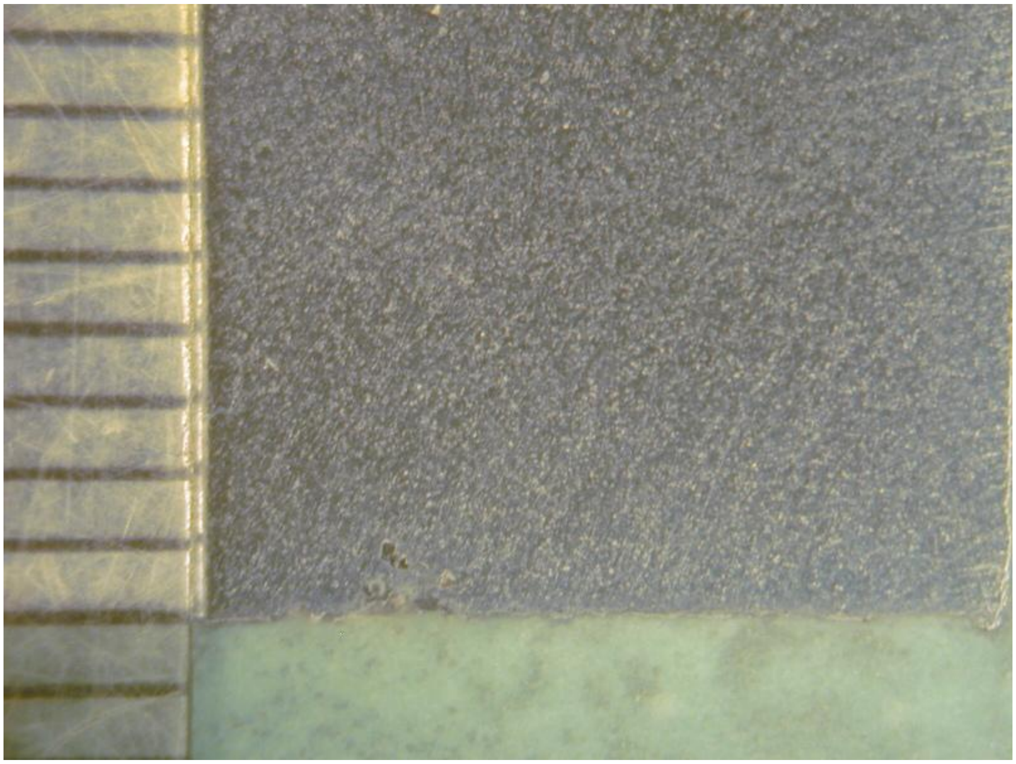

Fig. 30: 7x view of the pitting at the ID of sample #2.

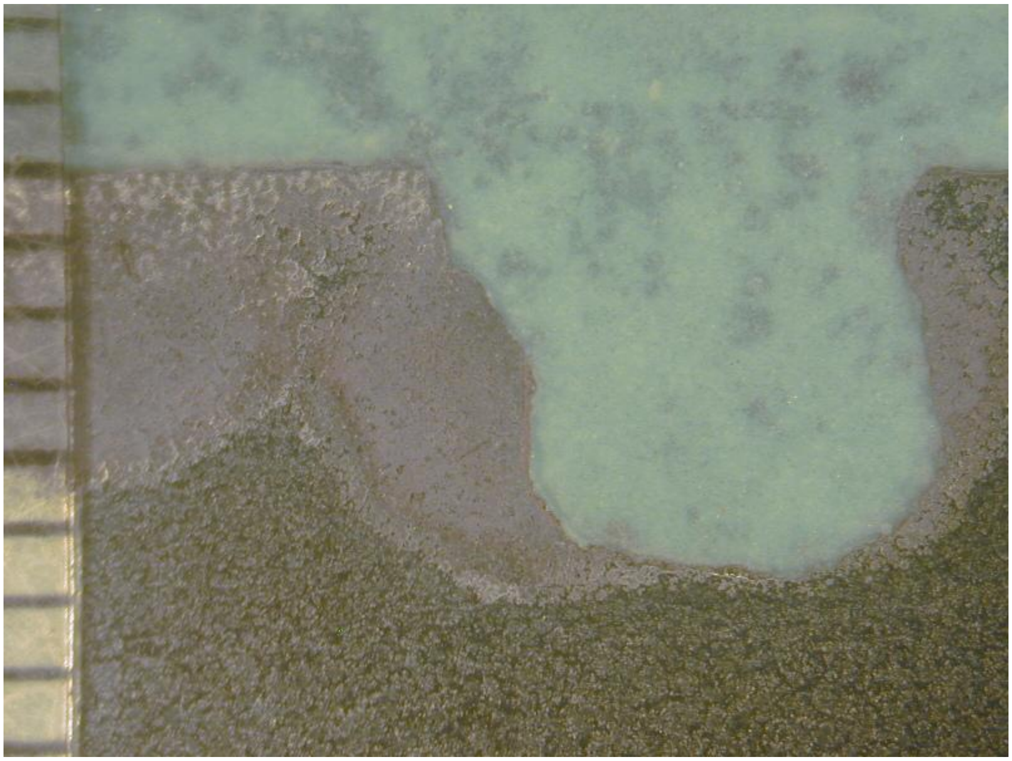

Fig. 31: 7x cross-sectional view of the pit and graphitic corrosion on sample #3.

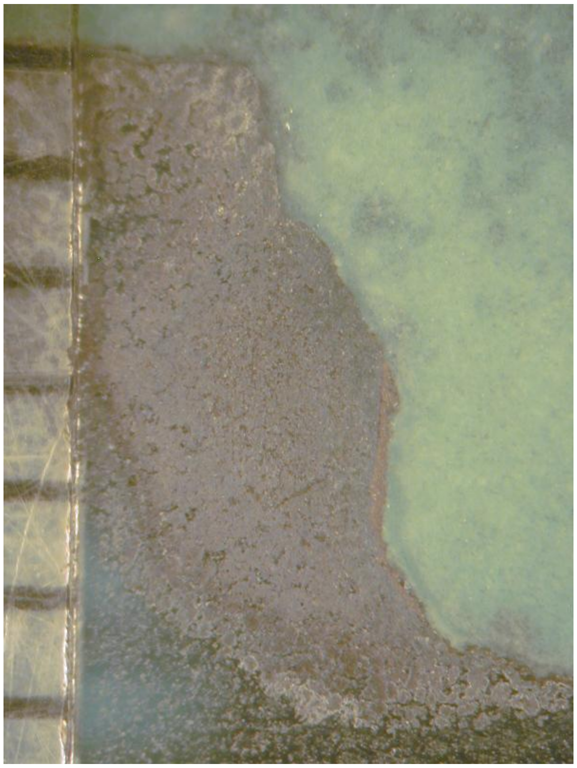

Fig. 32: 15x view of Fig. 31.

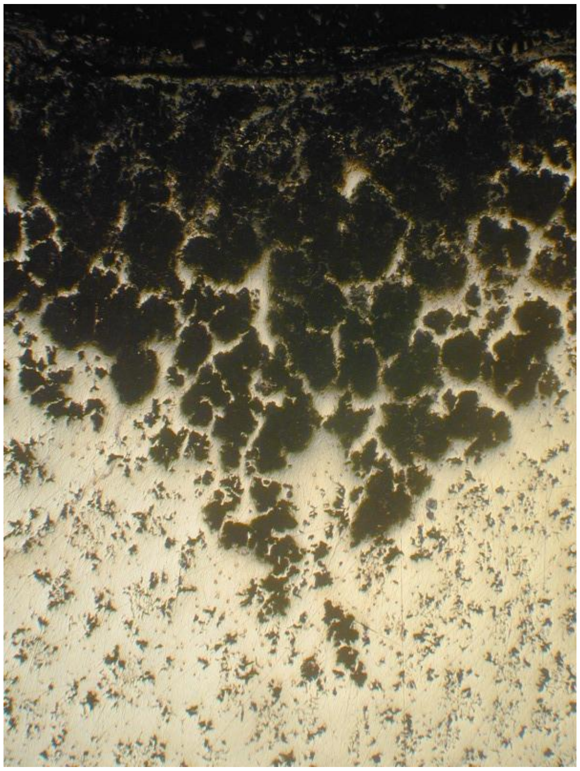

Fig. 33: 50x metallurgical view of the graphitic corrosion on sample #1.

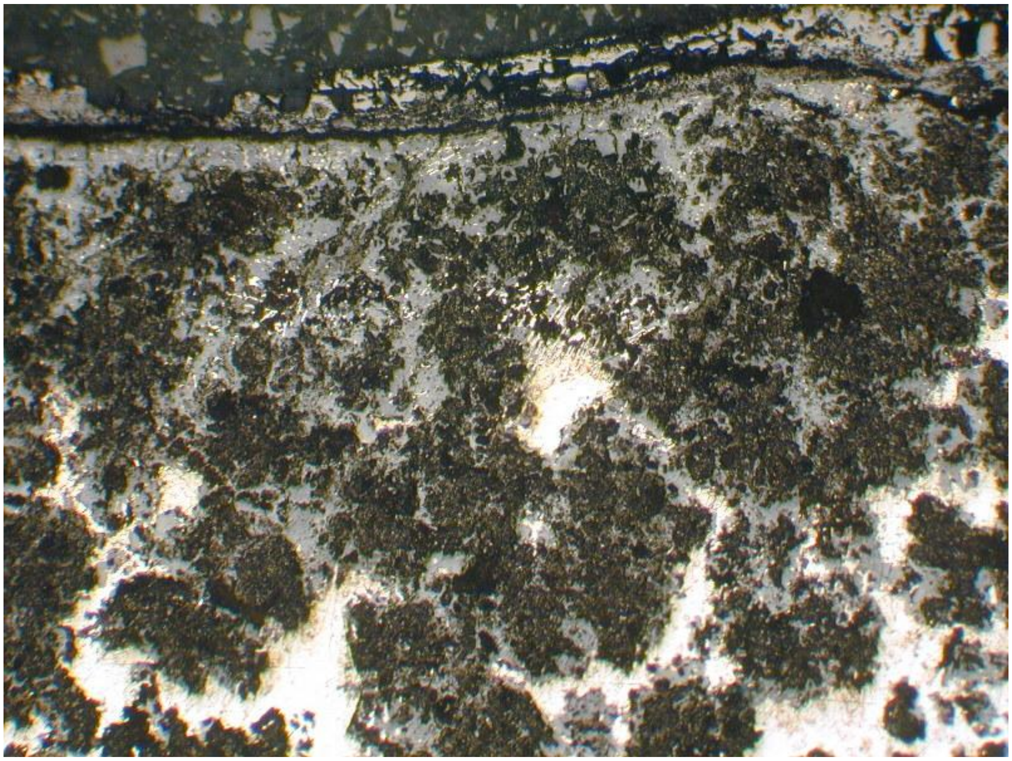

Fig. 34: 100x view of Fig. 33 at the outside edge.

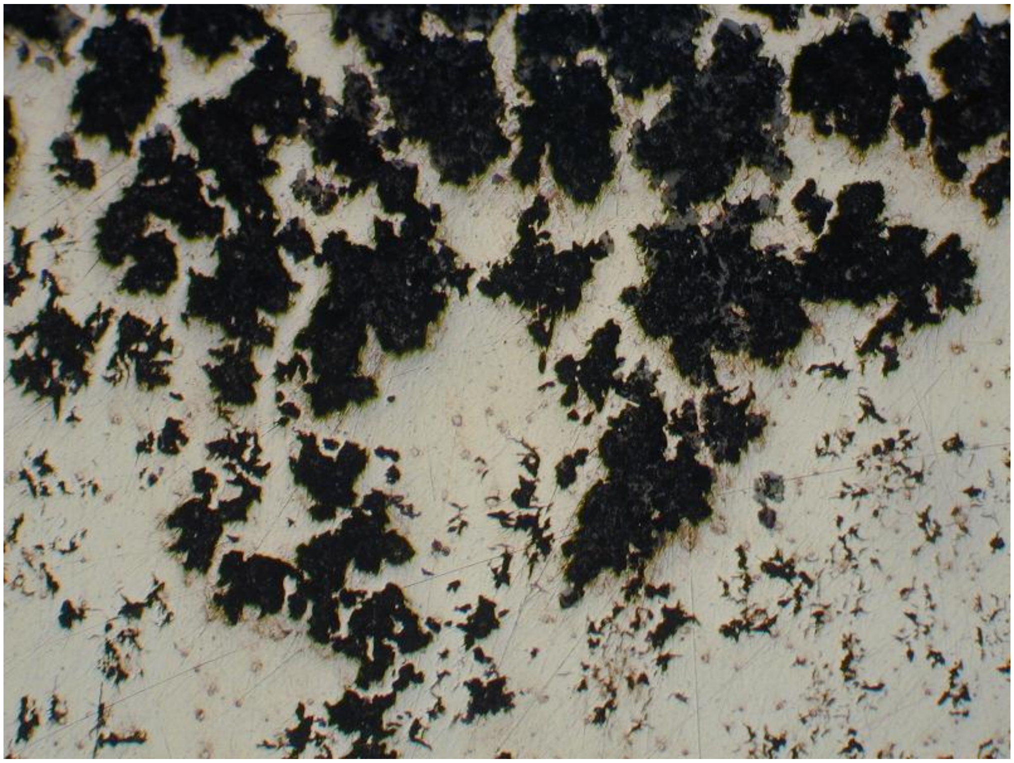

Fig. 35: 100x view of Fig. 33 at the deepest area of corrosion.

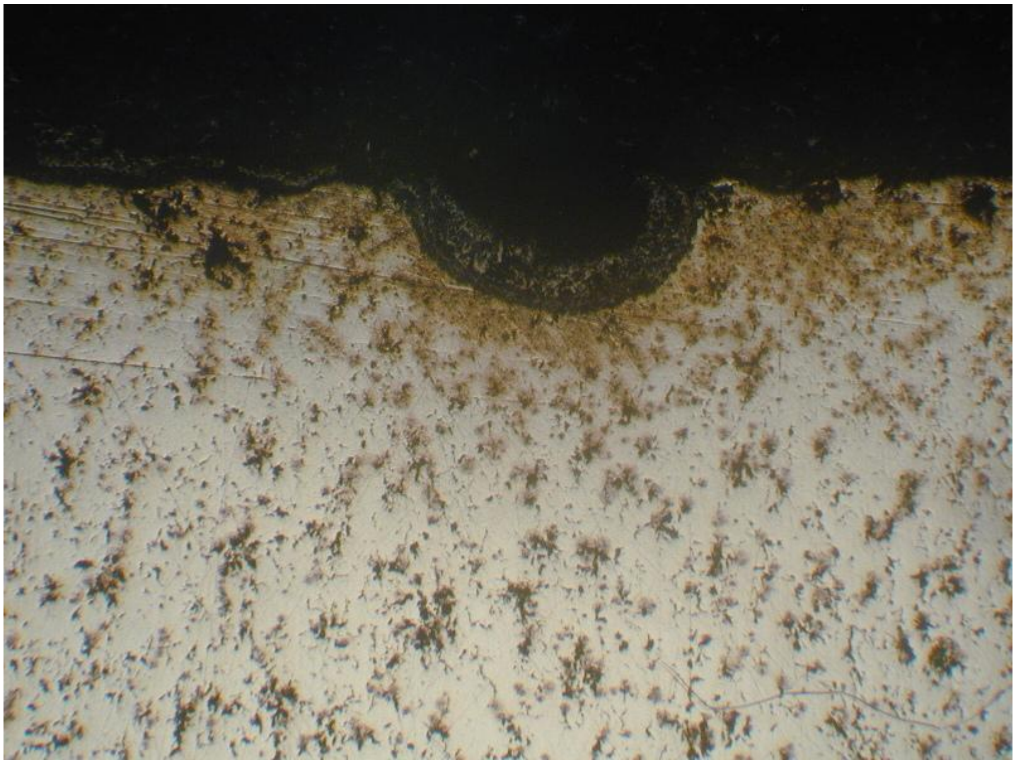

Fig. 36: 50x metallurgical view of the corrosion at the OD.

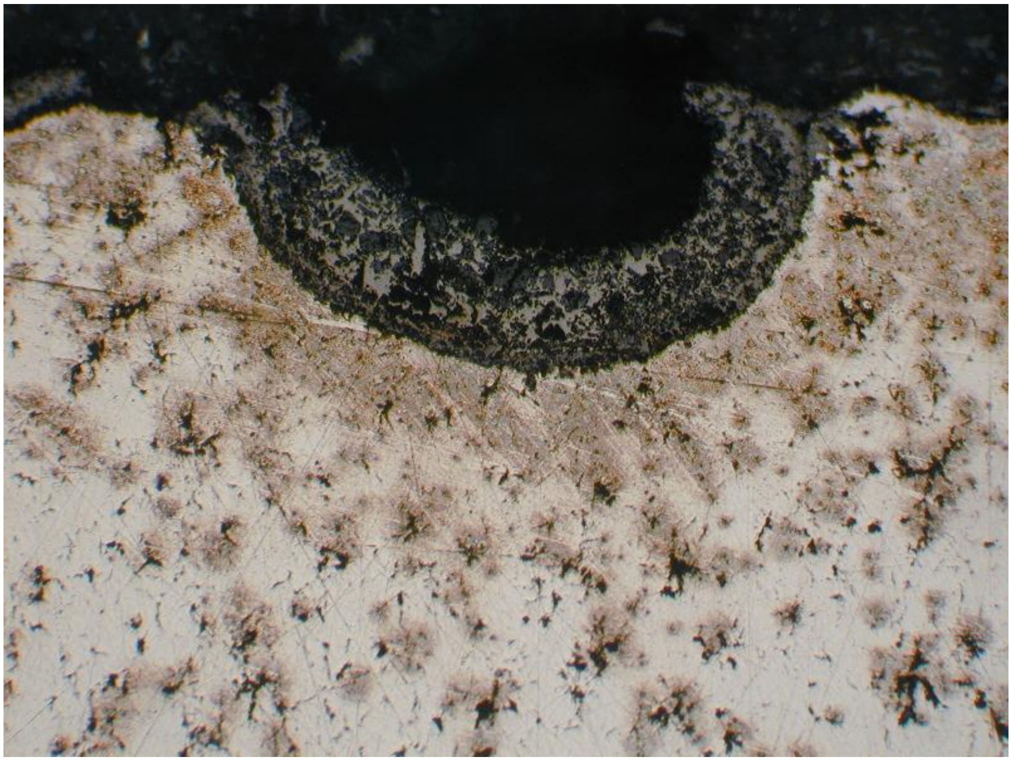

Fig. 37: 100x view of Fig. 36.

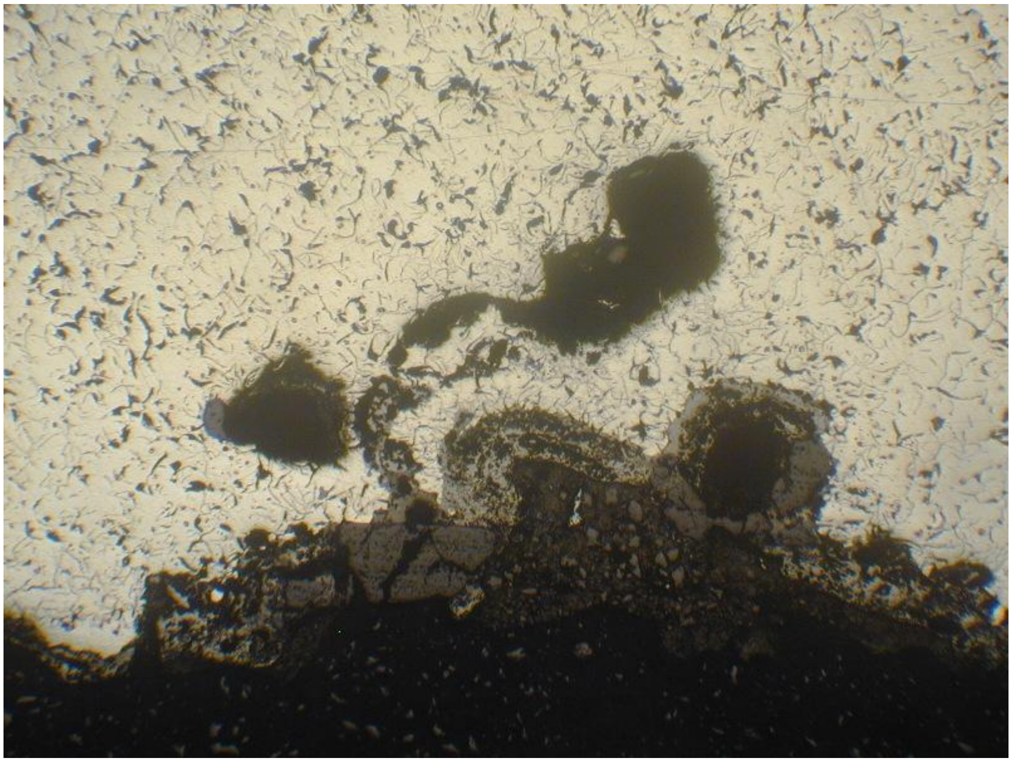

Fig. 38: 50x cross-sectional view of the pitting at the ID.

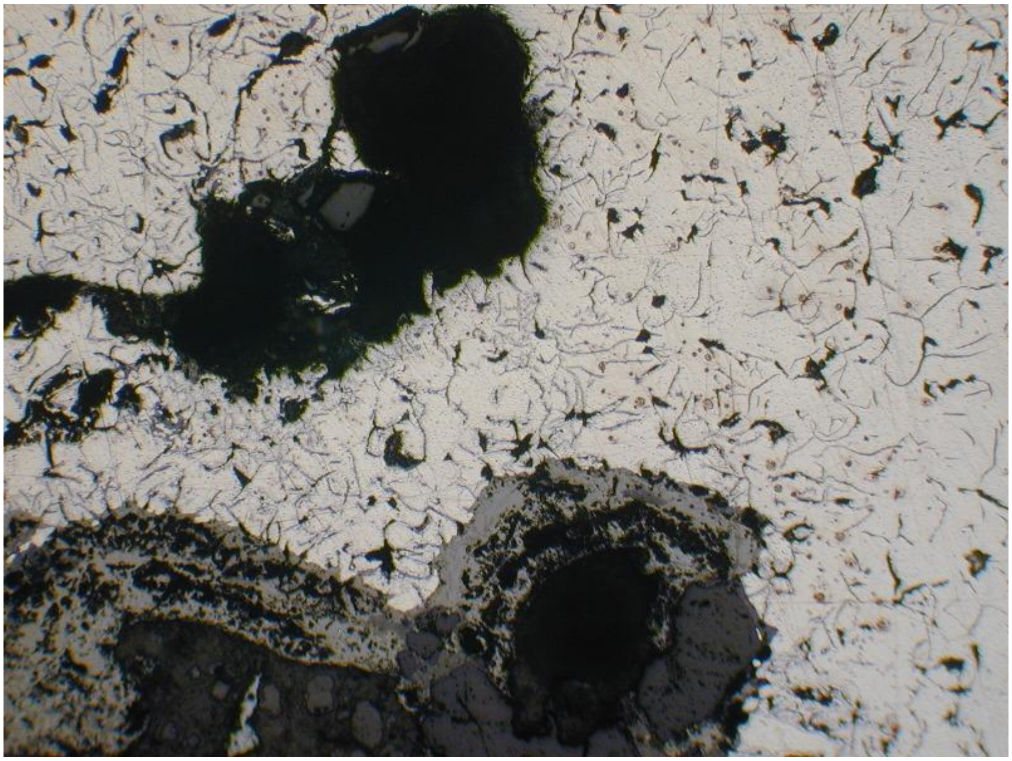

Fig. 39: 100x view of Fig. 38.

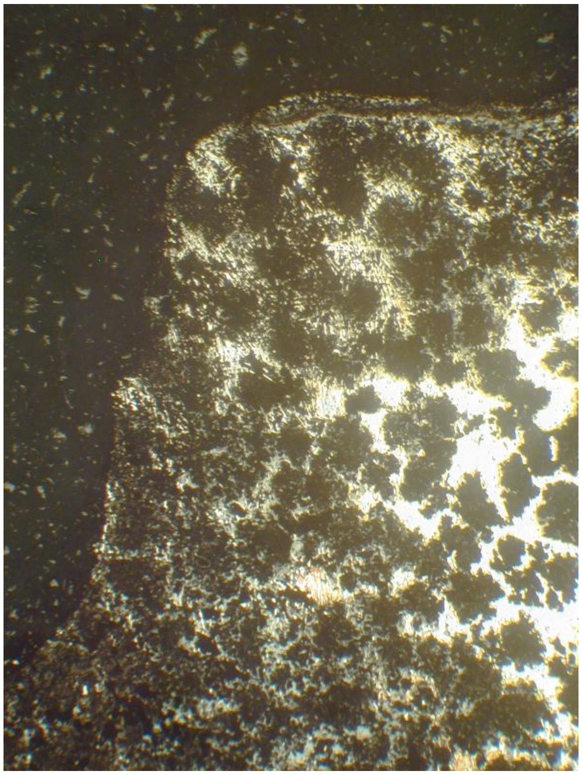

Fig. 40: 50x cross-sectional view at the edge of the pit on sample #3.

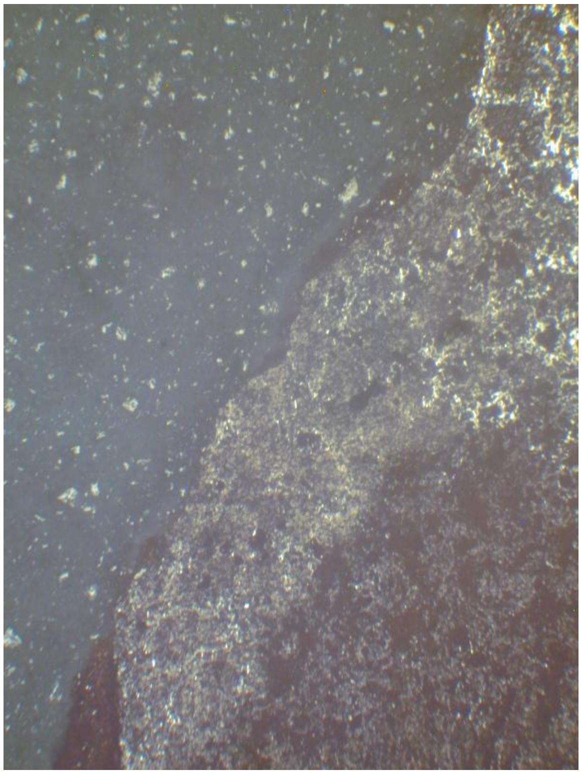

Fig. 41: Same as Fig. 40 except the pit is viewed further down.

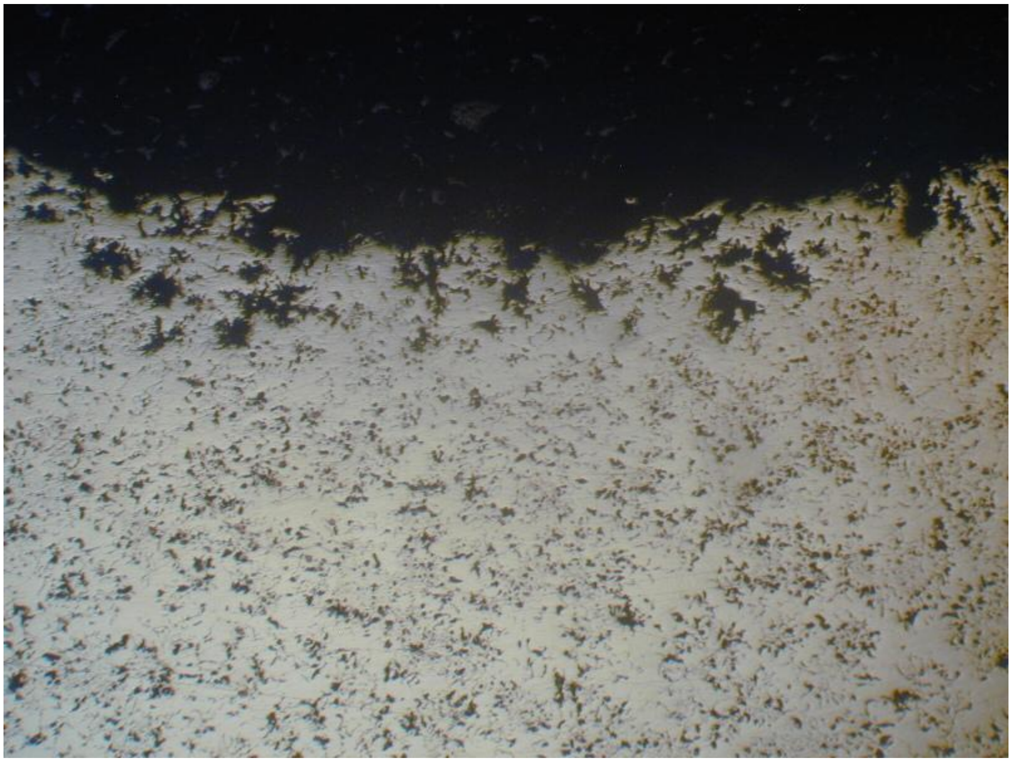

Fig. 42: Same as Fig. 41 except the base of the pit is viewed.

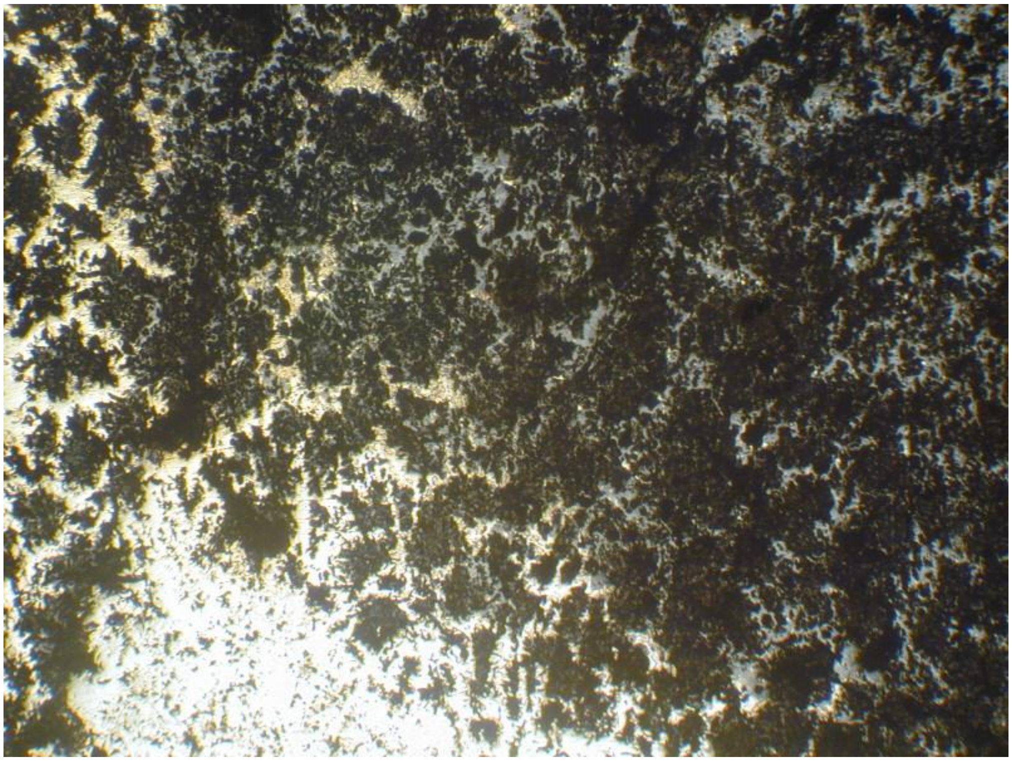

Fig. 43: 50x view of another area of graphitic corrosion.

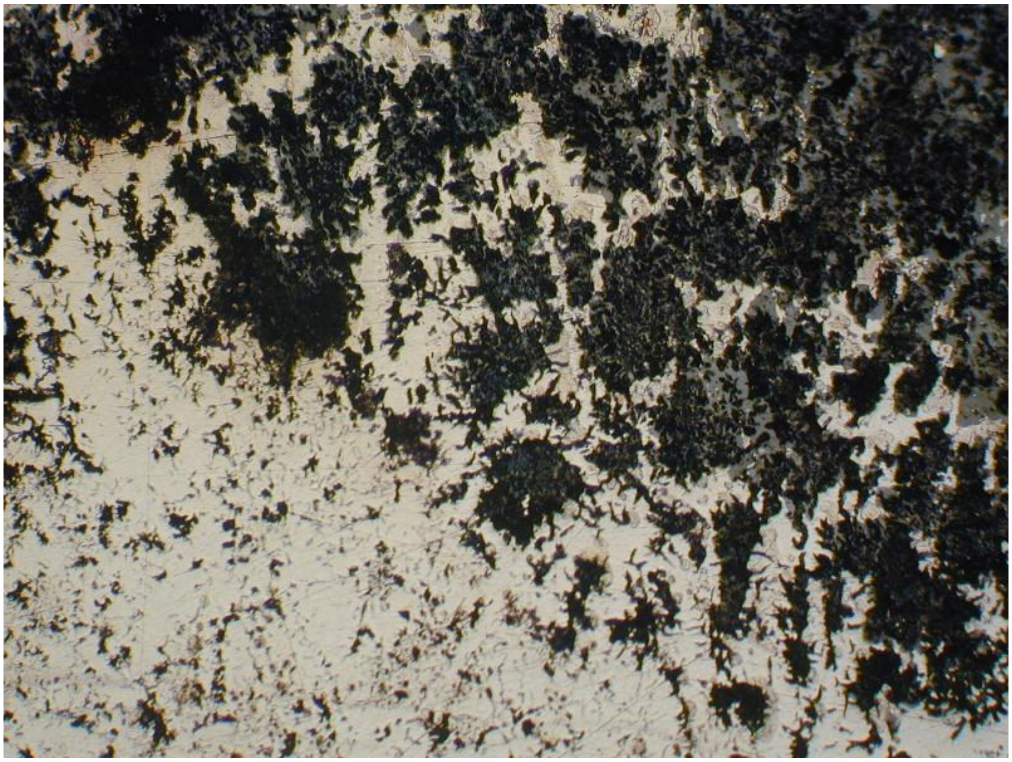

Fig. 44: 100x view of Fig. 43.

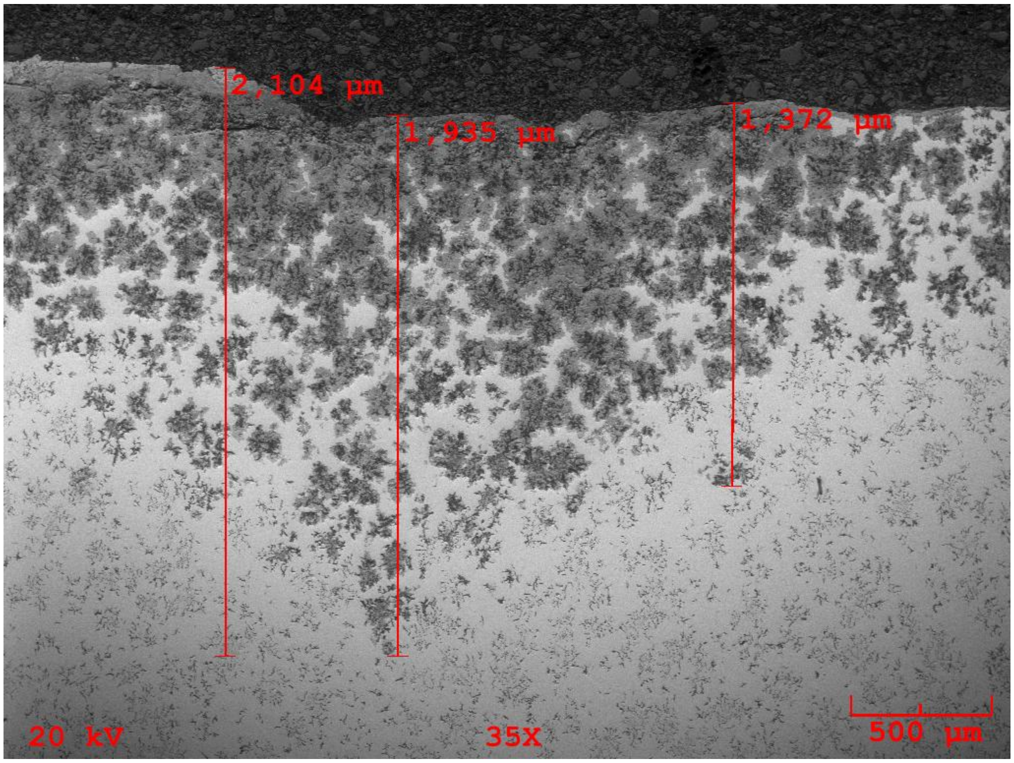

Fig. 45: 35x SEM image of the depth of corrosion on sample #1.

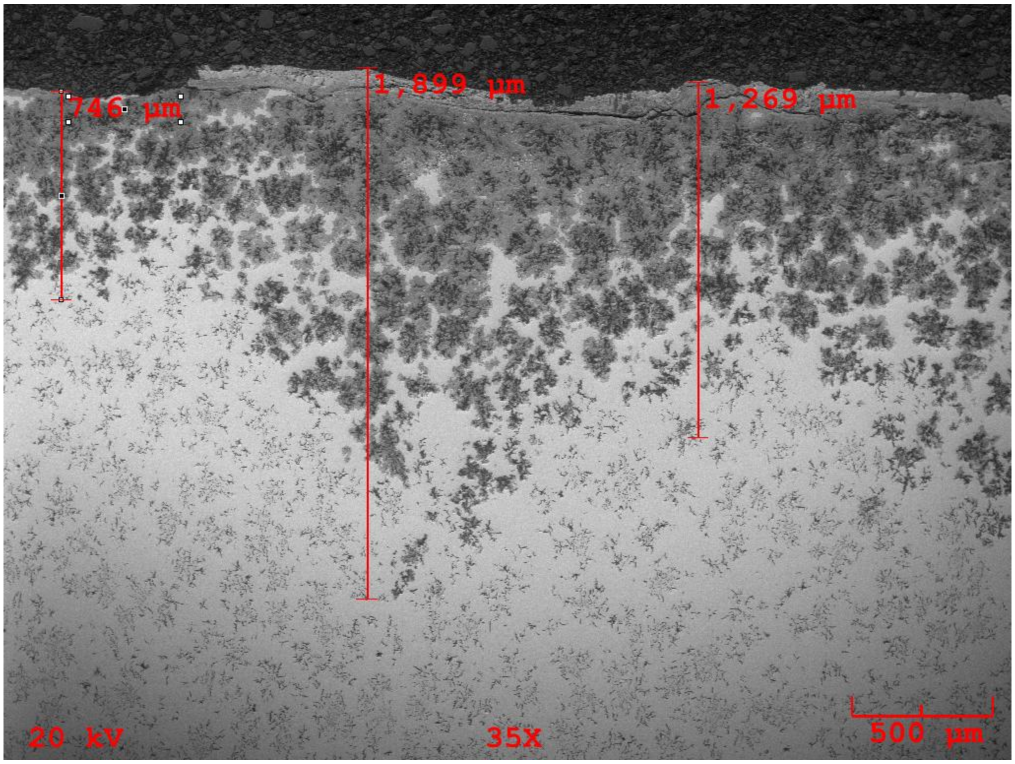

Fig. 46: Same as Fig. 45 except another area is viewed.

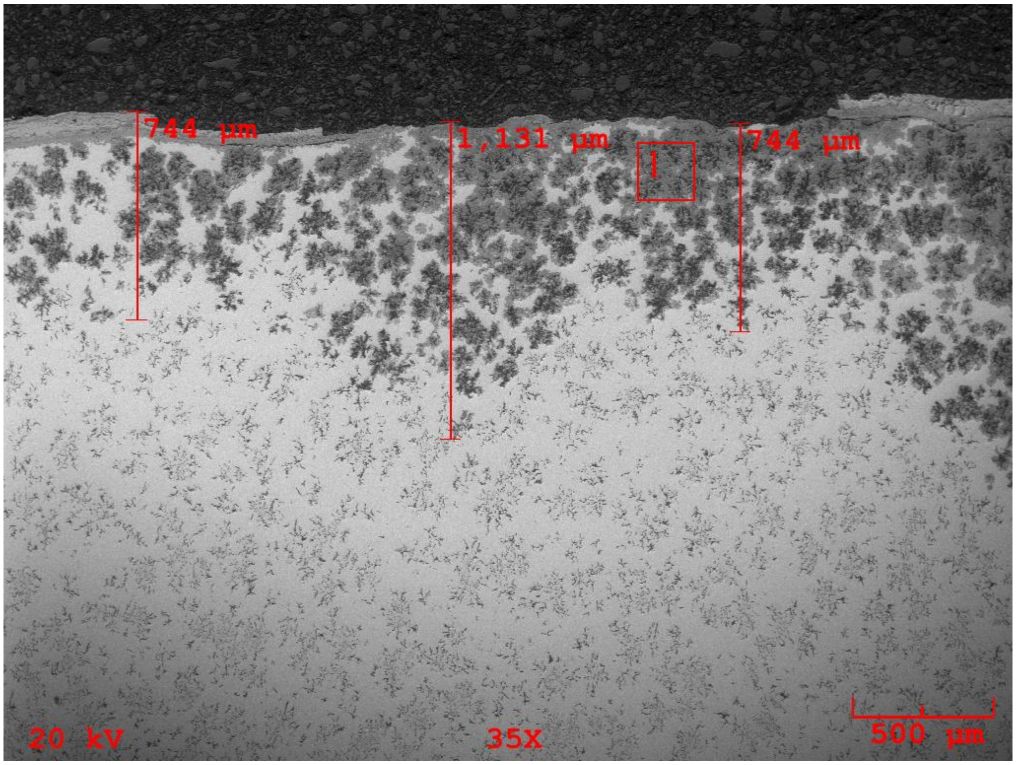

Fig. 47: Same as Fig. 45 except another area is viewed.

Analysis Report: Pipe sample 1-4-1

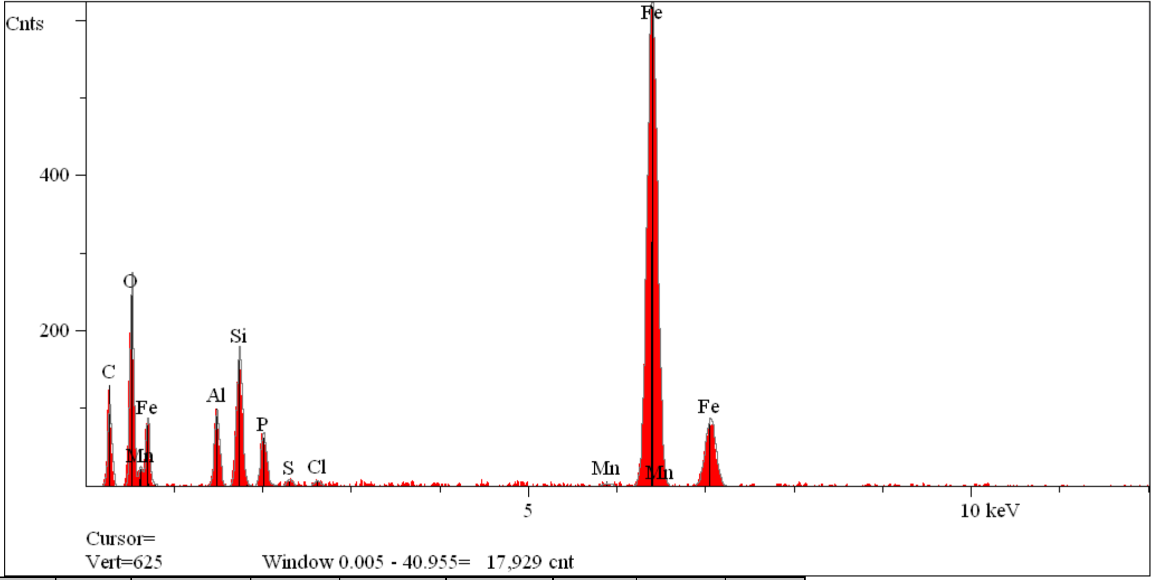

Elt.	Line	Intensity (c/s)	Error 2-sig	Atomic %	Conc	Units	Error 2-sig	
C	Ka	22.09	1.901	34.939	14.267	wt.%	1.227	
O	Ka	48.92	2.632	22.277	12.117	wt.%	0.652	
Al	Ka	24.39	2.089	2.397	2.198	wt.%	0.188	
Si	Ka	48.19	2.811	3.983	3.803	wt.%	0.222	
P	Ka	19.55	2.096	1.447	1.524	wt.%	0.163	
S	Ka	2.83	1.510	0.199	0.217	wt.%	0.116	
Cl	Ka	2.49	1.462	0.161	0.194	wt.%	0.114	
Mn	Ka	2.01	1.317	0.184	0.343	wt.%	0.225	
Fe	Ka	302.49	6.461	34.413	65.336	wt.%	1.396	
				100.000	100.000	wt.%		Total

kV 17.3
Takeoff Angle 45.0°
Elapsed Livetime 30.0

Fig. 48: EDS of area 1 marked in Fig. 47.

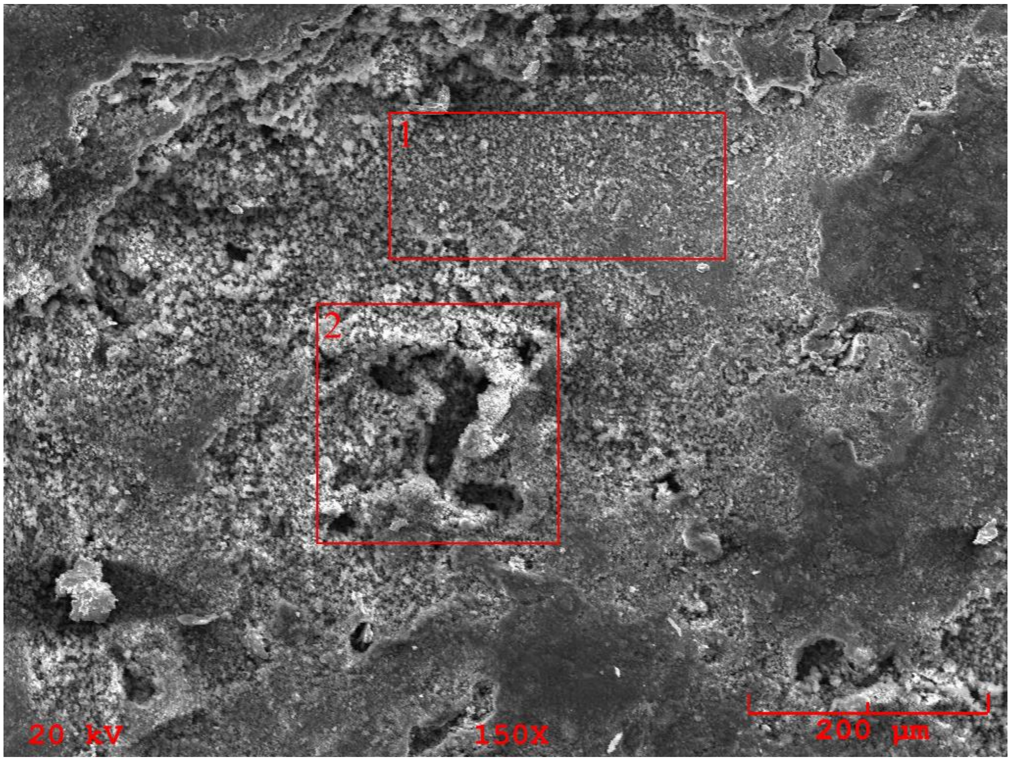

Fig. 49: 150x SEM image of corrosion scale on the OD of sample #1.

Analysis Report: Pipe sample 1 OD scale-1-1

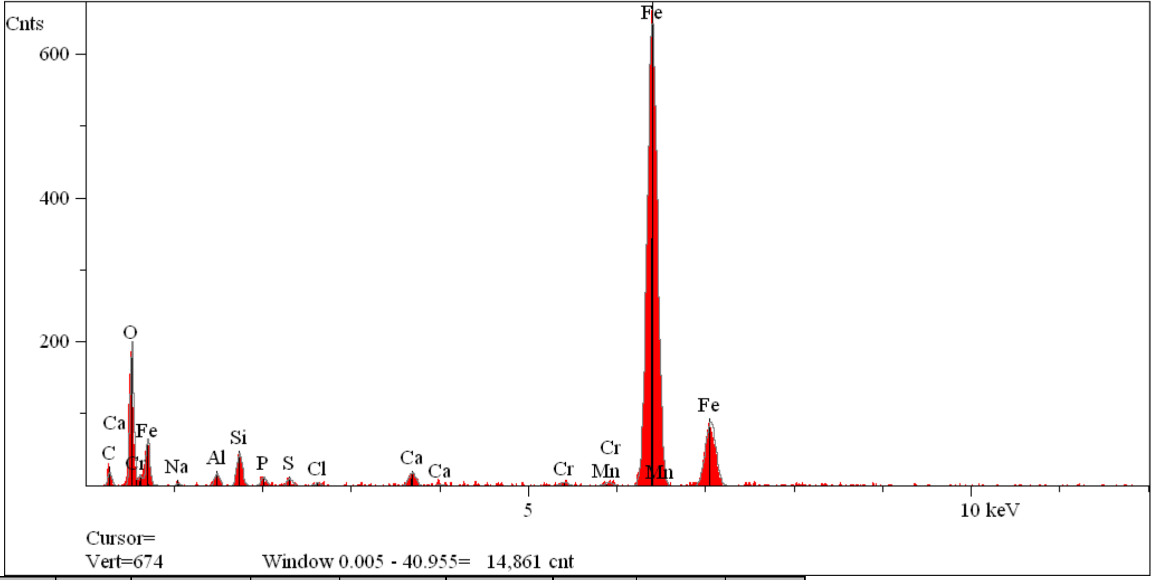

Elt.	Line	Intensity (c/s)	Error 2-sig	Atomic %	Conc	Units	Error 2-sig	
C	Ka	4.11	0.946	11.649	3.527	wt.%	0.812	
O	Ka	35.63	2.216	24.611	9.927	wt.%	0.617	
Na	Ka	0.98	0.709	0.409	0.237	wt.%	0.172	
Al	Ka	4.39	1.203	0.834	0.567	wt.%	0.155	
Si	Ka	12.30	1.658	1.894	1.341	wt.%	0.181	
P	Ka	3.55	1.354	0.472	0.368	wt.%	0.140	
S	Ka	3.13	1.389	0.388	0.314	wt.%	0.139	
Cl	Ka	1.44	1.361	0.162	0.144	wt.%	0.137	
Ca	Ka	6.90	1.587	0.724	0.732	wt.%	0.168	
Cr	Ka	2.45	1.319	0.215	0.282	wt.%	0.152	
Mn	Ka	2.16	1.263	0.327	0.453	wt.%	0.264	
Fe	Ka	304.88	6.514	58.316	82.106	wt.%	1.754	
				100.000	100.000	wt.%		Total

kV 17.7
Takeoff Angle 45.0°
Elapsed Livetime 30.0

Fig. 50: EDS of area 1 marked in Fig. 45.

Analysis Report: Pipe sample 1 OD scale-1-2

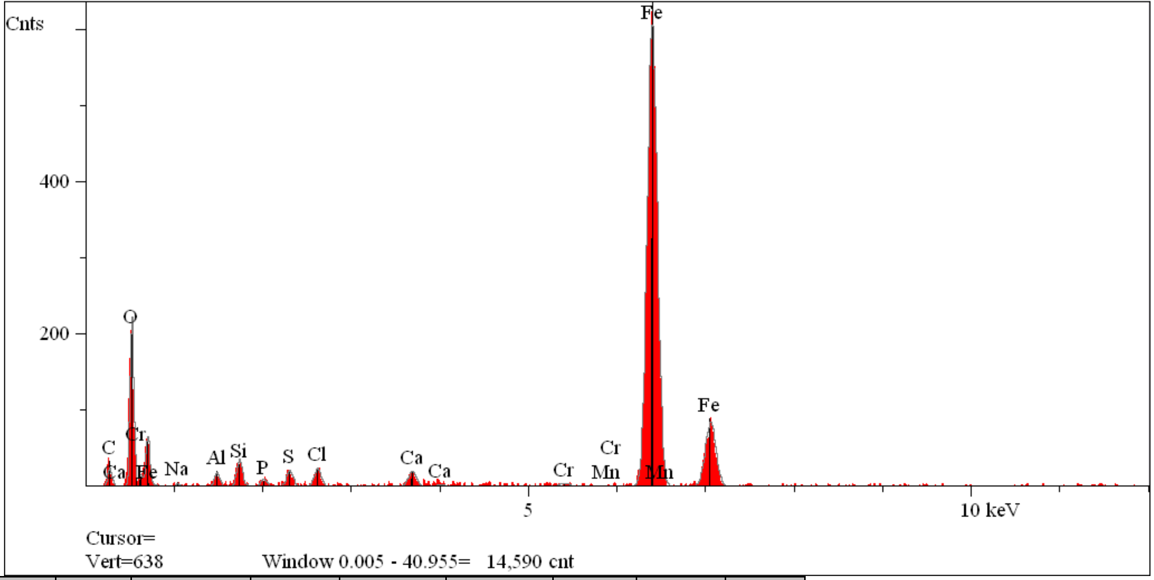

Elt.	**Line**	**Intensity (c/s)**	**Error 2-sig**	**Atomic %**	**Conc**	**Units**	**Error 2-sig**	
C	Ka	5.22	1.039	14.389	4.605	wt.%	0.916	
O	Ka	39.62	2.348	27.030	11.523	wt.%	0.683	
Na	Ka	0.55	0.662	0.221	0.135	wt.%	0.161	
Al	Ka	4.44	1.134	0.804	0.578	wt.%	0.148	
Si	Ka	9.51	1.465	1.398	1.046	wt.%	0.161	
P	Ka	2.75	1.197	0.348	0.287	wt.%	0.125	
S	Ka	6.19	1.457	0.735	0.628	wt.%	0.148	
Cl	Ka	7.37	1.624	0.800	0.755	wt.%	0.166	
Ca	Ka	7.19	1.534	0.732	0.782	wt.%	0.167	
Cr	Ka	1.71	1.257	0.147	0.204	wt.%	0.150	
Mn	Ka	0.26	1.154	0.039	0.056	wt.%	0.248	
Fe	Ka	287.54	6.327	53.358	79.399	wt.%	1.747	
				100.000	100.000	wt.%		Total

kV 17.6
Takeoff Angle 45.0°
Elapsed Livetime 30.0

Fig. 51: EDS of area 2 marked in Fig. 45.

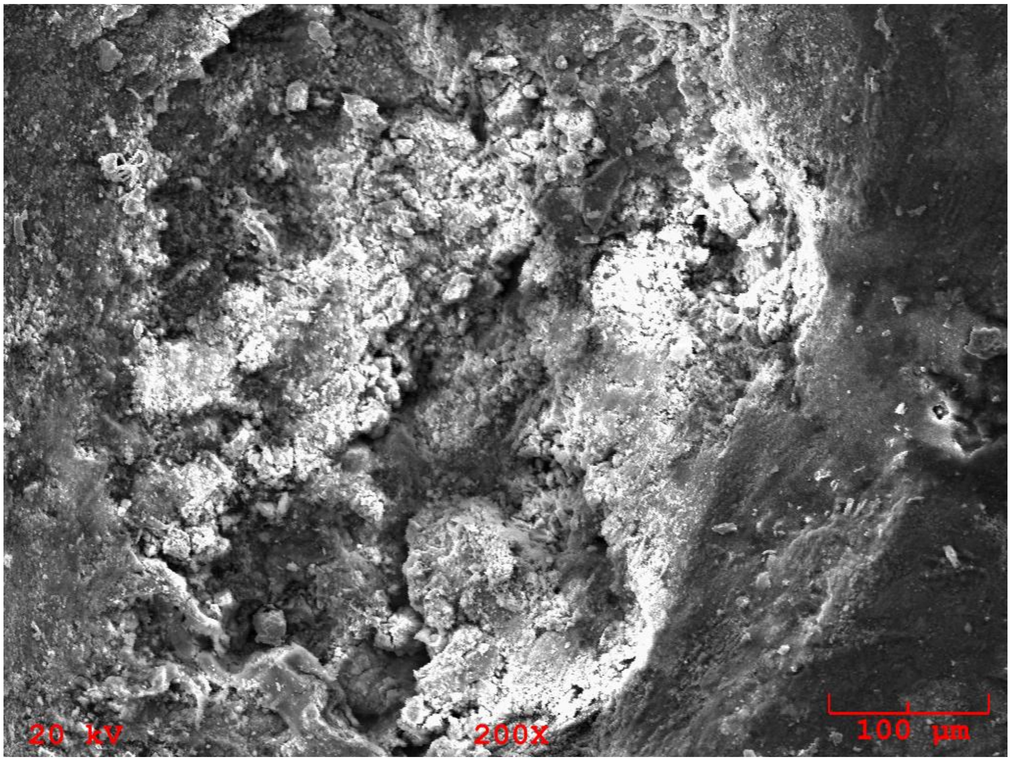

Fig. 52: 200x SEM image of area on sample #1.

Analysis Report: Pipe sample 1 OD scale-4-1

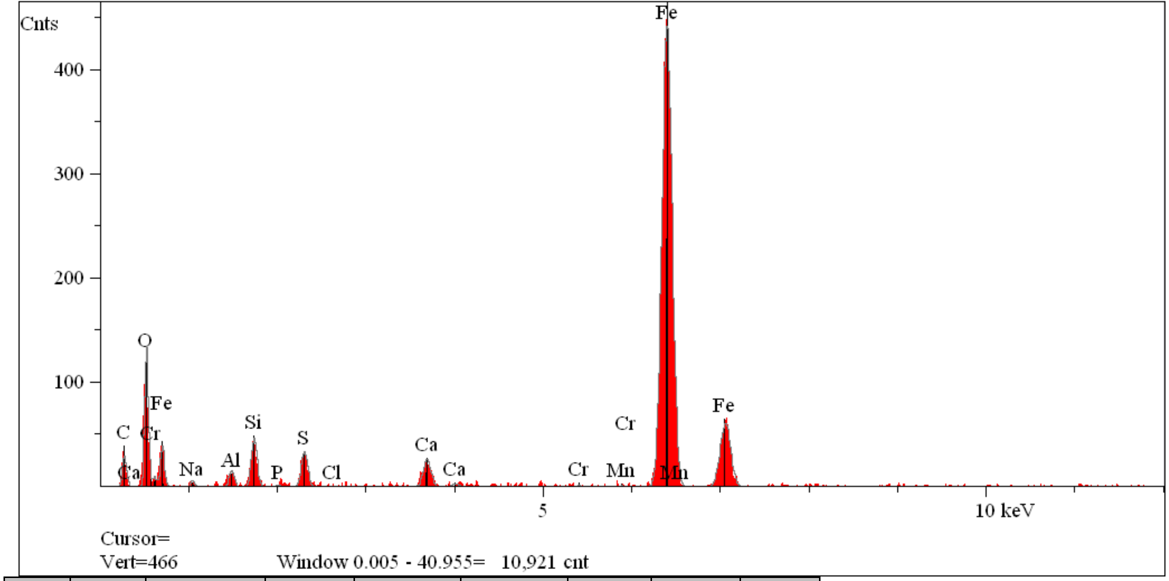

Elt.	**Line**	**Intensity (c/s)**	**Error 2-sig**	**Atomic %**	**Conc**	**Units**	**Error 2-sig**	
C	Ka	6.26	1.058	19.697	6.305	wt.%	1.066	
O	Ka	23.60	1.833	20.174	8.602	wt.%	0.668	
Na	Ka	1.18	0.644	0.550	0.337	wt.%	0.184	
Al	Ka	3.84	1.040	0.843	0.606	wt.%	0.164	
Si	Ka	12.61	1.541	2.282	1.708	wt.%	0.209	
P	Ka	0.59	0.937	0.093	0.077	wt.%	0.123	
S	Ka	10.19	1.490	1.530	1.308	wt.%	0.191	
Cl	Ka	0.07	1.025	0.010	0.010	wt.%	0.134	
Ca	Ka	9.40	1.523	1.257	1.343	wt.%	0.218	
Cr	Ka	0.66	1.028	0.079	0.109	wt.%	0.170	
Mn	Ka	0.68	1.063	0.136	0.199	wt.%	0.313	
Fe	Ka	209.26	5.401	53.348	79.396	wt.%	2.049	
				100.000	100.000	wt.%		Total

kV 16.7
Takeoff Angle 45.0°
Elapsed Livetime 30.0

Fig. 53: EDS of the area viewed in Fig. 52.

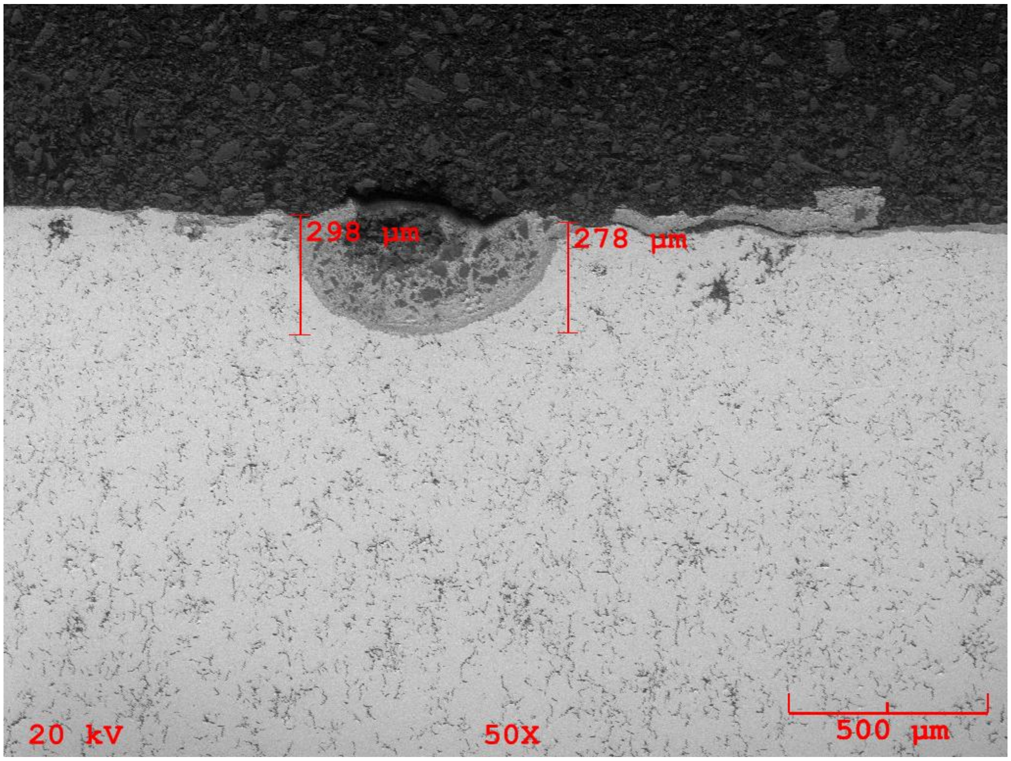

Fig. 54: 50x SEM cross-sectional view of sample #2 at the OD.

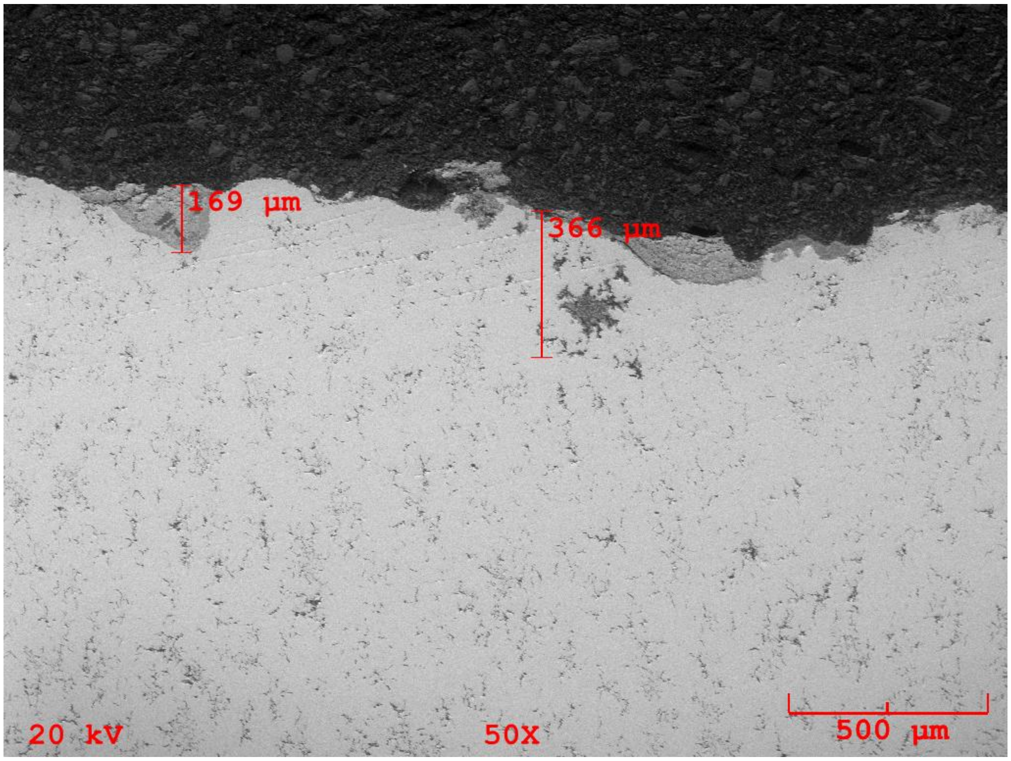

Fig. 55: Same as Fig. 54 except another area is viewed.

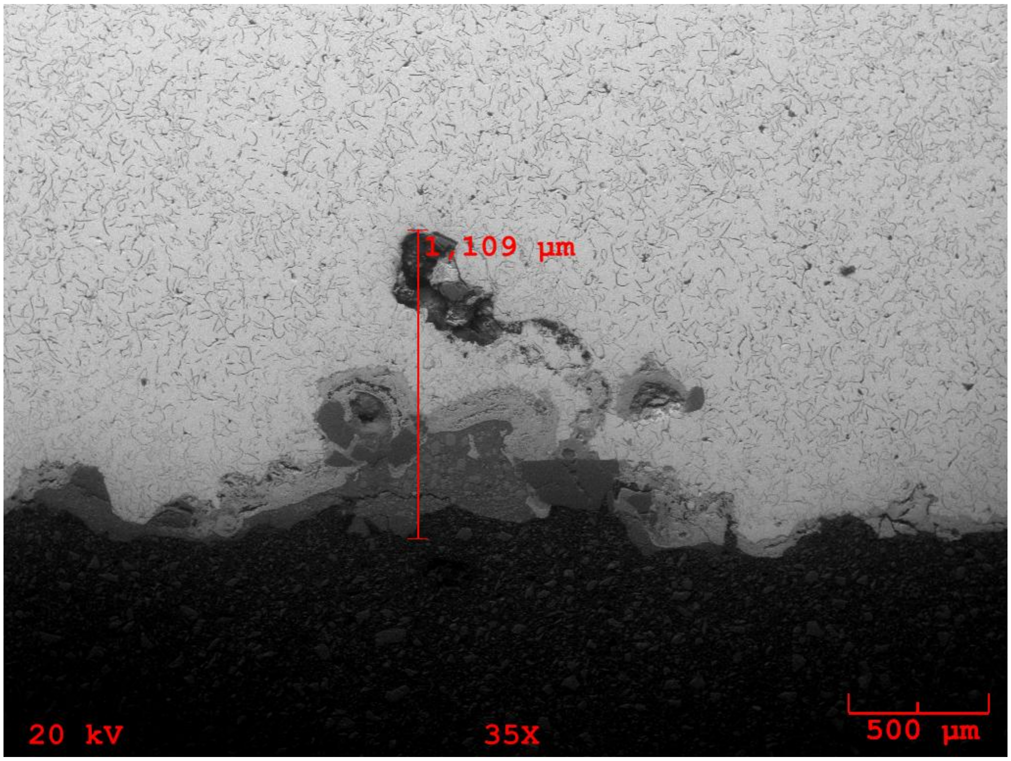

Fig. 56: 35x SEM cross-section of the pitting at the ID of sample #2.

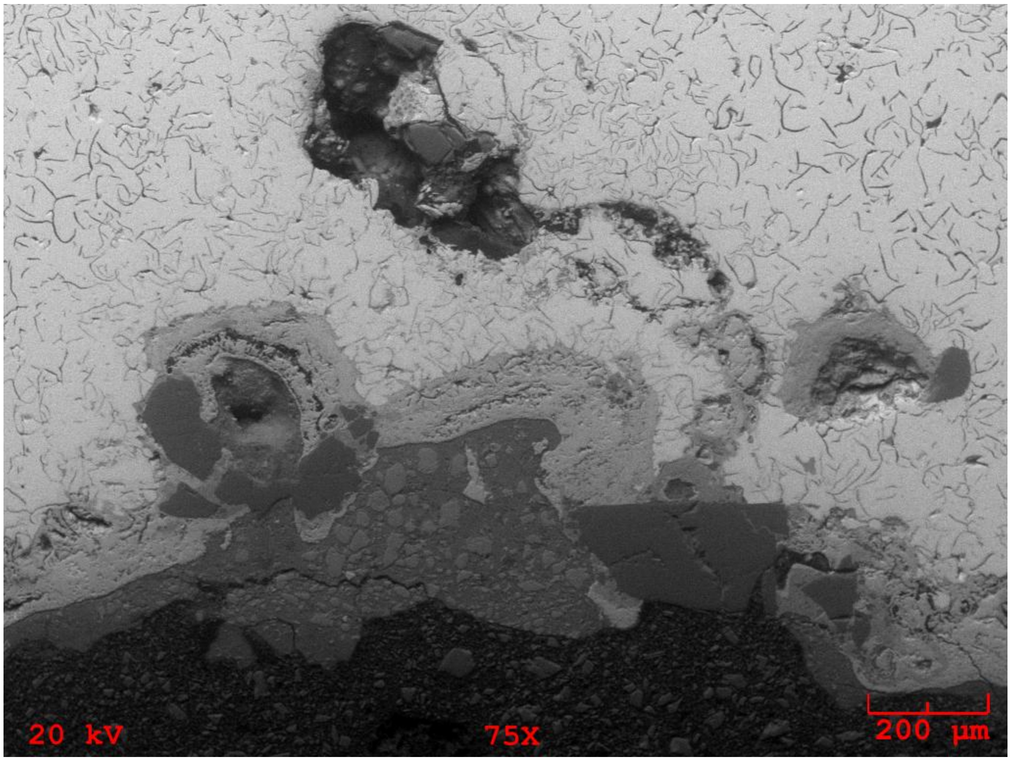

Fig. 57: 75x view of Fig. 56.

Analysis Report: Pipe sample 2 ID-2-1

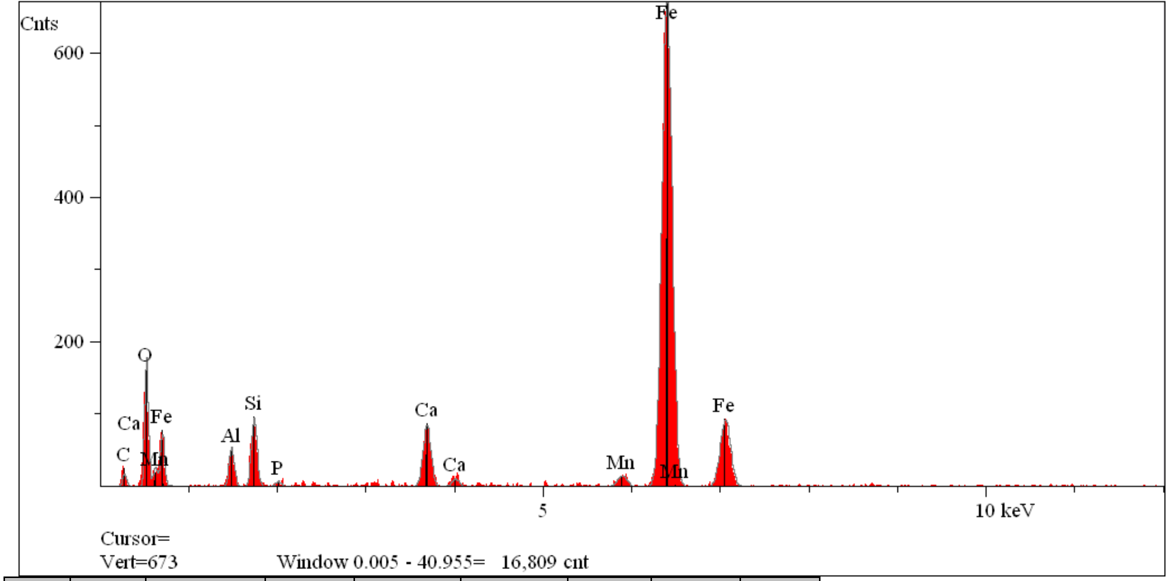

Elt.	Line	Intensity (c/s)	Error 2-sig	Atomic %	Conc	Units	Error 2-sig	
C	Ka	3.82	0.999	10.217	3.047	wt.%	0.797	
O	Ka	31.81	2.123	22.172	8.808	wt.%	0.588	
Al	Ka	13.46	1.630	2.359	1.580	wt.%	0.191	
Si	Ka	25.32	2.131	3.639	2.538	wt.%	0.214	
P	Ka	2.12	1.236	0.265	0.204	wt.%	0.119	
Ca	Ka	31.07	2.404	3.112	3.097	wt.%	0.240	
Mn	Ka	6.80	1.497	0.996	1.359	wt.%	0.299	
Fe	Ka	318.33	6.648	57.239	79.368	wt.%	1.658	
				100.000	100.000	wt.%		Total

kV 17.6
Takeoff Angle 45.0°
Elapsed Livetime 30.0

Fig. 58: EDS of one area of corrosion by products in Fig. 57.

Analysis Report: Pipe sample 2 ID-2-2

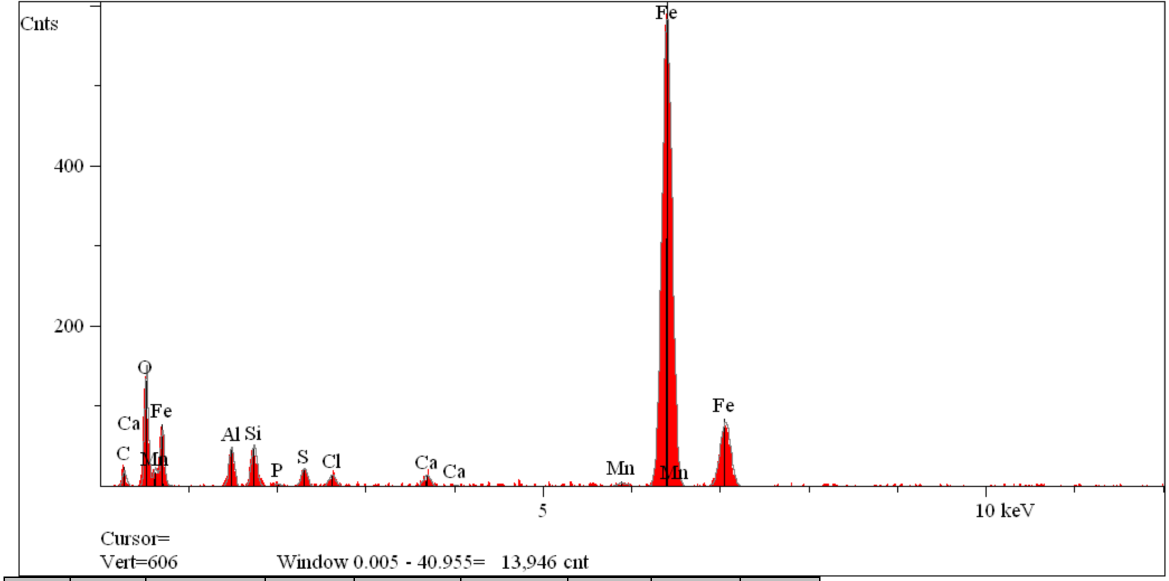

Elt.	Line	Intensity (c/s)	Error 2-sig	Atomic %	Conc	Units	Error 2-sig	
C	Ka	4.09	0.920	13.084	3.924	wt.%	0.884	
O	Ka	26.77	1.945	20.567	8.217	wt.%	0.597	
Al	Ka	12.46	1.490	2.555	1.722	wt.%	0.206	
Si	Ka	14.09	1.628	2.372	1.664	wt.%	0.192	
P	Ka	1.04	1.114	0.152	0.117	wt.%	0.126	
S	Ka	6.83	1.468	0.928	0.743	wt.%	0.160	
Cl	Ka	4.75	1.473	0.589	0.522	wt.%	0.162	
Ca	Ka	5.03	1.434	0.585	0.586	wt.%	0.167	
Mn	Ka	2.21	1.200	0.372	0.510	wt.%	0.277	
Fe	Ka	276.78	6.198	58.796	81.995	wt.%	1.836	
				100.000	100.000	wt.%		Total

kV 17.5
Takeoff Angle 45.0°
Elapsed Livetime 30.0

Fig. 59: Same as Fig. 58 except another location was analyzed.

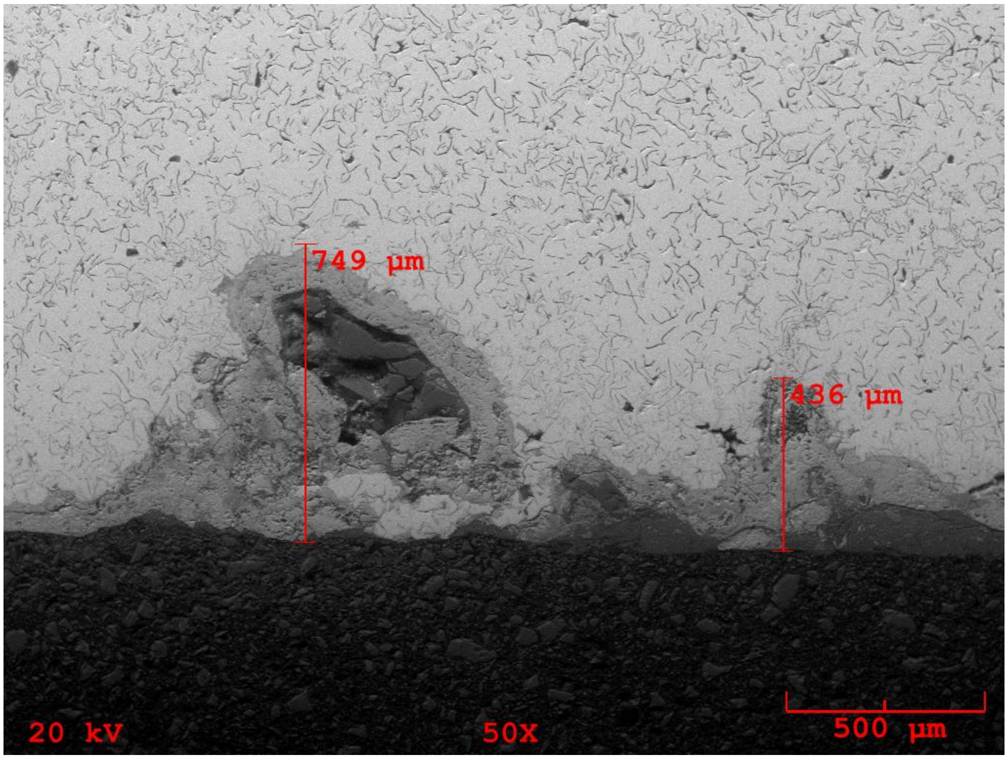

Fig. 60: 50x SEM view of another area of pitting at the ID.

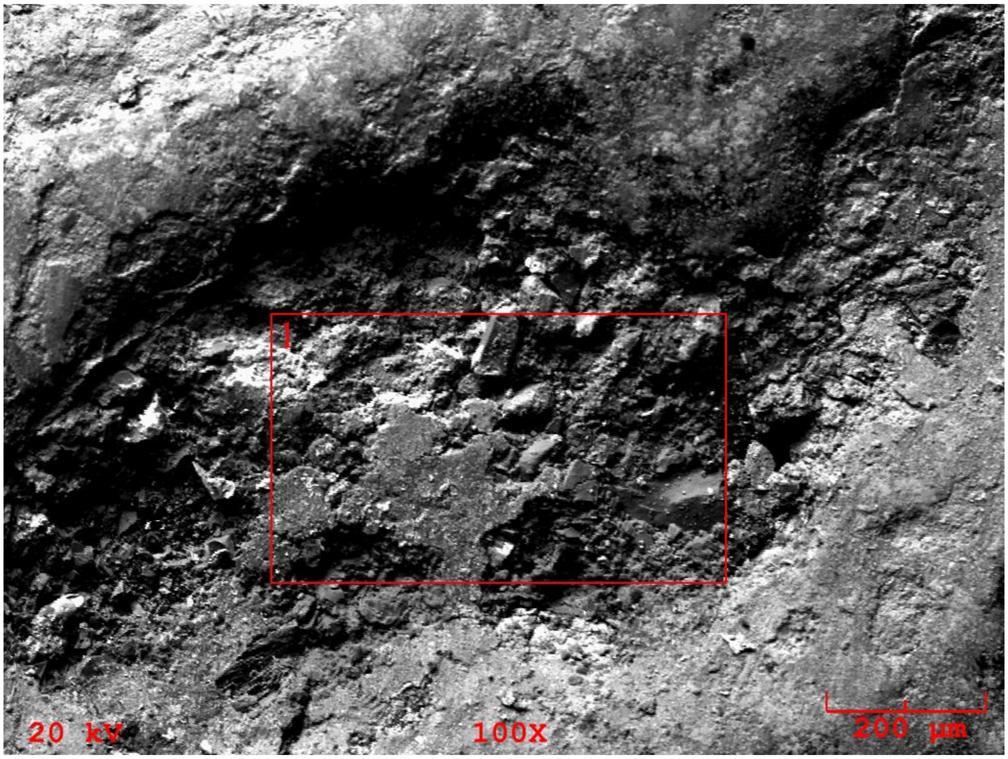

Fig. 61: 100x SEM image of the scale at the OD of sample #2.

Analysis Report: Pipe sample 2 OD scale-1-1

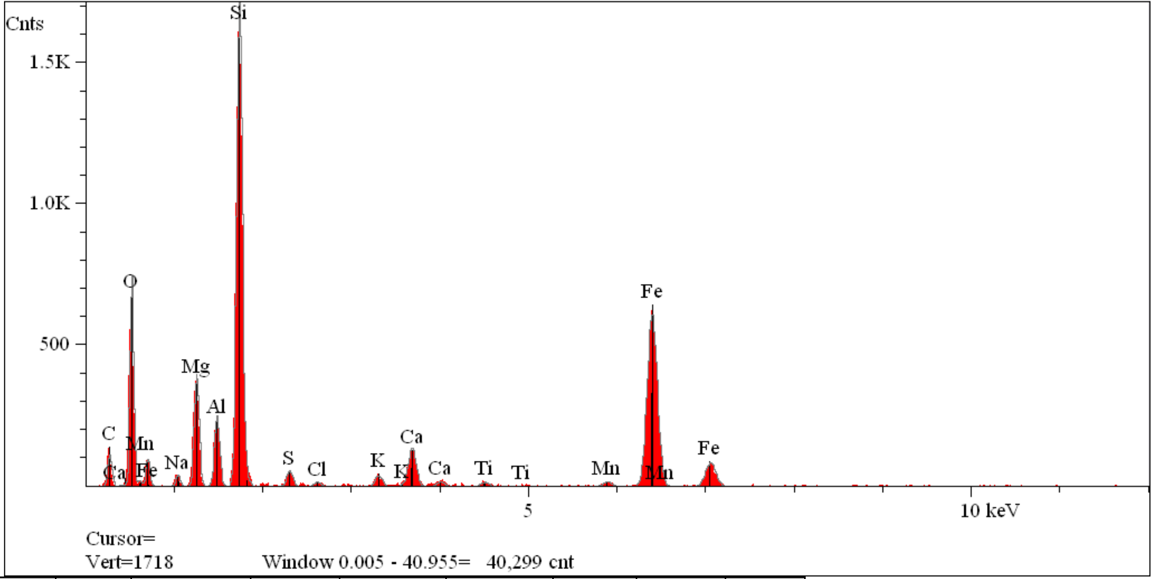

Elt.	Line	Intensity (c/s)	Error 2-sig	Atomic %	Conc	Units	Error 2-sig	
C	Ka	24.10	2.069	23.465	11.284	wt.%	0.969	
O	Ka	131.82	4.283	32.593	20.879	wt.%	0.678	
Na	Ka	8.94	1.603	0.679	0.625	wt.%	0.112	
Mg	Ka	93.74	3.841	4.727	4.600	wt.%	0.189	
Al	Ka	62.42	3.350	2.537	2.741	wt.%	0.147	
Si	Ka	469.40	8.122	16.732	18.815	wt.%	0.326	
S	Ka	16.46	2.379	0.562	0.721	wt.%	0.104	
Cl	Ka	5.21	2.169	0.164	0.232	wt.%	0.097	
K	Ka	13.79	2.451	0.421	0.659	wt.%	0.117	
Ca	Ka	49.89	3.189	1.574	2.526	wt.%	0.161	
Ti	Ka	6.34	2.183	0.214	0.411	wt.%	0.141	
Mn	Ka	7.61	2.106	0.360	0.793	wt.%	0.220	
Fe	Ka	287.84	6.449	15.972	35.714	wt.%	0.800	
				100.000	100.000	wt.%		Total

kV 17.1
Takeoff Angle 45.0°
Elapsed Livetime 30.0

Fig. 62: EDS of area 1 marked in Fig. 61.

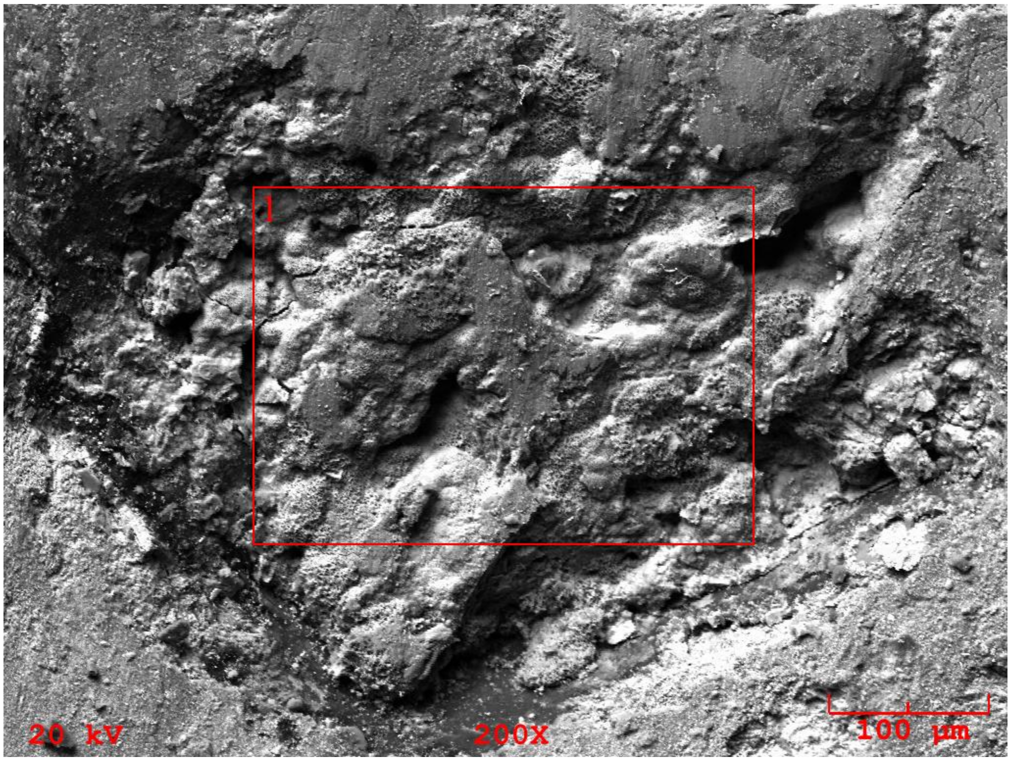

Fig. 63: 200x SEM image of another area of the OD on sample #2.

Analysis Report: Pipe sample 2 OD scale-3-1

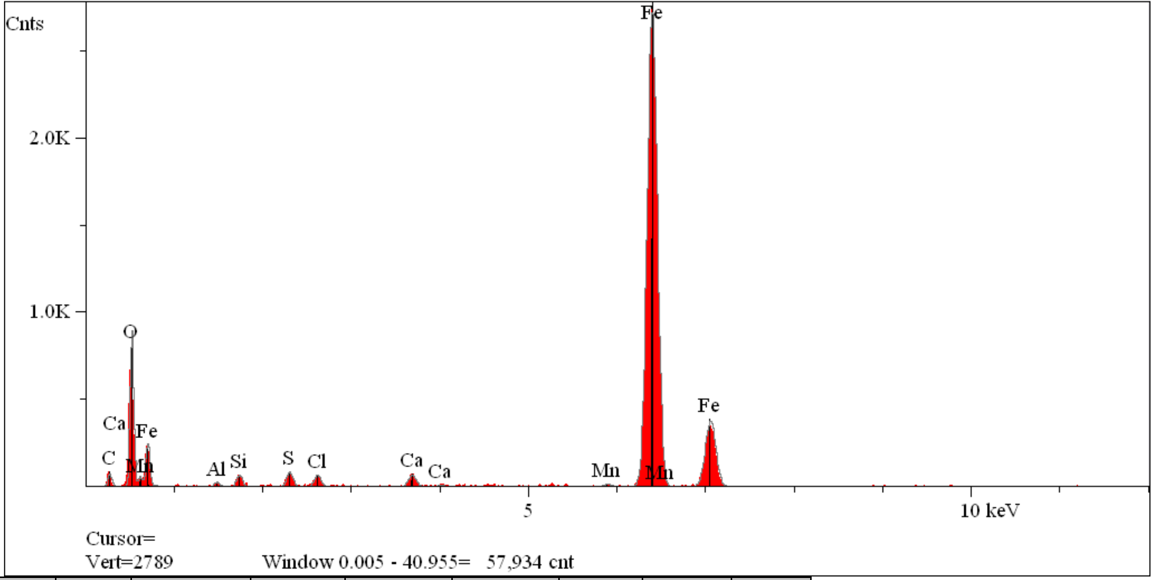

Elt.	**Line**	**Intensity (c/s)**	**Error 2-sig**	**Atomic %**	**Conc**	**Units**	**Error 2-sig**	
C	Ka	15.11	1.872	12.481	3.982	wt.%	0.494	
O	Ka	159.07	4.688	30.174	12.823	wt.%	0.378	
Al	Ka	6.38	1.901	0.322	0.231	wt.%	0.069	
Si	Ka	18.74	2.498	0.747	0.557	wt.%	0.074	
S	Ka	25.48	2.983	0.781	0.665	wt.%	0.078	
Cl	Ka	21.11	3.033	0.581	0.547	wt.%	0.079	
Ca	Ka	24.84	3.199	0.612	0.652	wt.%	0.084	
Mn	Ka	6.32	2.574	0.211	0.308	wt.%	0.125	
Fe	Ka	1,289.43	13.322	54.091	80.236	wt.%	0.829	
				100.000	100.000	wt.%		Total

kV 19.3
Takeoff Angle 45.0°
Elapsed Livetime 30.0

Fig. 64: EDS of area 1 marked in Fig. 63.

Analysis Report: Pipe sample 2 OD scale-5

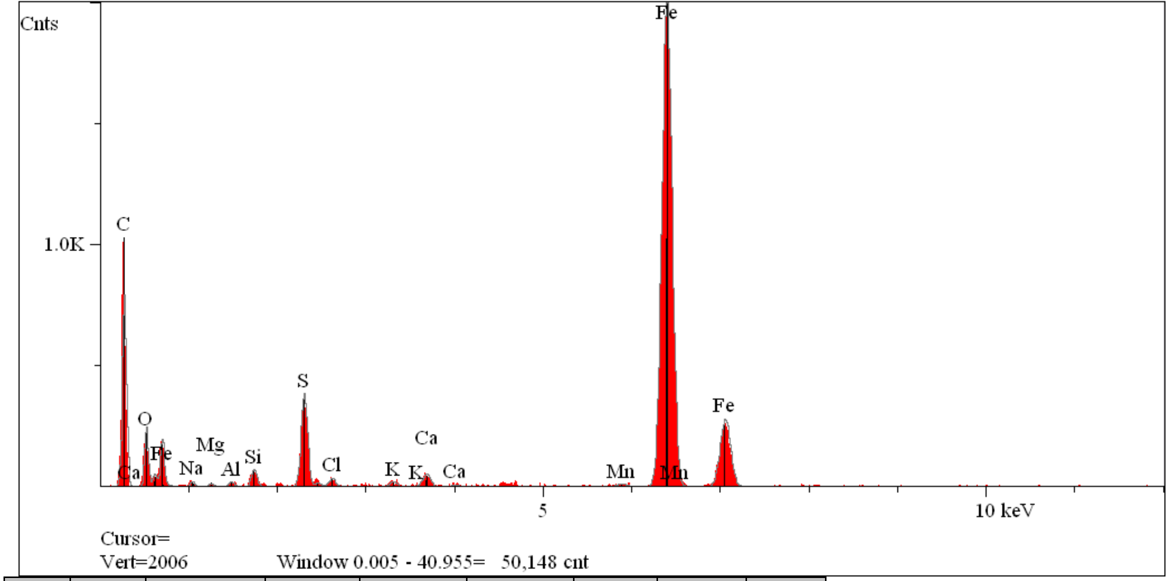

Elt.	**Line**	**Intensity (c/s)**	**Error 2-sig**	**Atomic %**	**Conc**	**Units**	**Error 2-sig**	
C	Ka	166.09	4.861	64.110	32.084	wt.%	0.939	
O	Ka	44.21	2.544	7.314	4.876	wt.%	0.281	
Na	Ka	4.78	1.475	0.259	0.248	wt.%	0.076	
Mg	Ka	2.98	1.725	0.101	0.102	wt.%	0.059	
Al	Ka	5.34	2.033	0.134	0.151	wt.%	0.057	
Si	Ka	19.29	2.659	0.397	0.464	wt.%	0.064	
S	Ka	115.02	4.708	1.945	2.599	wt.%	0.106	
Cl	Ka	10.92	2.999	0.173	0.255	wt.%	0.070	
K	Ka	7.52	2.860	0.113	0.184	wt.%	0.070	
Ca	Ka	19.09	3.041	0.288	0.480	wt.%	0.077	
Mn	Ka	5.73	2.357	0.123	0.282	wt.%	0.116	
Fe	Ka	948.53	11.451	25.044	58.275	wt.%	0.704	
				100.000	100.000	wt.%		Total

kV 18.5
Takeoff Angle 45.0°
Elapsed Livetime 30.0

Fig. 65: EDS of another area of corrosion scale on the OD of sample #2.

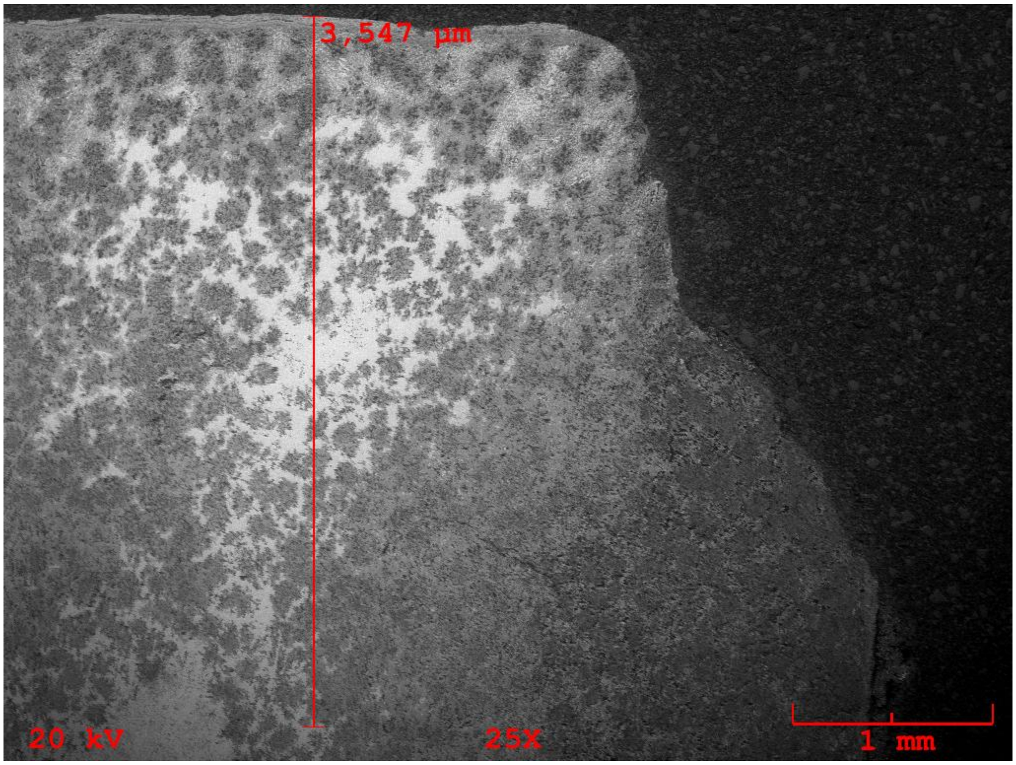

Fig. 66: 25x SEM cross-sectional image of the pit on sample #3. Note, the entire pit could not be captured in one image. Therefore, the pitting depth was determined by combining this measurement with the subsequent one.

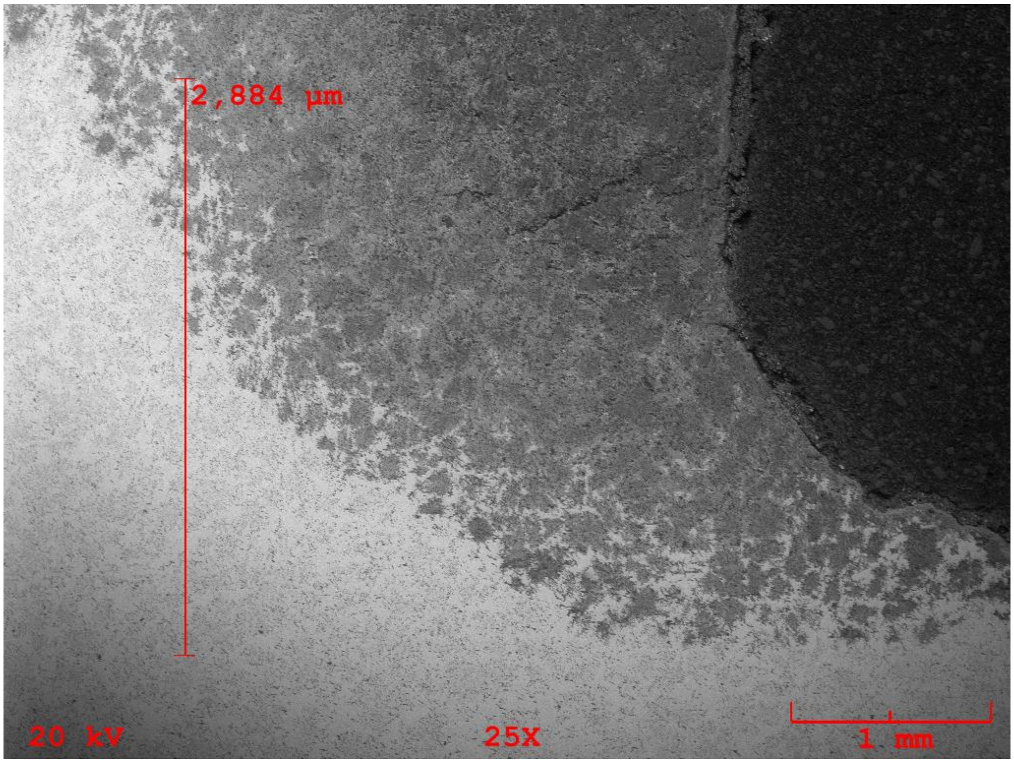

Fig. 67: Same as Fig. 66 except the base of the pit is viewed.

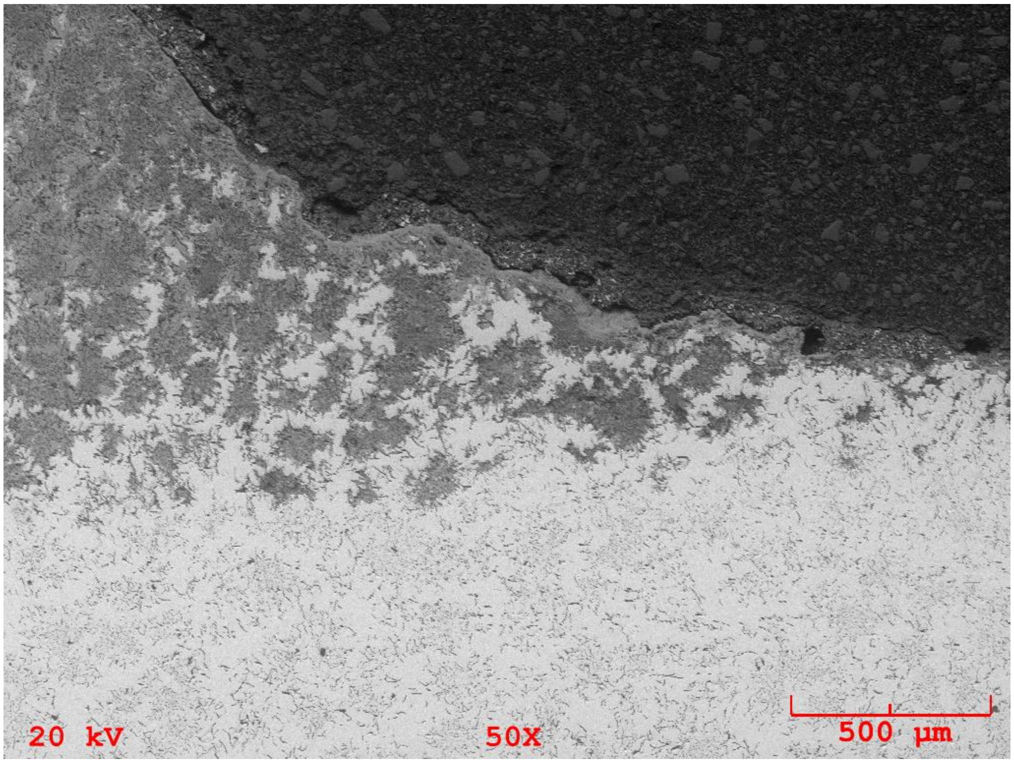

Fig. 68: 50x SEM view of Fig. 67.

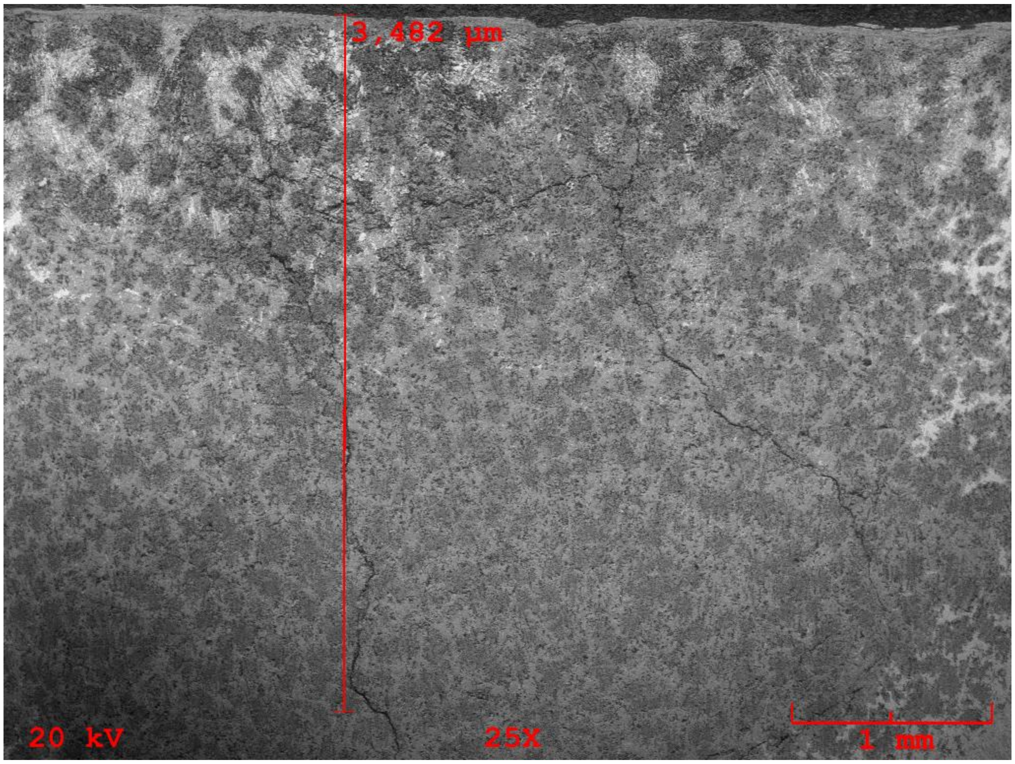

Fig. 69: 25x SEM image of an area of graphitic corrosion on sample #3.

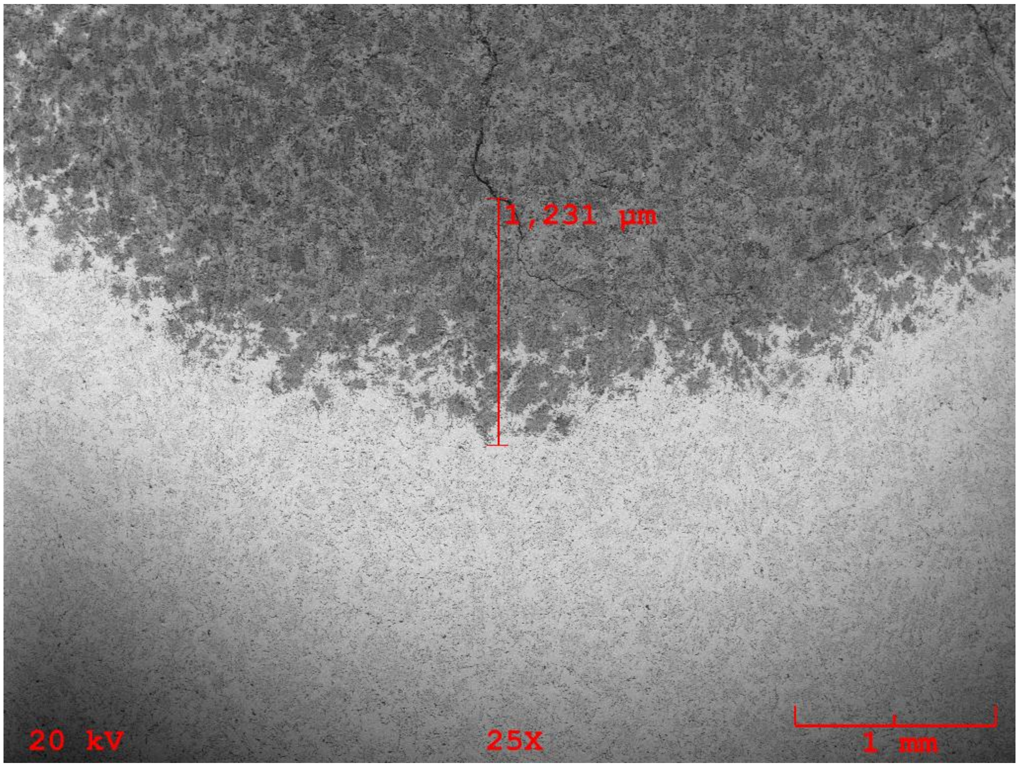

Fig. 70: Same as Fig. 69, except the base of the corrosion cell is viewed.

Analysis Report: Pipe sample 3 removed OD scale-1

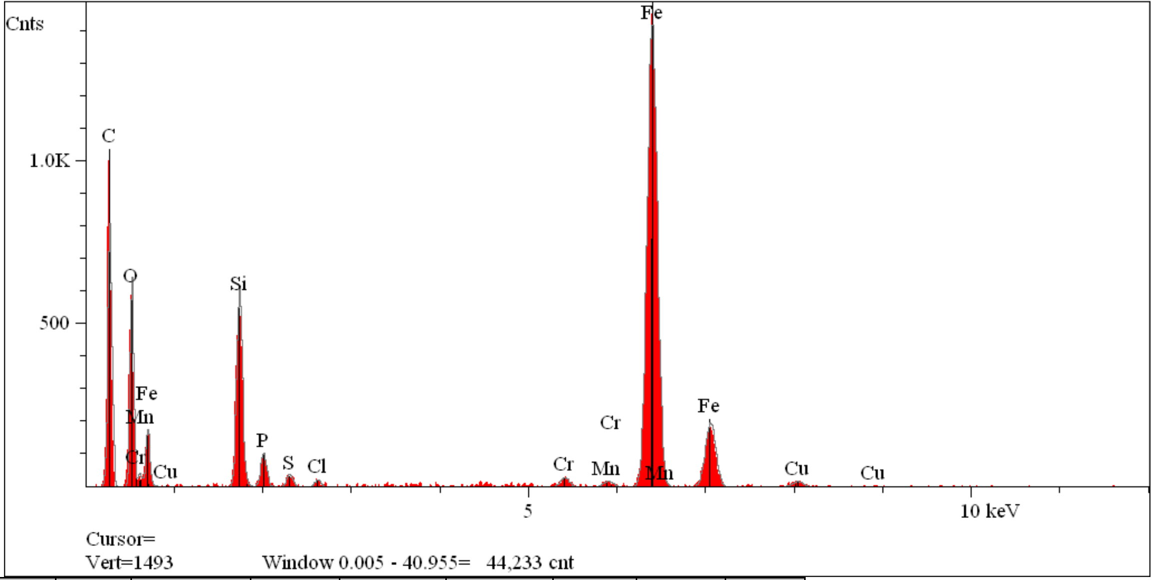

Elt.	**Line**	**Intensity (c/s)**	**Error 2-sig**	**Atomic %**	**Conc**	**Units**	**Error 2-sig**	
C	Ka	170.03	4.957	60.034	33.968	wt.%	0.990	
O	Ka	114.31	4.003	18.244	13.751	wt.%	0.481	
Si	Ka	163.47	5.103	3.103	4.105	wt.%	0.128	
P	Ka	29.39	2.952	0.507	0.739	wt.%	0.074	
S	Ka	11.88	2.582	0.195	0.294	wt.%	0.064	
Cl	Ka	6.89	2.574	0.104	0.174	wt.%	0.065	
Cr	Ka	12.95	2.396	0.183	0.449	wt.%	0.083	
Mn	Ka	7.12	2.283	0.150	0.388	wt.%	0.124	
Fe	Ka	673.05	9.679	17.078	44.928	wt.%	0.646	
Cu	Ka	9.59	1.832	0.402	1.203	wt.%	0.230	
				100.000	100.000	wt.%		Total

kV 18.5
Takeoff Angle 45.0°
Elapsed Livetime 30.0

Fig. 71: EDS on area 1 of scale removed from the OD of sample #3.

Analysis Report: Pipe sample 3 removed OD scale-2

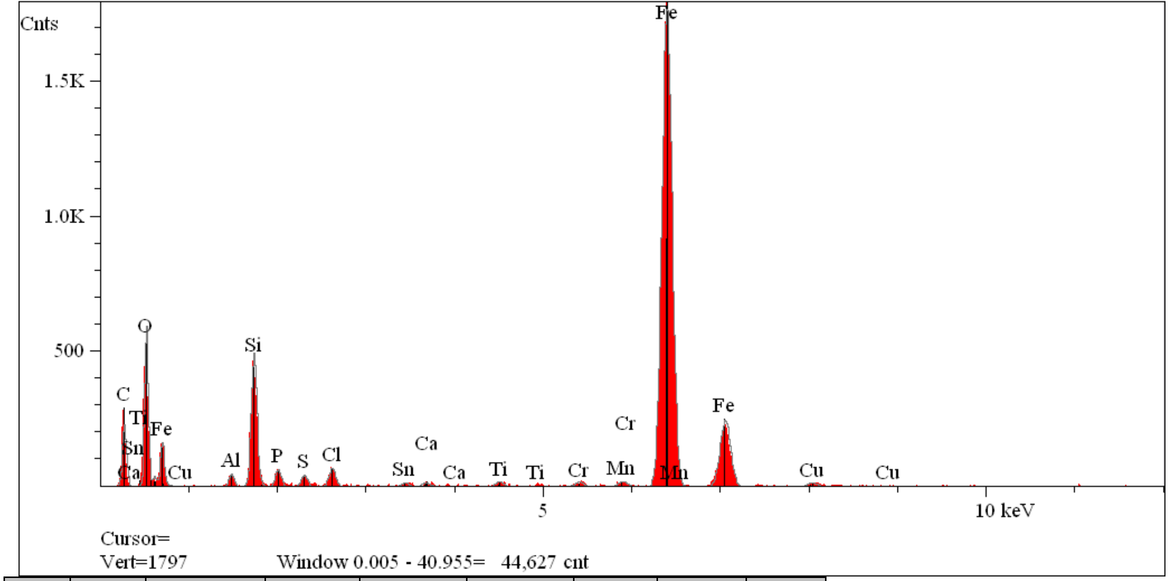

Elt.	Line	Intensity (c/s)	Error 2-sig	Atomic %	Conc	Units	Error 2-sig	
C	Ka	48.02	2.775	36.280	14.822	wt.%	0.856	
O	Ka	104.12	3.803	22.268	12.119	wt.%	0.443	
Al	Ka	11.56	1.969	0.494	0.454	wt.%	0.077	
Si	Ka	131.92	4.536	4.575	4.370	wt.%	0.150	
P	Ka	17.86	2.385	0.547	0.576	wt.%	0.077	
S	Ka	12.85	2.347	0.365	0.398	wt.%	0.073	
Cl	Ka	21.30	2.762	0.548	0.661	wt.%	0.086	
Ca	Ka	2.82	2.411	0.068	0.092	wt.%	0.079	
Ti	Ka	7.33	2.449	0.170	0.276	wt.%	0.092	
Cr	Ka	7.69	2.354	0.168	0.297	wt.%	0.091	
Mn	Ka	7.66	2.317	0.255	0.477	wt.%	0.144	
Fe	Ka	836.41	10.789	33.664	63.946	wt.%	0.825	
Cu	Ka	7.28	1.814	0.482	1.041	wt.%	0.259	
Sn	La	5.44	2.472	0.117	0.470	wt.%	0.214	
				100.000	100.000	wt.%		Total

kV 19.0
Takeoff Angle 45.0°
Elapsed Livetime 30.0

Fig. 72: Same as Fig. 71 except another area was analyzed.

Analysis Report: Pipe sample 3 removed OD scale-3

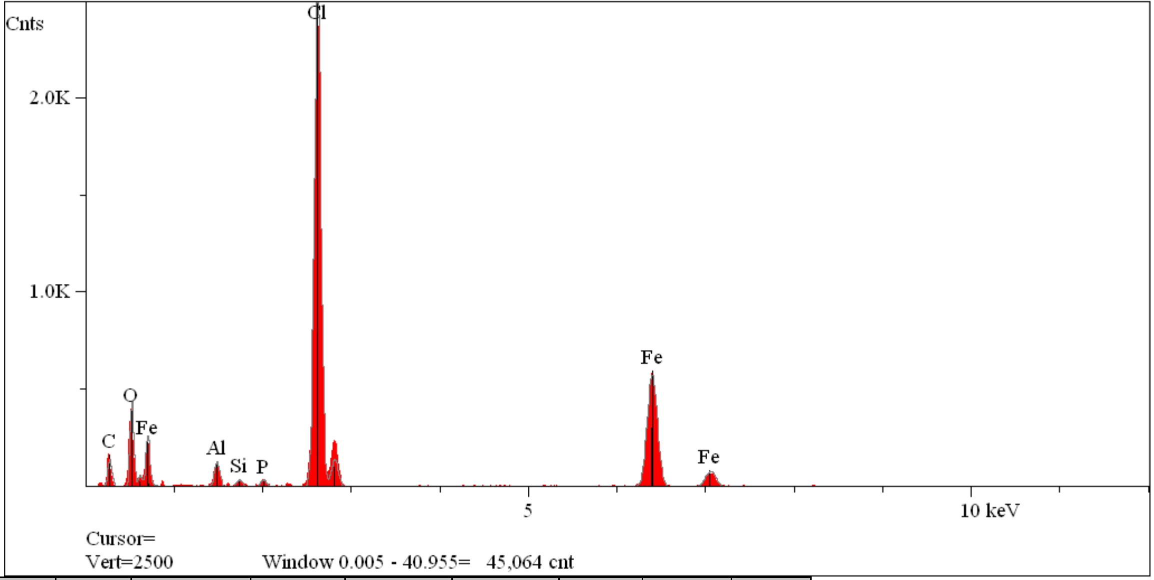

Elt.	**Line**	**Intensity (c/s)**	**Error 2-sig**	**Atomic %**	**Conc**	**Units**	**Error 2-sig**	
C	Ka	29.33	2.307	39.017	18.589	wt.%	1.462	
O	Ka	78.51	3.370	21.613	13.717	wt.%	0.589	
Al	Ka	32.20	2.701	1.114	1.192	wt.%	0.100	
Si	Ka	9.68	2.213	0.292	0.325	wt.%	0.074	
P	Ka	9.90	2.267	0.271	0.333	wt.%	0.076	
Cl	Ka	808.78	10.589	21.830	30.700	wt.%	0.402	
Fe	Ka	272.76	6.216	15.864	35.143	wt.%	0.801	
				100.000	100.000	wt.%		Total

kV 15.9
Takeoff Angle 45.0°
Elapsed Livetime 30.0

Fig. 73: Same as Fig. 71 except another area was analyzed.

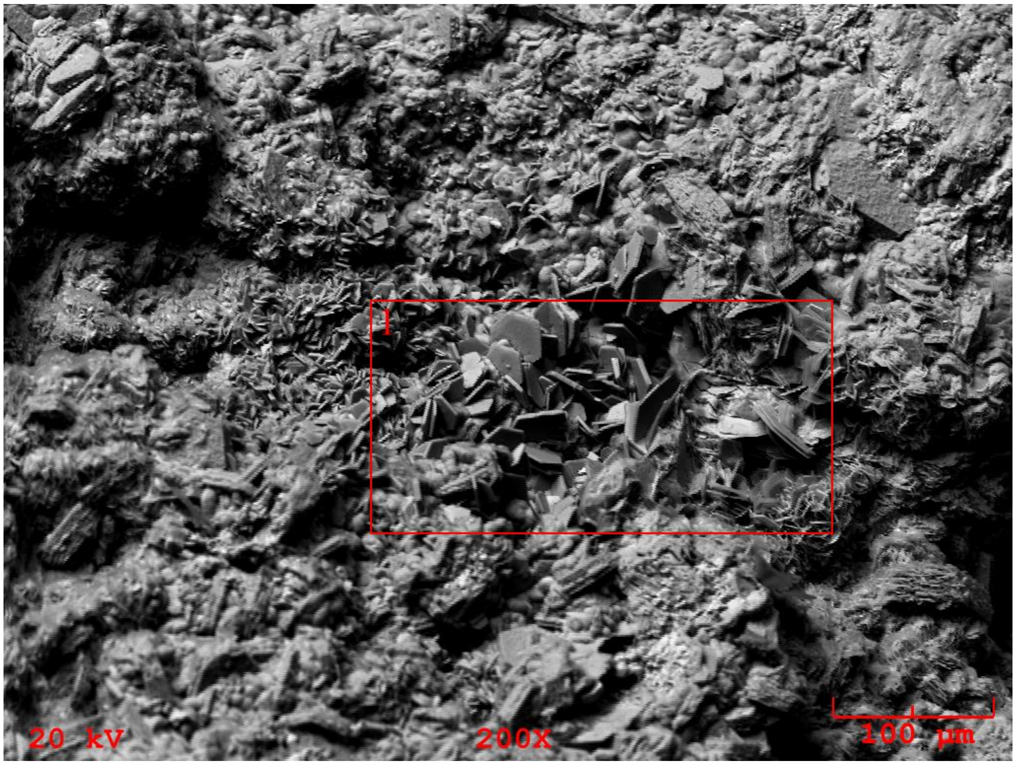

Fig. 74: 200x SEM image of corrosion scale from sample #4.

Analysis Report: Sample 4-1-1

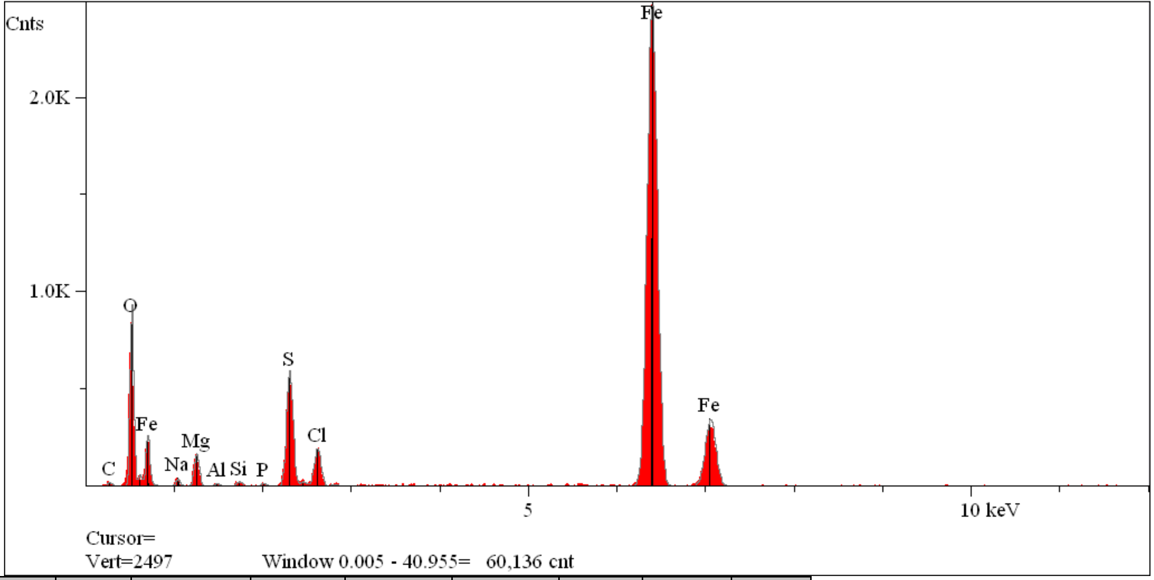

Elt.	**Line**	**Intensity (c/s)**	**Error 2-sig**	**Atomic %**	**Conc**	**Units**	**Error 2-sig**	
C	Ka	4.71	1.345	4.652	1.468	wt.%	0.419	
O	Ka	166.44	4.796	32.035	13.467	wt.%	0.388	
Na	Ka	7.81	1.586	0.874	0.528	wt.%	0.107	
Mg	Ka	39.84	2.752	2.738	1.748	wt.%	0.121	
Al	Ka	3.63	1.797	0.182	0.129	wt.%	0.064	
Si	Ka	6.68	2.148	0.265	0.196	wt.%	0.063	
P	Ka	4.28	2.286	0.143	0.117	wt.%	0.062	
S	Ka	177.66	5.441	5.518	4.649	wt.%	0.142	
Cl	Ka	60.68	3.911	1.751	1.631	wt.%	0.105	
Fe	Ka	1,172.03	12.722	51.842	76.068	wt.%	0.826	
				100.000	100.000	wt.%		Total

kV 18.9
Takeoff Angle 45.0°
Elapsed Livetime 30.0

Fig. 75: EDS of area 1 marked in Fig. 74.

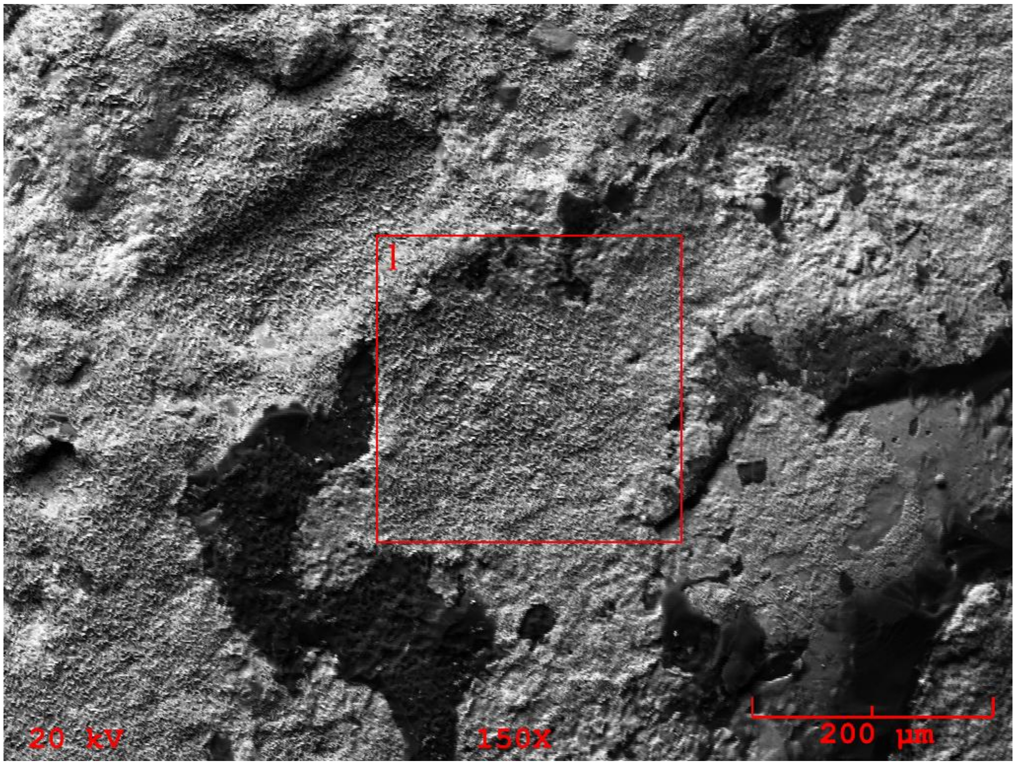

Fig. 76: 150x SEM image of another piece of corrosion scale from sample #4.

Analysis Report: Sample 4-3-1

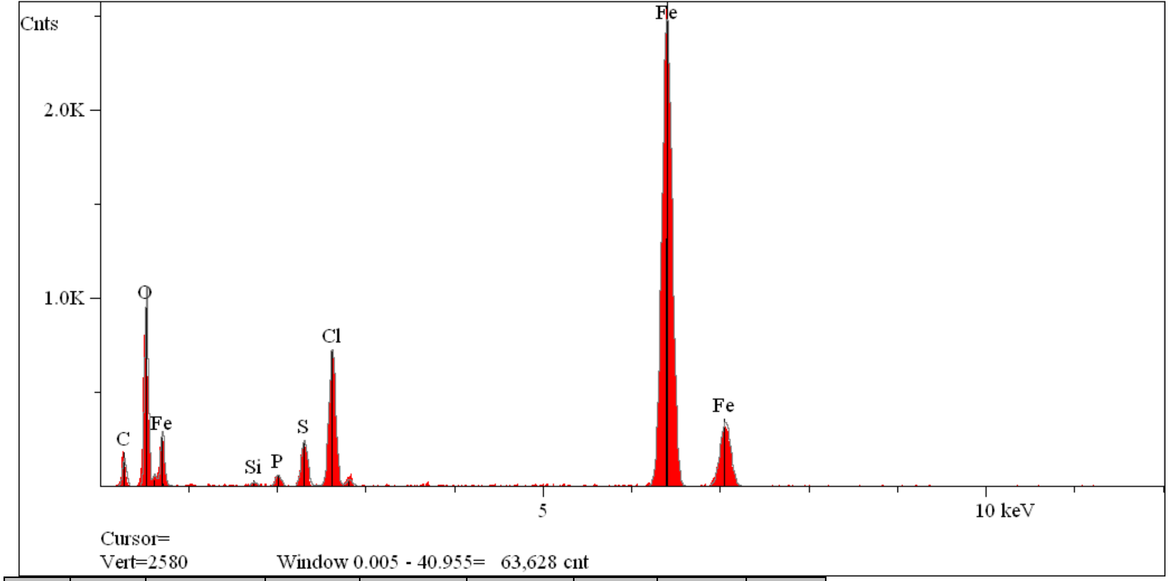

Elt.	Line	Intensity (c/s)	Error 2-sig	Atomic %	Conc	Units	Error 2-sig	
C	Ka	31.10	2.395	22.869	8.629	wt.%	0.665	
O	Ka	189.10	5.105	31.244	15.704	wt.%	0.424	
Si	Ka	6.87	2.350	0.197	0.174	wt.%	0.059	
P	Ka	17.75	2.970	0.432	0.420	wt.%	0.070	
S	Ka	74.16	4.202	1.680	1.692	wt.%	0.096	
Cl	Ka	229.23	6.328	4.797	5.343	wt.%	0.148	
Fe	Ka	1,177.50	12.741	38.781	68.037	wt.%	0.736	
				100.000	100.000	wt.%		Total

kV 19.1
Takeoff Angle 45.0°
Elapsed Livetime 30.0

Fig. 77: EDS of area 1 marked in Fig. 76.

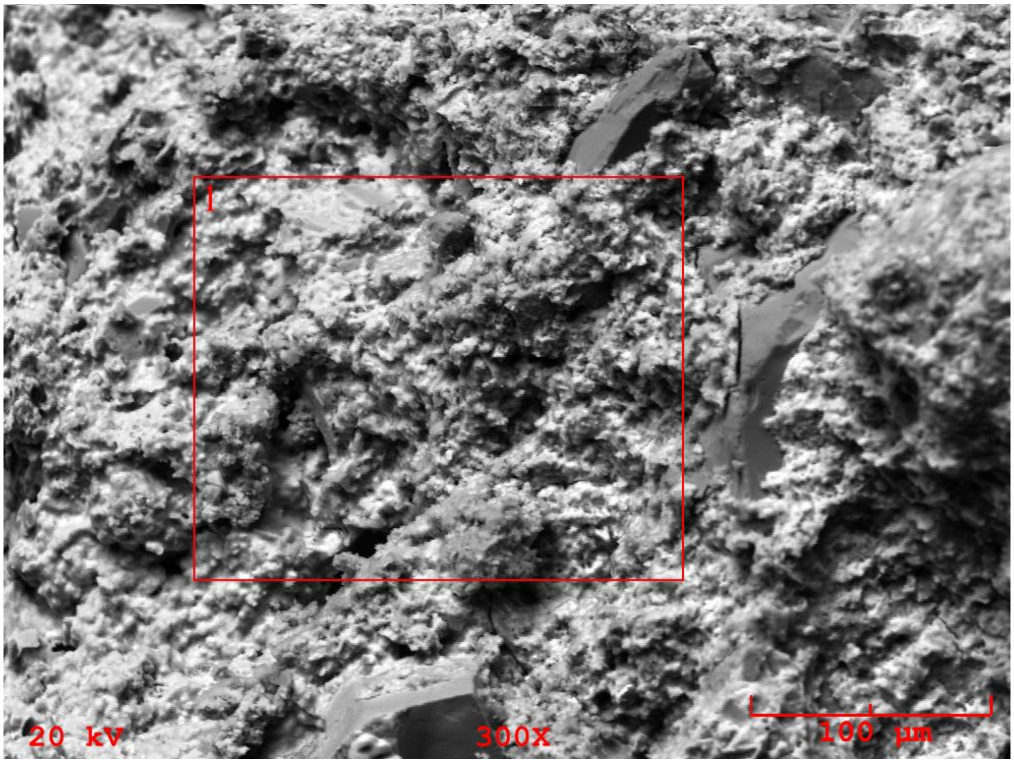

Fig. 78: 300x SEM image of another piece of corrosion scale from sample #4.

Analysis Report: Sample 4-5-1

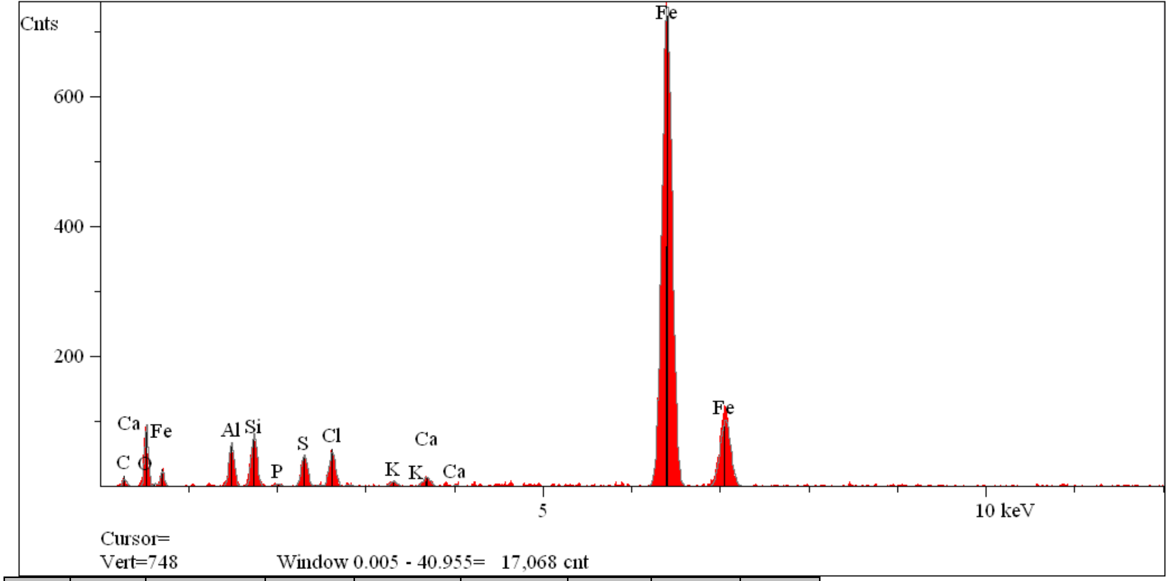

Elt.	**Line**	**Intensity (c/s)**	**Error 2-sig**	**Atomic %**	**Conc**	**Units**	**Error 2-sig**	
C	Ka	2.60	0.589	9.722	2.705	wt.%	0.612	
O	Ka	16.96	1.536	13.597	5.040	wt.%	0.456	
Al	Ka	16.74	1.586	3.378	2.112	wt.%	0.200	
Si	Ka	21.93	1.801	3.596	2.340	wt.%	0.192	
P	Ka	1.25	0.831	0.175	0.126	wt.%	0.084	
S	Ka	14.55	1.647	1.882	1.398	wt.%	0.158	
Cl	Ka	16.55	1.811	1.942	1.595	wt.%	0.175	
K	Ka	2.89	1.205	0.314	0.285	wt.%	0.119	
Ca	Ka	5.15	1.297	0.554	0.514	wt.%	0.130	
Fe	Ka	350.54	6.980	64.840	83.886	wt.%	1.670	
				100.000	100.000	wt.%		Total

kV 18.5
Takeoff Angle 45.0°
Elapsed Livetime 30.0

Fig. 79: EDS of area 1 marked in Fig. 78.

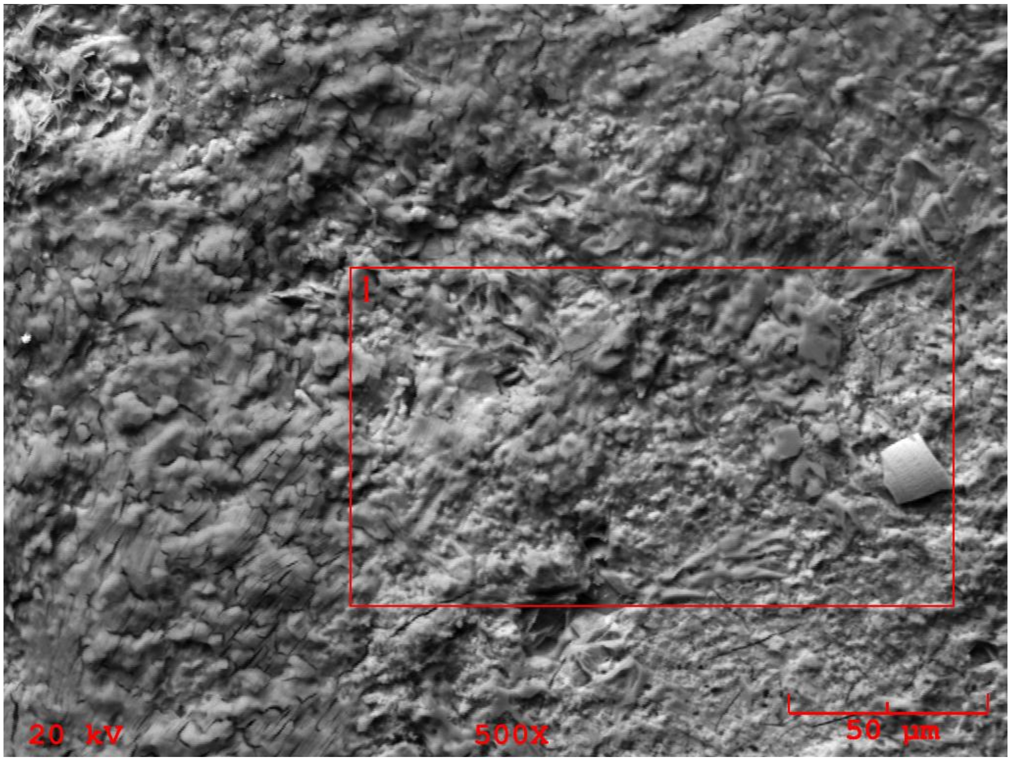

Fig. 80: 500x SEM image of another area of corrosion scale from sample #4.

Analysis Report: Sample 4-7-1

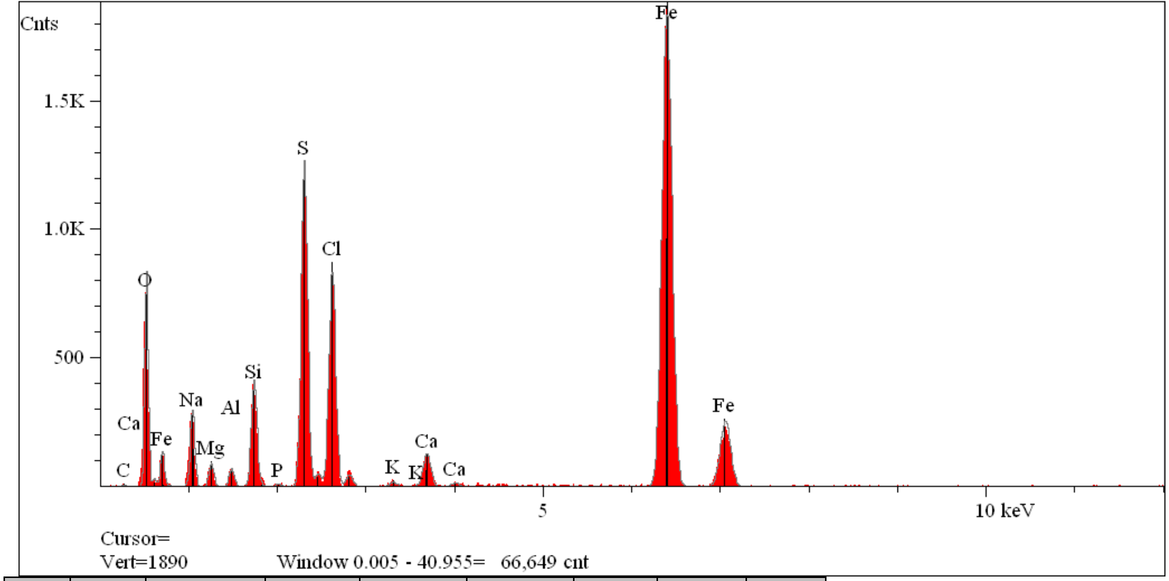

Elt.	Line	Intensity (c/s)	Error 2-sig	Atomic %	Conc	Units	Error 2-sig	
C	Ka	1.44	1.118	1.828	0.634	wt.%	0.492	
O	Ka	149.03	4.547	32.097	14.822	wt.%	0.452	
Na	Ka	65.46	3.225	5.654	3.752	wt.%	0.185	
Mg	Ka	21.52	2.362	1.203	0.844	wt.%	0.093	
Al	Ka	17.42	2.410	0.716	0.557	wt.%	0.077	
Si	Ka	111.18	4.417	3.705	3.003	wt.%	0.119	
P	Ka	3.20	2.536	0.093	0.083	wt.%	0.066	
S	Ka	377.32	7.655	10.365	9.593	wt.%	0.195	
Cl	Ka	262.20	6.709	7.013	7.176	wt.%	0.184	
K	Ka	6.33	2.787	0.163	0.184	wt.%	0.081	
Ca	Ka	46.66	3.603	1.202	1.390	wt.%	0.107	
Fe	Ka	870.48	11.007	35.961	57.963	wt.%	0.733	
				100.000	100.000	wt.%		Total

kV 18.6
Takeoff Angle 45.0°
Elapsed Livetime 30.0

Fig. 81: EDS of area 1 marked in Fig. 80.

APPENDIX D

MIC TEST RESULTS


MICkit Site #1
Anaerobes (ANA)

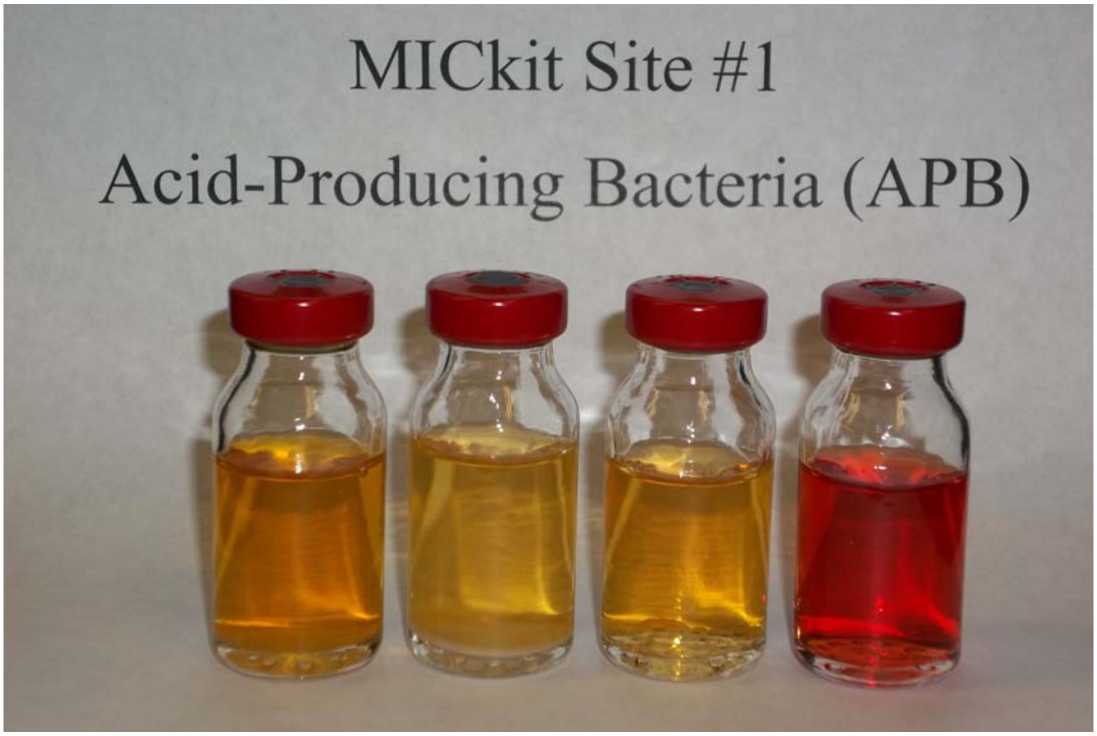
MICkit Site #1
Acid-Producing Bacteria (APB)

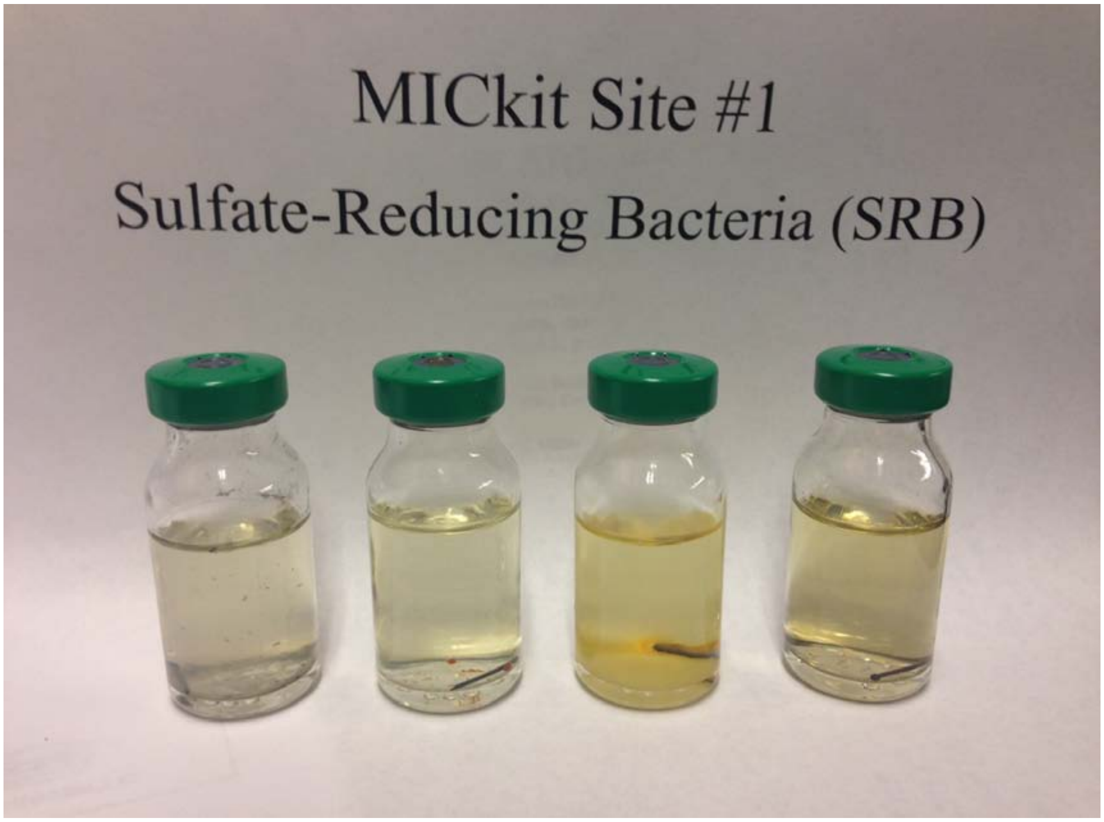
MICkit Site #1
Sulfate-Reducing Bacteria (SRB)


MICkit Site #2
Low Nutrient Bacteria (LNB)

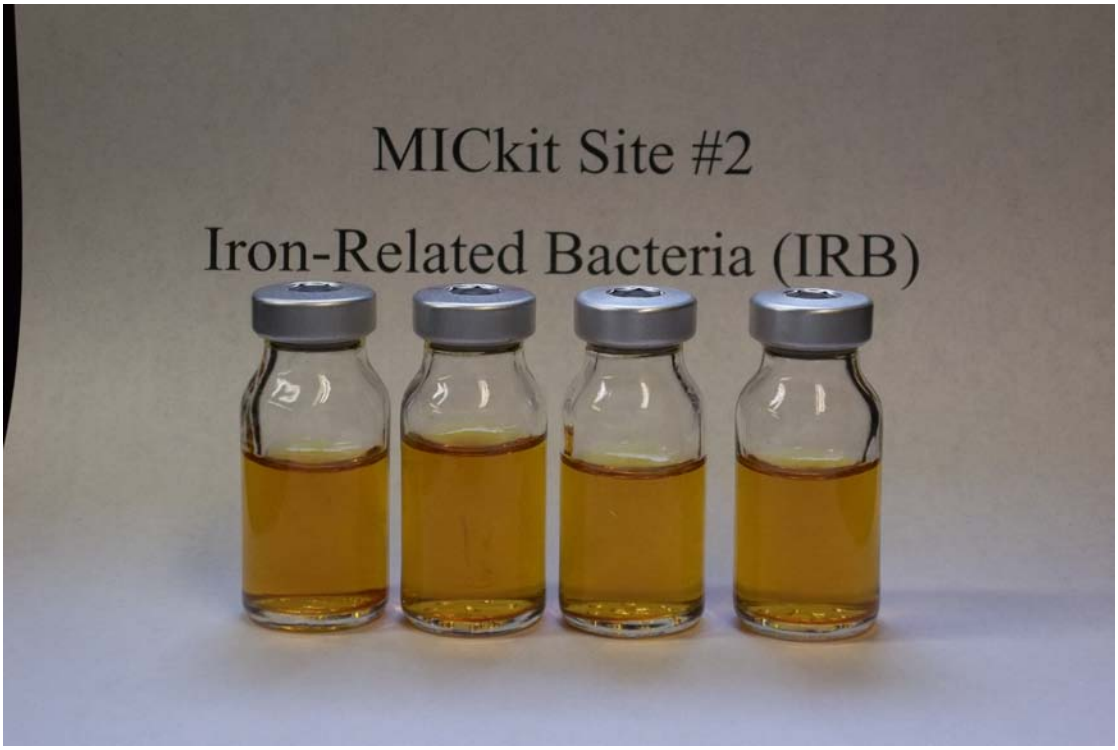
MICkit Site #2
Iron-Related Bacteria (IRB)


MICkit Site #2
Anaerobes (ANA)

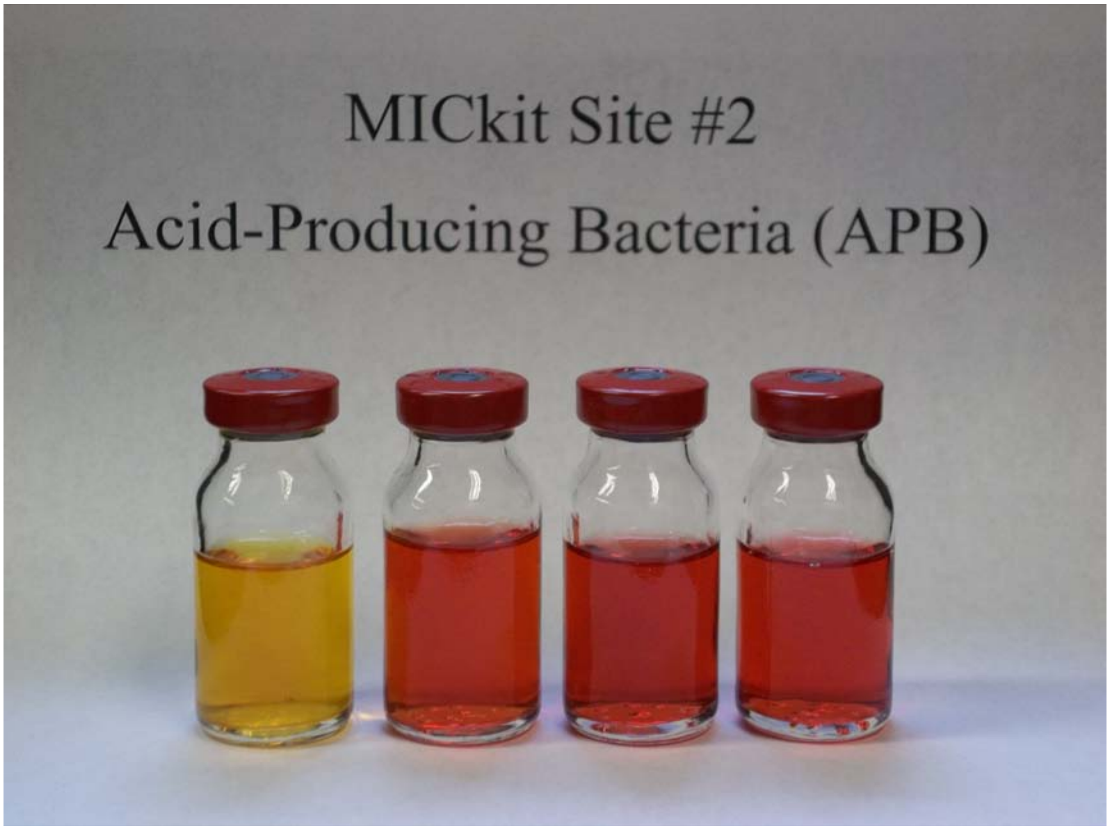
MICkit Site #2
Acid-Producing Bacteria (APB)


MICkit Site #2
Sulfate-Reducing Bacteria (SRB)


MICkit Site #3
Low Nutrient Bacteria (LNB)


MICkit Site #3
Iron-Related Bacteria (IRB)

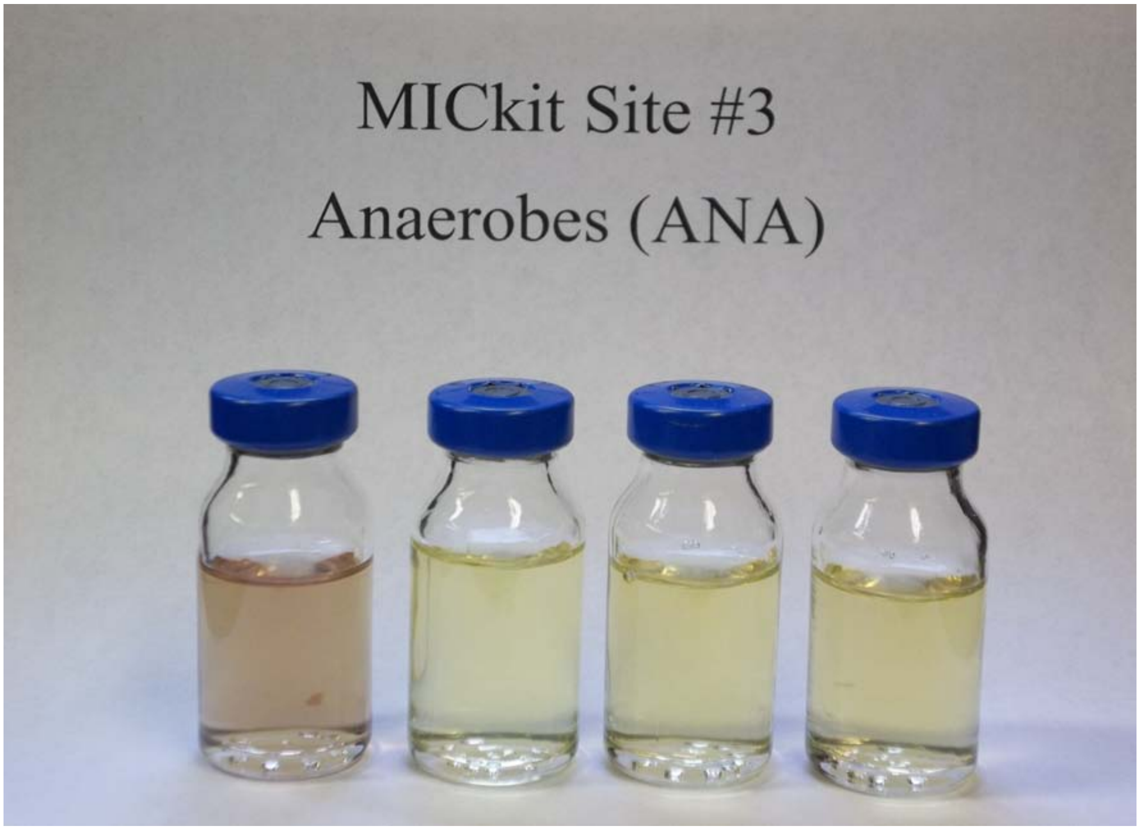
MICkit Site #3
Anaerobes (ANA)


MICkit Site #3
Acid-Producing Bacteria (APB)

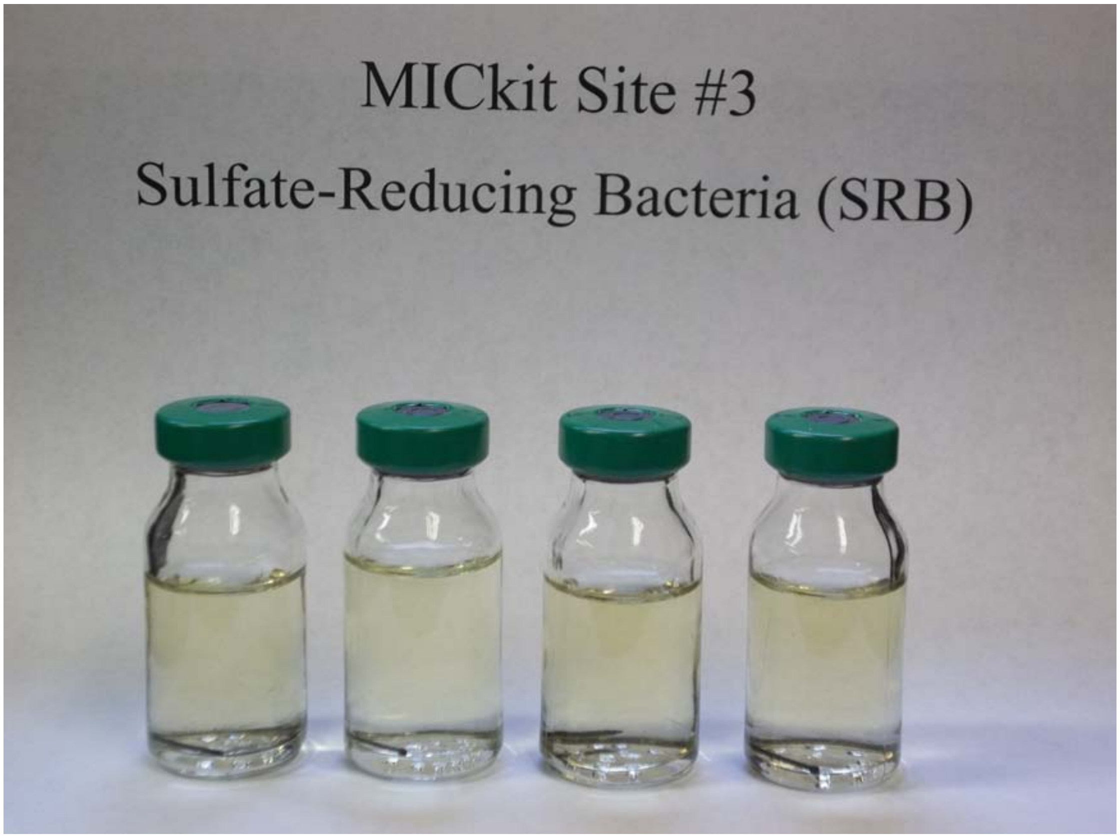
MICkit Site #3
Sulfate-Reducing Bacteria (SRB)

MICROBIOLOGICAL INFLUENCED CORROSION ANALYSIS

Customer: Tetra Tech/King County
Date Collected: 8/14/2012-8/16/2012
Date Tested: 9/20/2012

NCL Job #: 20806
Project: North Beach Force Main
Sample Description: Metal Coupons

	Date Collected	Low Nutrient Bacteria (LNB)	Iron Related Bacteria (IRB)	Anaerobic Bacteria (ANA)	Acid Producing Bacteria (APB)	Sulfate Reducing Bacteria (SRB)
Coupon #1	9/14/2012	None Detected	None Detected	1-10 Per mL	1-10,000 Per mL	None Detected
Coupon #2	9/15/2012	None Detected	None Detected	None Detected	1-10 Per mL	None Detected
Coupon #3	9/16/2012	None Detected	None Detected	None Detected	1-10 Per mL	None Detected

APPENDIX E

CORROSION FUNDAMENTALS

Corrosion of metal can be defined as deterioration due to interaction with the environment. The exact mechanism of that process occurring at the metal/environment interface varies and is highly complex. However, the following conditions must be present before the galvanic corrosion process commences.

(1) Two areas on a metallic structure must differ in electrical potential.

(2) These anodes and cathodes must be electrically interconnected.

(3) These anodes and cathodes must be subjected to a common electrolyte.

When these conditions exist, a galvanic corrosion cell is formed in which oxidation of the metal (occurs at the anode) and reduction of the species in solution (occurs at the cathode). As a result of this process, electrical direct current flows through the metal interconnecting the anode and the cathode. Metal at the anode is consumed while metal at the cathode is protected from corrosion damage. The quantity of metal loss is directly proportional to the DC current flow. For cast iron, the metal loss is approximately 1 to 2 pounds/ampere per year.

Anodes and cathodes can exist on the same metallic surface at a microscopic level or can be created by coupling dissimilar metals exposed to a common electrolyte. All metals have intrinsic energy associated with the smelting process and a typical galvanic series represents that energy as electrical potential when the metals are submerged in a conductive medium. The metals located high on the series are more energetic than those listed lower and are therefore more active.

TYPICAL GALVANIC SERIES

METAL	VOLTS (CSE)
Commercially Pure Magnesium	-1.75
Magnesium Alloy	-1.60
Zinc	-1.10
Aluminum Alloy	-1.05
Commercially Pure Aluminum	-0.80
Mild Steel (clean & shiny)	-0.50 to -0.80
Mild Steel (rusted)	-0.20 to -0.50
Cast Iron (not graphitized)	-0.50
Lead	-0.50
Mild Steel in Concrete	-0.20
Copper, Brass, Bronze	-0.20
High Silicon Cast Iron	-0.20
Carbon, Graphite, Coke	+0.30

The galvanic series provides an indicator of typical metals that can be safely coupled without promoting significant corrosion current flow. The corrosion current generated is proportional to the potential difference between those metals. Metals located near the top of the galvanic series are quite active and typically utilized as sacrificial material when coupled with more passive metals lower on the series.

The amount of corrosion current that eventually flows whether by exposure to a corrosive environment or a galvanic couple is a function of several variables, including an inverse relationship of circuit resistance and pH value of the electrolyte as well as the direct relationship of dissolved oxygen concentration, electrical potential developed between the cathode and anode, and the cathode-to-anode area ratio. Depending upon the physical and metallurgical nature of the metal, and the prevailing environmental conditions, different types of corrosion activity are likely to occur. Some of these common corrosion types are listed below:

CORROSION TYPE	CHARACTERISTIC
Uniform or near uniform	Corrosion attacks all areas of the metal at the same or similar rate. This type of attack can be limited.
Localized	Some areas of the metal corrode at different rates due to heterogeneities in the metal or environment. This type of attack can approach pitting.
Pitting	Very highly localized attack resulting in small pits that may penetrate to perforation.

Many metal structures can continue to perform the design function while experiencing limited corrosion rates, particularly when corrosion is uniform. However, a structure functioning as a vessel may not tolerate localized and pitting corrosion since rapid failure can occur with little volumetric metal loss.

Soils and natural waters constitute very complex electrolytes in which corrosion rates can greatly vary. Soils and natural waters can be heterogeneous providing a non-uniform environment that promotes electrical potential differences between portions of exposed metal creating corrosion cells. Differentials in moisture content, oxygen concentration, salt content, hydrogen ion concentration and other factors are responsible for both producing corrosion cells and controlling corrosion rates.

Corrosion rates are limited by the electrical conductivity of the electrolyte and metallic paths in a corrosion cell. However, electrolyte resistivity is often the limiting factor and low electrolyte resistivity permits high corrosion rates. Also, resistivity differentials of electrolyte in contact with a metal will result in the metal becoming anodic in the electrolyte with low resistivity. Resistivity is dependent upon the type and quantity of ion producing species present. High concentrations of chloride ions greatly reduce resistivity, which further promotes the flow of destructive corrosion currents.

The concentration of free hydrogen ions (pH) and dissolved oxygen control the corrosion process. An acidic electrolyte with a pH value less than 7 contains excess hydrogen ions, which promote electron transfer and enhance the flow of damaging corrosion current. A tenuous by-product of the corrosion activity is the accumulation of gaseous hydrogen film on the cathode surface. This cathodic passivation acts to naturally reduce the corrosion current. However, any available dissolved oxygen can react with this hydrogen to form water. This activity destroys the passivation film, which then allows the corrosion process to continue.

Corrosion is also caused by electrical interference when stray currents moving through an electrolyte collect onto steel structures. Those currents will eventually discharge from the steel and re-enter the electrolyte to complete the circuit to ground. Corrosion damage occurs at the discharge point of the current where metal is oxidized.

APPENDIX F

CORROSION CONTROL METHODS

Corrosion can be mitigated by any of the following methods:

(1) Selection of corrosion resistant material (stainless alloys, fiberglass, concrete).

(2) Alteration of the environment (chemical treatment, remove moisture).

(3) Utilization of coatings and linings, which electrically isolate the structure from the electrolyte (paints, plastic films, etc.).

(4) Application of cathodic protection.

Selection of corrosion resistant material is typically applicable during original construction but similar remedial measures can sometimes be successfully applied.

Local environmental alteration can be effective as a remedial corrosion control method providing the structure is configured properly. A steel tank filled with corrosive liquid can be protected by chemically treating the liquid, but providing a moisture barrier on one surface of a concrete slab may not be effective in controlling rebar corrosion. Electrical isolation of the susceptible surface is also effective in controlling corrosion providing that isolation is not compromised. Concrete encasement of steel can sometimes be an effective method of retrofit to existing structures compromised by corrosion.

Coatings used exclusively for corrosion control by isolation of the environment are quite effective but can sometimes exacerbate corrosion by concentrating the damaging effects at small coating holidays resulting in accelerated local corrosion and premature failure. However, consumable coatings such as zinc and aluminum are generally effective in controlling corrosion as are zinc rich primers used under high-build coatings.

Cathodic protection utilizes an external source of electrical current, which forces the entire structure to become a cathode. The external power source may include either the natural galvanic metallic couple with a sacrificial metal or the operation of an impressed current system using a rectifier to power non-consumable anodes. Cathodic protection is frequently used in conjunction with coatings, which reduce the amount of exposed metal and thus the current requirement for corrosion control.

Galvanic cathodic protection systems using zinc or magnesium anodes as sacrificial material are best suited for applications with low electrolyte resistivity and small protective current requirements. Impressed current systems may be utilized in a wider range of conditions and are advantageous when protective current requirements are large. These latter systems utilize non-soluble anodes to discharge the cathodic protection current directly into the electrolyte.